



ISLAMIC UNIVERSITY OF TECHNOLOGY
DHAKA, BANGLADESH
ORGANISATION OF ISLAMIC COOPERATION



**Study of the Effect of Stacking Sequence on the Tensile and
Flexural Behaviour of Carbon/Jute Epoxy Composite
Materials: Experimental and Numerical/FE Analysis**

B.Sc. Engineering (Mechanical) Thesis

Authored by

Teena Mohaimen

Student ID: 160011085

Hakim Dina Anjum

Student ID: 160011035

Md. Enamul Haque

Student ID: 160011060

Mokid Mohammad Shelley Serajee

Student ID: 160011086

Supervised by

Prof. Dr. Mohammad Ahsan Habib

Department of Mechanical & Production Engineering (MPE)

Islamic University of Technology

Board Bazar, Gazipur

Dhaka, Bangladesh.

Department of Mechanical and Production Engineering (MPE)

Islamic University of Technology (IUT)

March 2021

Research Certification

The thesis title “**Study of the Effect of Stacking Sequence on the Tensile and Flexural Behaviour of Carbon/Jute Epoxy Composite Materials: Experimental and Numerical/FE Analysis**” submitted by **Teena Mohaimen (160011085), Hakim Dina Anjum (160011035), Md. Enamul Haque (160011060) and Mokid Mohammad Shelley Serajee (160011086)** has been accepted as satisfactory in partial fulfillment of the requirement for the Degree of Bachelor of Science in Mechanical Engineering on March 2021.

Signature of the Supervisor



A handwritten signature in black ink, appearing to read 'Ahsan', is written over a horizontal line. Below the signature, the date '01/03/2021' is written in the same ink.

Prof. Dr. Mohammad Ahsan Habib
Department of Mechanical & Production Engineering (MPE)
Islamic University of Technology
Board Bazar, Gazipur
Dhaka, Bangladesh.

Candidate's Declaration

It is hereby declared that this thesis or any part of it has not been submitted elsewhere for the award of any degree or professional qualification.

Signature of the Candidates

Teena
01/03/21

Hakim Dina Anjum
01.03.21

Teena Mohaimen
Student ID: 160011085

Hakim Dina Anjum
Student ID: 160011035

Enamul Haque
01.03.21

Mokid Mohammad Shelley Serajee
01/03/21

Md. Enamul Haque
Student ID: 160011060

Mokid Mohammad Shelley Serajee
Student ID: 160011086

Department of Mechanical and Production Engineering (MPE)
Islamic University of Technology (IUT), OIC
Board Bazar, Gazipur
Dhaka, Bangladesh

Signature of the Supervisor

Ahsan Habib
01/03/2021

Prof. Dr. Mohammad Ahsan Habib
Department of Mechanical & Production Engineering (MPE)
Islamic University of Technology
Board Bazar, Gazipur
Dhaka, Bangladesh.

Abstract

Currently, there is an increasing trend of utilizing composite materials in various sectors of engineering and technology, particularly aerospace and industrial application, for their exceptional mechanical and thermal properties, lightweight, and lower cost. In a composite, the constituent materials collectively work to create a new substance whose properties are superior to those of the original components. A number of factors affect the properties of the composite material. This paper addresses the effects of the stacking sequence on the tensile and flexural behavior of Jute/Carbon Epoxy hybrid composites. Five specimens of unidirectional Jute/Carbon fiber reinforced composite were fabricated for each of the five stacking sequences of a test to investigate the mechanical properties of the composite. The distinct stacking sequences consisted of equal quantity of fiber components. Specimens were fabricated using vacuum assisted resin infusion process under the ASTM guidelines. Experiment results revealed that similar amount of load or force generated varying responses on specimens with varying stack up sequences. Further, identical stacking sequences had different effects on different tests. Sandwiching four Carbon plies between six Jute plies proved beneficial for the composite's tensile behavior, but derogatory for its flexural one. The experimental results were validated using ACP in ANSYS by recreating the composite laminate, taking into account the distinct stacking sequences and exact experimental conditions. The FE Analysis of the tensile and flexural tests consisted outcomes similar to those of the experimental results, with acceptable errors ranging from 3%-5%.

Acknowledgements

Our deepest gratitude to our thesis supervisor, Prof. Mohammad Ahsan Habib for his assistance at every stage of the research project. We sincerely acknowledge his insightful comments and suggestion that motivated us throughout the thesis.

We would like to extend our sincere thanks to Mr. Md. Abu Shaid Sujon for his valuable guidance and encouragement extended to us. In addition, we are greatly indebted to him for sharing the experimental data of his research as well as software expertise with us.

We wish to acknowledge the help provided by Prof. Mohammad Zoynal Abedin in facilitating the testing of the fabricated samples in Dhaka University of Engineering Technology (DUET), Gazipur.

We also place on record, our gratitude to one and all, who directly or indirectly, have lent their hand in this venture.

Table of Contents

Abstract	i
Acknowledgements	ii
Table of Contents	iii
Abbreviations	v
List of figures	vi
List of tables	xi
Chapter 1. Introduction	1
1.1 Research Aims and Objectives	2
1.2 Composite Materials	3
1.3 Categories of Composite Materials	3
1.4 Types of Fibers	4
1.5 Thesis Outline	4
Chapter 2. Literature Review	6
Chapter 3. Experimental Procedure and Numerical Methodology	11
3.1 Materials and Fabrication	11
3.1.1 Materials	11
3.1.1.1 Jute Fiber	12
3.1.1.2 Carbon Fiber	14
3.1.1.3 Matrix	15
3.1.2 Stacking sequence	16
3.1.3 Fabrication Method of Composite Laminates	18
3.1.3.1 Vacuum Assisted Resin Infusion Process	18
3.1.3.2 Infusion Procedure	20
3.2 Flexural Test	25
3.2.1 Experimental Procedure	25
3.2.2 Finite Element Analysis	28

3.2.2.1	Flexural Analysis	29
3.2.2.2	Simulation Steps	31
3.3	Tensile Test	52
3.3.1	Experimental Procedure	52
3.3.2	Finite Element Analysis	53
3.3.2.1	Simulation Steps	54
Chapter 4.	Results and Discussion.....	80
4.1	Tensile Test Result Analysis	81
4.1.1	Experimental Result Analysis	81
4.1.2	FEA Simulation Results of Tensile Properties.....	86
4.2	Flexural Test Result Analysis.....	87
4.2.1	Experimental result analysis	87
4.2.2	FEA Simulation Results of Flexural Properties	91
Chapter 5.	Conclusion	93
Chapter 6.	References	96

Abbreviations

NFRC-Natural Fiber Reinforced Composite

VARI- Vacuum Assisted Resin Infusion

UD-Unidirectional

VARI- Vacuum Assisted Resin Infusion

UTS-Ultimate Tensile Strength

GF- Glass Fiber

FFRP-Flax Fiber Reinforced Polymer

GFRP-Glass Fiber Reinforced Polymer

CFRP- Carbon Fiber Reinforced Polymer

HP- Hybrid Plain Woven

BP-Banana Plain

KP-Kenaf Plain

SLS-Sodium Lauryl Sulphate

FEA-Finite Element Analysis

TS- Tensile Strength

BS-Bending Strength

TM-Tensile Modulus

BM-Bending Modul

List of figures

Figure 3.1 Jute fiber fabric	12
Figure 3.2 Carbon fiber fabric.....	14
Figure 3.3 Stacking Sequences	17
Figure 3.4 Schematic Diagram of Vacuum Assisted Resin Infusion Process	19
Figure 3.5 Setup of mould with composite layer	21
Figure 3.6 Placement of fiber, peel ply and infusion mesh on the composite layer	22
Figure 3.7 Installation of infusion spiral tube, silicon connector and sealant tape	23
Figure 3.8 Vacuum-Bagging Procedure.....	24
Figure 3.9 Specimen dimension for flexural test	26
Figure 3.10 Flexural testing equipment with the specimen	27
Figure 3.11 Prepared mesh of pusher, base and specimen for flexural test.....	30
Figure 3.12 Saving file.....	31
Figure 3.13 Creating ACP PrePost.....	32
Figure 3.14 Insertion of density and elasticity	33
Figure 3.15 Properties of carbon/epoxy	34
Figure 3.16 Properties of jute/epoxy	34
Figure 3.17 Selection of geometry	35
Figure 3.18 Dimension of ply	36
Figure 3.19 The splitting of the ply	37
Figure 3.20 Selection of geometry	37
Figure 3.21 The arbitrary assignment of values of properties	38
Figure 3.22 The geometry and type of ply	39

Figure 3.23 Usage of method	40
Figure 3.24 Selection of acp setup	40
Figure 3.25 Creation of fabrics	41
Figure 3.26 Flipping axes.....	42
Figure 3.27 Rosette directions.....	42
Figure 3.28 Selection of orientated selection set	43
Figure 3.29 Upward direction	43
Figure 3.30 Stacking sequence.....	44
Figure 3.31 Setting of stack up	45
Figure 3.32 Creation of static structural.....	46
Figure 3.33 Deselection of ‘show mesh’	46
Figure 3.34 Modification of analysis settings	47
Figure 3.35 Addition of simply support.....	48
Figure 3.36 Insertion of force.....	48
Figure 3.37 Addition of displacement.....	49
Figure 3.38 Branches of solution tree	50
Figure 3.39 Data for graph plotting and animation.....	51
Figure 3.40 Marking of the positions with the greatest and smallest ‘solution’ results.....	51
Figure 3.41 Specimen dimension for tensile test	52
Figure 3.42 Tensile testing equipment with the specimen.....	53
Figure 3.43 Prepared mesh of the fixture and specimen for tensile test	54
Figure 3.44 Designing the specimen in SolidWorks 2017.....	54
Figure 3.45 Designing fixtures to hold the specimen	55

Figure 3.46 Setting up ACP (ANSYS Composite Prepost)	56
Figure 3.47 Inputting the property values of Carbon Epoxy	56
Figure 3.48 Inputting the property values of Jute Epoxy.....	57
Figure 3.49 Importing the designed specimen into the workbench	58
Figure 3.50 Imported specimen on ANSYS ACP.....	58
Figure 3.51 Geometry assigned with a fake thickness.....	59
Figure 3.52 Prepared geometry for meshing.....	60
Figure 3.53 Finely meshed model of the specimen.....	60
Figure 3.54 Setting up workbench for importing fixture geometry	61
Figure 3.55 Importing the fixture geometry.....	61
Figure 3.56 Meshed fixtures	62
Figure 3.57 Setup window of ACP tool.....	63
Figure 3.58 Creating fabric on ANSYS ACP	63
Figure 3.59 Defining Carbon fabric	64
Figure 3.60 Defining Jute fabric	64
Figure 3.61 Creating new Rosette.....	65
Figure 3.62 Creating Oriented Selection Set	66
Figure 3.63 Defining coordinates for oriented selection set	66
Figure 3.64 Arrows showing the direction of fiber and the normal direction.....	67
Figure 3.65 Creating Modeling Groups	68
Figure 3.66 Creating composite plies	68
Figure 3.67 Creating Carbon ply.....	69
Figure 3.68 Creating ply for Jute	70

Figure 3.69 Creating Solid Model.....	70
Figure 3.70 Inputting necessary data for creating solid model	71
Figure 3.71 Creating Section Cut.....	72
Figure 3.72 Section Cut Window.....	72
Figure 3.73 Specimen after executing section cut	73
Figure 3.74 Setting up static structural tool and connecting with ACP tool.....	74
Figure 3.75 Connecting ACP and Mechanical model with Static Structural.....	75
Figure 3.76 Combined model of specimen and fixture in ANSYS Mechanical.....	76
Figure 3.77 Illustration of prepared mesh in both specimen and fixture	76
Figure 3.78 Defining fixed support.....	77
Figure 3.79 Assigning load on the fixture.....	78
Figure 3.80 Simulation option parameters for (a) Equivalent Stress (b) Equivalent Elastic Strain (c) Total Deformation.....	79
Figure 4.1 Experimental and numerical tensile test result for all the composite laminates	82
Figure 4.2 Rosen’s Tensile Failure Model.....	83
Figure 4.3 Fracture condition of Unidirectional composite (S1-S4) material after tensile test(a-d)	85
Figure 4.4 Total deformation after tensile load. (a) S1 = J3C4J3, (b) S2= J2C2J2C2JC, (c) S3 = C2J3C2J3, (d) S4= C2J6C2.....	86
Figure 4.5 Flexural stress vs Strain curve experimental and FEA (a) J3C4J3 (b) J2C2J2C2J2 (c) C2J3C2J3 (d) C2J6C2.....	89
Figure 4.6 Fracture configuration of the sample after the flexural test (a-d) for sample S1-S4 (unidirectional).....	90

Figure 4.7 Total deformation of FEA 3D specimen under flexural load of (a)J₃C₄J₃
(b)J₂C₂J₂C₂J₂ (c) C₂J₃C₂J₃ (d) C₂J₆C₂..... 92

List of tables

Table 3-1 Chemical configuration of jute	13
Table 3-2 Properties of jute fiber	13
Table 3-3 Properties of carbon fiber	15
Table 3-4 Material properties in Engineering Data, ACP (Pre).....	29

Chapter 1. Introduction

Over the past few decades, polymer composites have been used widely in various applications like automobiles, airships, fleet, fishing equipment etc. for having numerous advantages over their conventional metal counterparts. To give a few examples, depending on the reinforcements used, tensile strength of composites has the potential to be up to four to six times greater than that of steel or aluminium. They have higher fatigue strength, which values up to 60% of the ultimate tensile strength sometimes. Using composites results in 30% - 40% lighter structure compared to metallic structures designed to the same functional requirements. Composite parts can eliminate the need of joints or fasteners, providing simpler design, and can be tailored to meet complex design requirements as well, making them more versatile than metals. These materials exhibit excellent corrosion resistance and fire retardancy. They are less noisy while in operation and provide lower vibration transmission than metals.

In a nutshell, composites offer high specific strength, stiffness, better fatigue performances, corrosion resistance and have the ability to meet diverse design requirements with significant weight savings as well as strength-to-weight ratio, at a convenient cost [1].

Superior qualities like enhanced physical properties, higher elasticity, lower material quantity per unit volume, and brilliant heat resistance make carbon fibre a widely used reinforcement material [2], [3]. However, carbon fibres are costly, and tend to be more influenced by the stress-riser in practical operations due to their brittleness [4]. Replacing some layers of carbon fibres by ductile fibres can aid in increasing the strength and reducing the cost of Carbon Fibre Reinforced Polymers (CFRPs). For this hybridization, this paper uses jute. Apart from being notably ductile, natural fibres like jute are abundant and cheap

in the South Asian regions. Owing to the damping properties of jute fibres and the high tensile strength of carbon fibres, such hybrid composites of carbon and jute can replace carbon fibre reinforced composites in structures exposed to vibrations [5].

1.1 Research Aims and Objectives

This paper investigates the tensile and flexural properties of carbon-jute epoxy composites by varying the stacking sequences. The experimental results were validated by finite element analysis using ANSYS R20. This software is an important tool to validate experimental data as well as analyse any complex design. It is a comprehensive general-purpose finite element programme, which is being used in many engineering fields that include aerospace, automobile, electronics and nuclear sectors. In this work, the following objectives were met.

- Fabricating a composite material consisting of optimum mechanical properties using minimum amount of synthetic fiber and maximum amount of natural fiber to get the benefit of the abundance and low cost of natural fiber. Here, a composite with 27% carbon fiber and 73% jute fiber by weight was fabricated.
- Fabricating the composite using the Vacuum Assisted Resin Infusion process as this creates composites with the best mechanical properties, compared to other manufacturing processes.
- Determining the optimum stacking sequence achieved using four plies of unidirectional carbon fibers and six plies of unidirectional jute fibers.

1.2 Composite Materials

A composite material is a new material fabricated from the combination of two or more materials (different in terms of physical or chemical properties) to produce a material with better physical and chemical properties and a more robust structure [6]. The newly created composite tends to have features that are unique and absent in the individual materials [7].

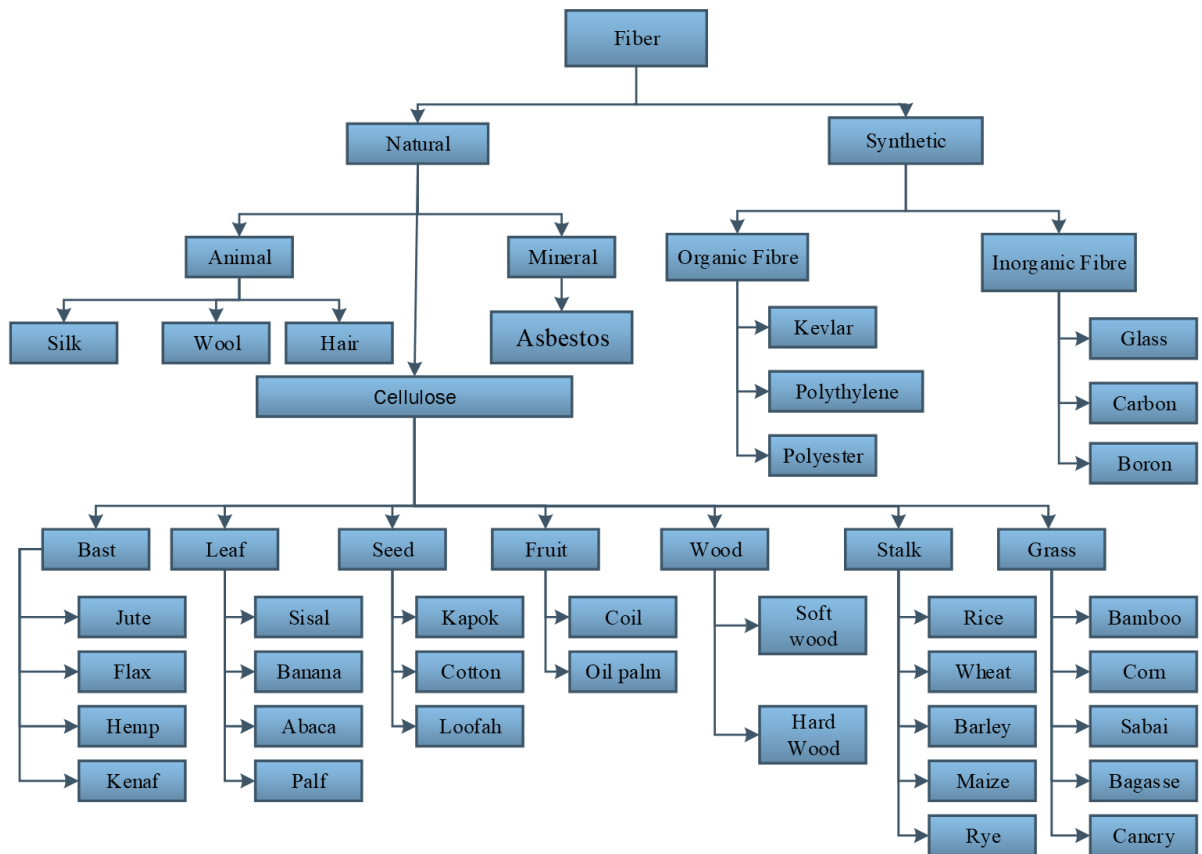
This improvement in properties is usually achieved by embedding reinforcement in the matrix, using natural fibers or synthetic fibers, or a combination of both. Such composite materials are being used in various applications, like aerospace, automotive, marine, infrastructure, military, aircraft, sports equipment, and construction [6]. Their superior properties and numerous applications in various fields have made them a better alternative to metals or alloys.

1.3 Categories of Composite Materials

Composite materials are generally of two kinds.

1. Natural composite
2. Artificial or synthetic composite

Wood is an example of a natural composite material. It is abundantly found in the environment. It comprises of lignin and cellulose. Artificial composite materials, on the other hand, are artificially fabricated with the combination of two or more material together. In the recent years, numerous composite materials have been produced with the advancement of technology.



1.4 Types of Fiber

It is seen from the chart that fibers are mainly of two kinds, natural and synthetic or artificial. Natural fibers again can be classified into three different kinds, animal, cellulose and mineral, jute being an example of bast type cellulose fibers. Among synthetic fibers, there are the organic fibers like Kevlar, Polythylene and the inorganic ones like glass and carbon. A fine composite material can be created with the combination of natural and synthetic fiber.

1.5 Thesis Outline

The fabrication, experimental and numerical analysis of a composite material created with four plies of carbon and six plies of jute has been presented in this thesis work. The elevated

mechanical properties of the newly created composite of various stacking sequence have been determined. The thesis work has been divided into 5 chapters. In the first chapter, a brief introduction to the subject was provided along with the different categories and types of fibers. Our research aims and objectives were speculated. In the second chapter, a detailed review of previous literary works related to the use of natural and synthetic fibers was provided. The detailed experimental procedure and numerical methodologies were provided in chapter 3. Chapter 3 also talks about the materials used in the fabrication, the stacking sequences followed and the fabrication method of the composite laminates, including the VARI process. A general introduction to the finite element analysis along with the detailed simulation steps for both the flexural and tensile tests were also provided in this chapter. Chapter 4 comprises of the results of the experimental tests and numerical simulation and provides relevant discussions. Finally, an overall conclusion of the research work was provided in chapter 5.

Chapter 2. Literature Review

A number of different studies were conducted on a wide variety of composite materials over the past few years, which describe the change in the mechanical properties of composites depending on varying parameters.

Ramesh et al. conducted tensile and flexural tests on composites he produced with sisal, jute, and glass fibre [8]. Results revealed that sisal fibre composite has a higher ultimate tensile strength than jute fibre composite. However, neither of them have a higher tensile strength than glass fibre composite. Results of Morton et al. also revealed that glass fibre composites has the highest tensile strength. Among the natural fibres, they found out that flax fibre had better properties compared to hemp and jute [9]. Dhakal evaluated some other mechanical properties of composite materials formed of flax fibre, carbon fibre, and a conjunction of both. From the results of the tests, a development in fractural strain is noticed in the flax/carbon fibre hybrid composite when compared to carbon fiber composites [10]. The naturally poorer strength of flax fibers causes a reduction in the flexural strength of carbon composites.

A number of researchers carried out experiments on the effect of stacking sequence of individual laminas on the tensile and flexural strength of hybrid composites [11]–[13]. Outcomes of the experiments revealed that the flexural strength is elevated by stacking the comparatively stronger fibre on the outer side. Results also exhibited an increase in tensile strength with the increase of the fibre density in the hybrid composite.

A.K. Bledzki, J. Gassan studied the influence of coupling agents on the mechanical properties of composites reinforced with cellulose based fibres. He found out that such properties of composites are mainly influenced by the adhesion between matrix and fibres [14].

The mechanical properties of annual fibre/PP composites were also studied by several researchers [15]–[17]. The properties of these materials can reach a satisfying level by increasing the compatibility between the fibre and the matrix using, for example, maleic anhydride (MAH) modified PP.

The study about the impact behavior of natural fibre reinforced composites is still developing. Pavithran et al. determined the fracture energies for sisal fibre-polyester and pineapple fibre-polyester composites (fibre content of approximately 50 vol. %) in a Charpy-impact-test. With an exception of coconut-fibre-polyester composites, they found an increase in fracture energy accompanied by increasing fiber toughness, determined by the stress–strain diagram of the fibers [18].

A study was undertaken by Hakim et al. to understand the effects of porosity on mechanical behavior and material properties of carbon fibre-reinforced polymer composite samples fabricated using hand lay-up. They observed that fabricating polymer composite samples using manufacturing processes such as pultrusion, vacuum infusion and autoclave molding yields better results than the traditional hand-layout method [19].

Subhankar Biswas analyzed the effect of ply angle in jute epoxy resin composite material and observed better tensile properties with 0-45-90-45-0 angles within the plies. He also compared the tensile strengths of woven and nonwoven jute-polypropylene composites and found the woven one to have higher tensile strength (~ 69 MPa) than the non-woven one (~ 49 MPa) when 0-90-0 fibre orientation was used. The value of Young's modulus did not fluctuate much. Comparing jute and bamboo fibres, jute fibre shows almost two times higher transverse flexural stress than that of bamboo fibres. It also shows better results for flexural modulus compared to bamboo fibre. This is due to their interfacial bonding, where jute fibres have more compact structure and broader surface area compared to bamboo fibre [20].

Researches conducted by Ismail et al. revealed that tensile strengths of rice husk fibre–polypropylene composites slightly decreased with increasing filler loading [6–8] and presented the peak value at a crosshead speed of 500 [21]–[23] .

Selver et al. researched on some of the physical properties of flax/glass and Jute/glass hybrid composite by altering the stacking sequence. The samples were formed by an infusion process. When the percentages of jute and flax fibre was augmented, and the glass fibre was added to the external layers, the transverse rupture strength was seen to have improved [24].

Jesthi et al. found that the flexural strength of the composite was upgraded more than the normal glass fibre reinforced polymer composite [25]. A number of researches are conducted on hybrid composites with the mixture of glass, Kevlar and carbon fibre as

artificial fibre and flax seed, hemp, banana skin, jute and so on as a regular fibre [8], [26]–[30].

The effect of fibre angles and placing sequence on hybrid composites made of jute/carbon epoxy is still being developed.

Studies of Vinšová et.al stated the method of obtaining different elastic engineering constants of the materials, eg. Young's modulus and Poisson's ratio (E_1 , E_2 and ν_{12}) of a woven lamina required for simulation of thick laminates by conducting thin laminate tensile tests [31].

Nirbhay et al. experimentally tested the tensile properties of carbon fibre reinforced composites consisting of fifteen plies. He numerically modeled them using ABAQUS to determine the tensile strength and strain at failure. The parametric study revealed that the composite strength of composite is depended on the ply orientation of reinforcing materials [32].

Experimental and numerical approaches (using ABAQUS) were made by Wang et al. to evaluate the Young's modulus of unidirectional fibre reinforced composites along different fibre orientations. The results of both approaches were found to be linear [33].

Experimental and numerical analysis of composite materials is a widely investigated topic and many research works are available in the literature. However, the topic is vast and still

has scope for more investigations and development. This paper focuses on the experimental and numerical investigation of the flexural and tensile behavior of carbon/jute epoxy composites. It aims to validate the experimental results of the mechanical properties by numerical analyses.

Chapter 3. Experimental Procedure and Numerical Methodology

3.1 Materials and Fabrication

The current world of composite materials observes an increase of interest in using natural fiber-reinforced composites in all aspects, starting from industrial applications to research purposes. Natural fibers are abundant, renewable, recyclable to great extent, cheap and biodegradable. Sustainability, biodegradability, and environmental friendliness are some of the important properties that advance the growth of natural fibre composites. Applications of natural fibres in various sectors have increased compared to that of synthetic fibres for these properties. However, due to data limitation of mechanical properties of different hybrid composites, natural fibre reinforced composites are only used in non-structural cases. Further improvement is needed in this area due to lack of sufficient scientific literature. This makes mechanical properties of composite materials a promising field for scientific research. This thesis work focuses on the mechanical properties of the composite laminates and the effect of the stacking sequence.

3.1.1 Materials

In this research work, unidirectional woven jute fiber fabrics along with carbon fiber had been used to produce the composite material. Epoxy resin and hardener were used to fabricate the composites of various stacking sequences to perform our experiments.

3.1.1.1 Jute Fiber

Jute is low cost, eco-friendly and extensively available in the textile fields of Bangladesh. It has low density along with relatively stiff and strong behavior. For these reasons, in most cases, jute is a suitable substitute of comparatively more expensive and non-renewable synthetic fibers, like glass. It has an aspect ratio (ratio of length to diameter) of greater than 1000, allowing it to be easier to weave. The chemical and physical properties of jute fiber are shown in *Table 3-1* and *Table 3-2*.

Jute fiber fabrics of unidirectional characteristics, shown in *Figure 3.1* have been used to produce the composite material. Bangladesh Jute Research Institute (BJRI), Bangladesh supplied with the jute fiber for the fabrication of the composite material for the research.



Figure 3.1 Jute fiber fabric

Table 3-1 Chemical configuration of jute [34]

Component	Content (%)
Cellulose	64.4
Hemicellulose	12.0
Pectin	0.2
Lignin	11.8
Water soluble	1.1
Wax	0.5
Water	10.0

Table 3-2 Properties of jute fiber [34]

Material	Weaving Pattern	Tensile Strength (MPa)	Modulus of Elasticity (GPa)	Thickness of a single fiber(mm)	GSM	Density g/cm³
Jute	Unidirectional	400	12	0.6	500	1.5

3.1.1.2 Carbon Fiber

When used in a composite structure, carbon fiber can offer enhanced strength and stiffness in a composite material. These properties can further be elevated with appropriate stacking sequences. Like jute, unidirectional carbon fibers have been used in this research. It was purchased from Easy Composites, England. In **Figure 3.2**, a sample picture of UD woven carbon fiber fabric has been shown.



Figure 3.2 Carbon fiber fabric

Unidirectional carbon fiber fabric is a type of carbon reinforcement where the fabric is non-woven. Here, all fibers are set in a single, parallel direction. This form of fabric ensures zero gaps between fiber threads. The fibers are lay smooth and flat, and there is no cross-section weave dividing the fiber strength in half with another direction.

The ultimate tensile strength of composite materials made with unidirectional carbon fibers is the direction of the fiber grains. Hence, composites that use carbon fiber fabric that are unidirectional provide maximum strength possible in the direction of the fiber and are incredibly stiff. This property of directional strength makes the composite an isotropic material, similar to wood.

Multidirectional isotropic behaviour can be achieved by stacking unidirectional plies at different angles. This produces a completely new composite material with anisotropic physical and mechanical properties [35].

The properties of the carbon fiber that has been used for this research is given below in *Table 3-3*.

Table 3-3 Properties of carbon fiber [34]

Material	Weaving Pattern	Tensile Strength (MPa)	Modulus of Elasticity (GPa)	Thickness of a single fiber(mm)	GSM	Density g/cm³
Carbon	Unidirectional	3500	240	0.4	300	1.8

3.1.1.3 Matrix

The most important aspect while selecting a resin is viscosity. Epoxy LY556 has a low viscosity that aids the infusion process and has been used by the other researchers as well [36], [37]. Choosing the correct hardener is also equally important. While selecting hardener it is important to monitor the hardening time while mixing it with the resin. If the hardening time is fast, the mixture might get immensely dense at a point blocking the flow through the tube. So in accordance with the resin Araldite HY951 has been selected as the hardener.

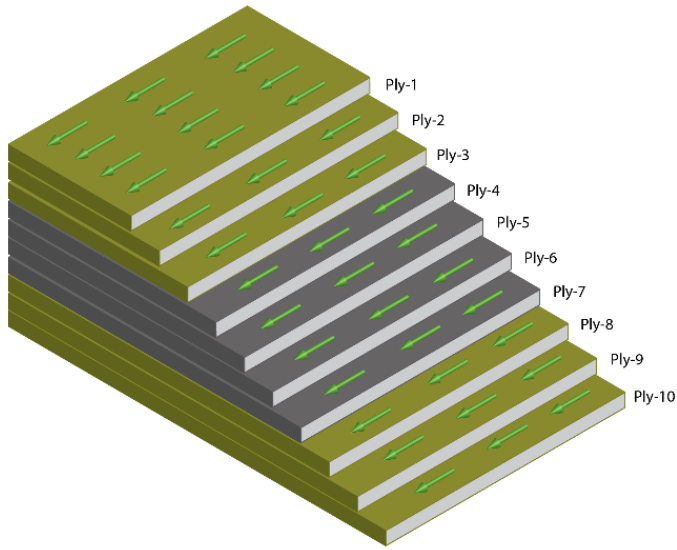
These were acquired from obtained from Fix-it Industries, Bangladesh. A fixed ratio of 10:1 by weight was used to mix the epoxy resin with the hardener.

The following outstanding properties make epoxy resin and hardener a great matrix: have the following outstanding properties:

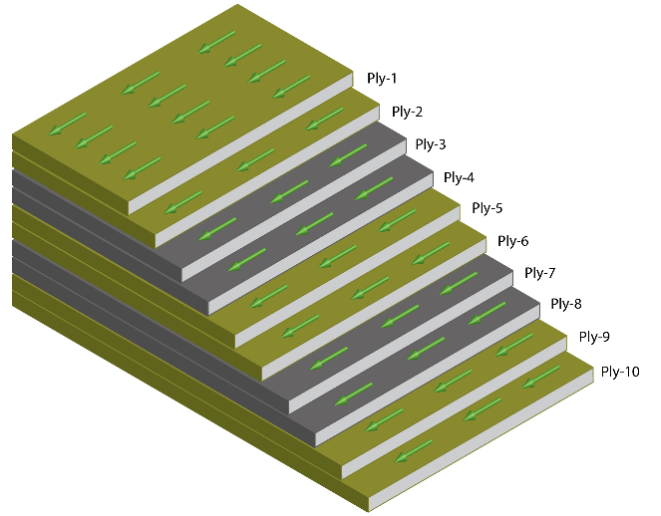
- Outstanding adhesion to various materials
- Immense strength, toughness resistance
- Brilliant resistance to chemical corrosion and moisture
- Excellent mechanical and electrical properties
- Odourless, tasteless and entirely nontoxic.
- Insignificant shrinkage

3.1.2 Stacking sequence

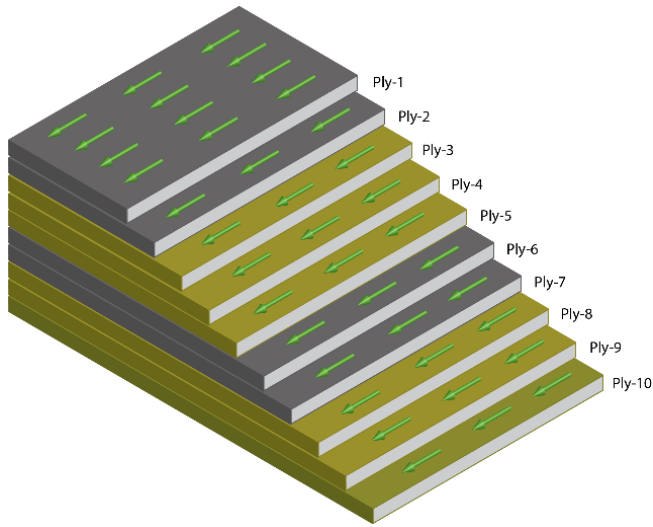
Each specimen constituted of six plies of jute fiber and four plies of carbon fiber. Four different stacking sequences were used to test its effect on the tensile and flexural behavior of the composites. The chosen stacking sequences are presented in *Figure 3.3*.



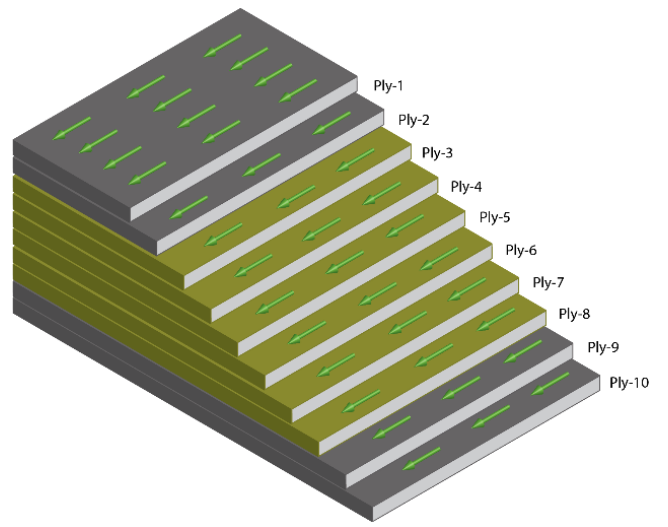
(a) $J_3C_4J_3$



(b) $J_2C_2J_2C_2J_2$



(c) $C_2J_3C_2J_3$



(d) $C_2J_6C_2$

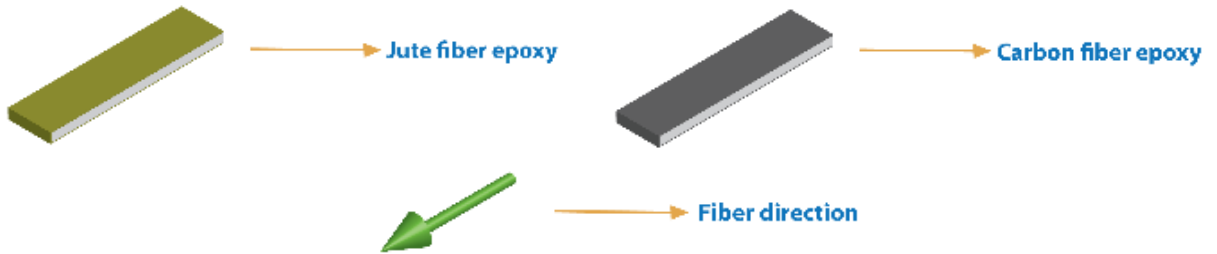


Figure 3.3 Stacking Sequences

Each of the composite samples are constructed using VARI process, which is described, in the section 3.1.3.

3.1.3 Fabrication Method of Composite Laminates

To facilitate the manufacturing process of the composite material Vacuum Assisted Resin Infusion kit was ordered online from easy composite, England.

3.1.3.1 Vacuum Assisted Resin Infusion Process

The hybrid samples of carbon and jute fiber were fabricated by a process called the ‘Vacuum Assisted Resin Infusion Process’. The Vacuum Assisted Resin Infusion (VARI) process is a technique that uses vacuum pressure to drive resin into a laminate. This is a widely accepted process in the field of composite research for having a number of advantages over other ones. Composites fabricated using VARI usually show better mechanical properties, such as more strength and less void formation, involve a cleaner process with better fiber to resin ratio, less resin waste and consistent resin usage, and can be molded to complex structures compared to composites fabricated by the traditional hand layup or vacuum bagging processes.

The VARI process is carried out by using the following steps and equipment:

1. Creating the mold, selecting reinforcement and flow media, and stacking the fabric
2. Sealing the mold and creating vacuum using sealant tape and vacuum pump, respectively
3. Catalyzing the epoxy resin in the resin storage

4. Degassing the mold
5. Infusion of resin through the resin pipe
6. Curing the fabricated plies

To aid the vacuum infusion process, an infusion mesh and vacuum bagging film were added sequentially over the stacked plies, along with a sealant tape taped around the setup. A spiral resin pipe was inserted to the mold through which the matrix was fed. An illustration of the whole setup is given in *Figure 3.4*.

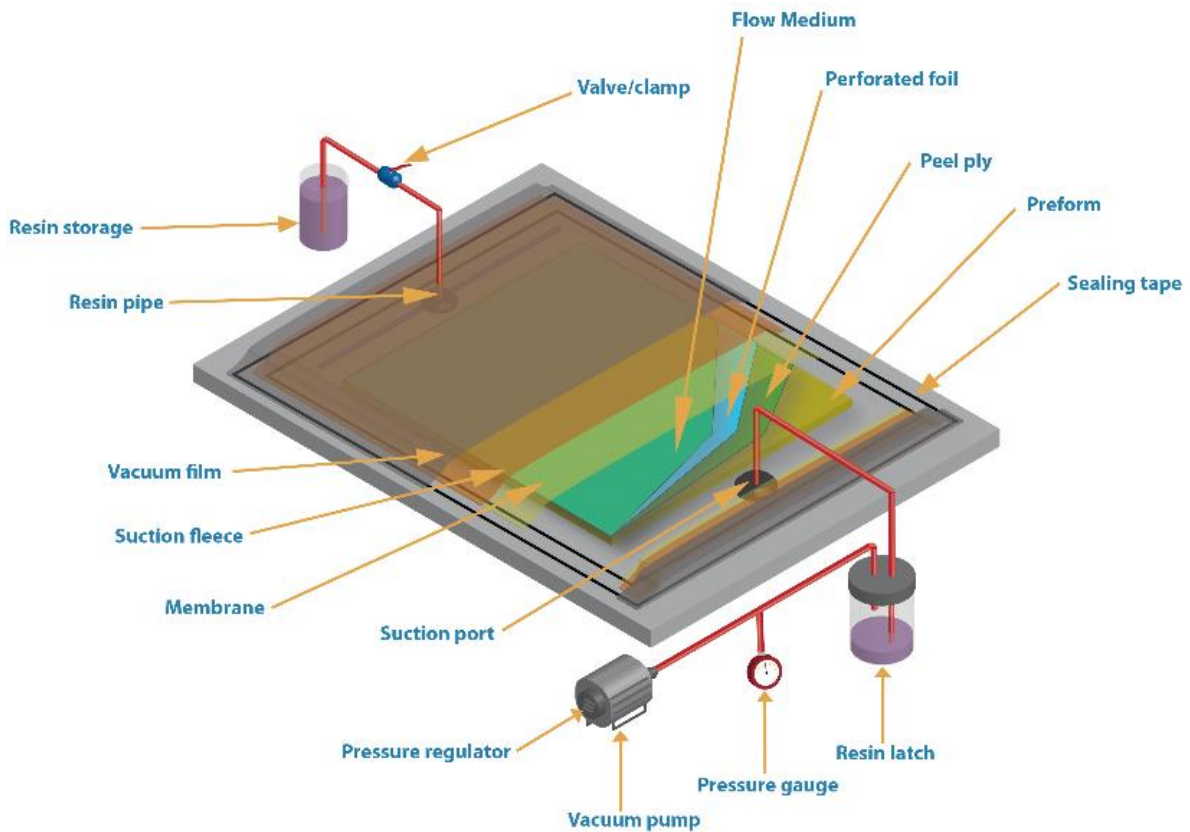


Figure 3.4 Schematic Diagram of Vacuum Assisted Resin Infusion Process

The vacuum infusion process is established by the setting up the following equipment: a vacuum pump, a professional resin infusion catch-pot and a resin infusion starter kit which

includes vacuum bagging gum, PVC vacuum hose, resin infusion line clamp, resin infusion spiral medium, flow coil, resin infusion silicon connector and vacuum bagging film. All this are set up to complete the initial preparation for the vacuum infusion process. This will be followed by the step-by-step infusion procedure to achieve the final composite material.

3.1.3.2 Infusion Procedure

The following steps were followed to infuse the specimen with epoxy-based resin:

Preparation of mould:

Initially, the mold was prepared where the samples will be placed for infusion. A rigid mold helps in acquiring the best quality samples. Here, an acrylic glass plate have been used as the mold for the fabricating of the composite samples. It has enough flanges to put the vacuum sealant tape and vacuum bagging film around the sample without any interference.

In *Figure 3.5* a picture of mould has been shown.

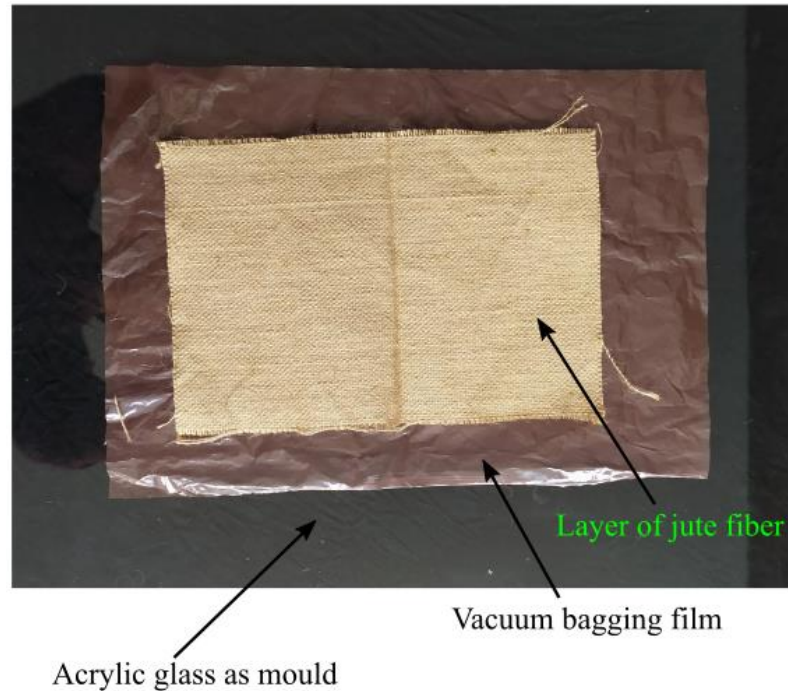


Figure 3.5 Setup of mould with composite layer

After selection, the mold was cleaned thoroughly before moving to the next step.

Adding Vacuum Bag Film on the Mould:

The vacuum bagging film of the size of the plate had been cut out and placed on the glass plate keeping the flange area out. It acts as the separator between the resin flow and acrylic and ensures the proper removal of the composite from the acrylic layer. If a vacuum bagging film is not used, the composite will permanently stick to the acrylic. Generally, a plastic bag is used for this purpose.

From *Figure 3.5* a layer of vacuum bagging film has been illustrated.

Placement of fiber, peel ply and infusion mesh:

The sample is then carefully placed on top of the vacuum bagging film. It is crucial to ensure that the layers were aligned in a proper uniform way. The composite is then placed in the middle of the acrylic. Enough room is kept for the resin to flow across the sample. After that, a layer of peel ply is placed over the composite layer. Finally goes a layer of infusion mesh. The infusion mesh has been illustrated in *Figure 3.6*.

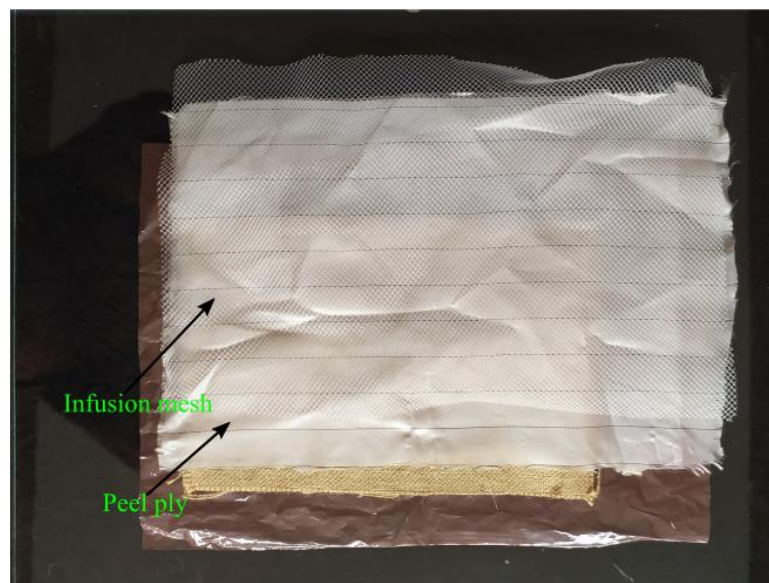


Figure 3.6 Placement of fiber, peel ply and infusion mesh on the composite layer

Double-sided tapes were used to attach the peel ply and infusion mesh with the mold perfectly.

Installation of infusion spiral tube, silicon connector and sealant tape:

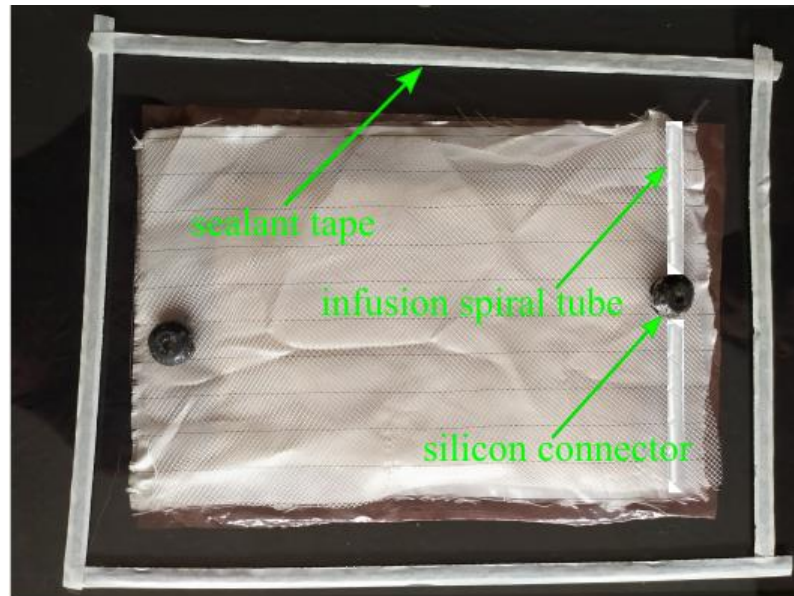


Figure 3.7 Installation of infusion spiral tube, silicon connector and sealant tape

Resin is passed from the source bucket to the composite sample through an infusion spiral tube. The tube is constructed in a way that resin can enter and leave through its entire length. This is ideal for the in-bag vacuuming feed lines. The spiral tube was attached to the resin infusion silicon connector. It was then put at one end of the prepared bed. When not stretched, the spiral tubes tend to straighten up. Hence, double-sided tape was used to attach it with the infusion mesh. The silicon connector has a four-way channel that allows the resin to flow smoothly through the spiral tubes. Another silicon connector is attached to the other side of the bed to draw out any excess resin inside the vacuum bag. A vacuum hose of proper diameter can also be used. The setup of infusion spiral tube, silicon connector and sealant tape is shown in *Figure 3.7*.

Sealing:

The vacuum bag is created using a vacuum seal. Firstly, the sealant tape is attached (*Figure 3.7*) around the flange area to keep all dry materials at the centre. The vacuum film is then carefully attached to the sealant tape at all sides. It was ensured that no air entered and no air leak was formed during the whole bagging placement procedure.

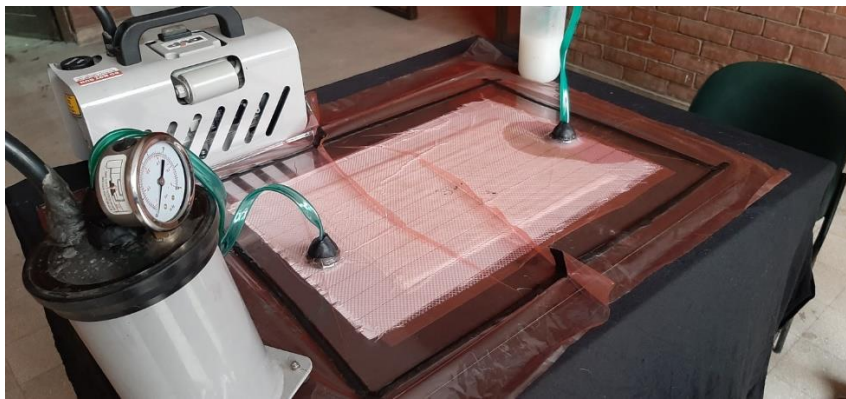


Figure 3.8 Vacuum-Bagging Procedure

In this step a PVC vacuum hose is attached to the resin infusion catch-pot. A catch pot was used to store the excess resin. The vacuum hose is inserted through the tight infusion line, called the gland nut to gather the excess resin in the catch pot. Again, sealant tapes were used at both ends to avoid any kind of leakage. A second vacuum hose is entered into the silicon connector that holds the spiral tubes. The whole setup for VARI process has been shown in *Figure 3.8*.

After completing the setup, the vacuum pump was turned on and air was sucked out of the vacuum bag shortly. The pressure was monitored for 30 minutes to check for air leakages in the whole setup. In case of the presence of a leakage, the pressure reading of the pressure gauge will increase. This checking is important as even a small leakage can hamper the infusion process. After inspection, no leakage was found. The pump was turned off when the pressure inside the vacuum bag reached **-1 bar**.

After proper inspection, the clamp was opened to let the mixture of resin and hardener flow through the pipe. The vacuum inside the chamber sucks in the resin-hardener mixture and transfers it throughout the whole layout. When the infusion is done, the excess resin-hardener mixture travels through to tube connected to the catch pot.

The composite was then cured for 24 hours. After curing, the setup was disassembled and the completed composite was freed out from it.

3.2 Flexural Test

3.2.1 Experimental Procedure

The capability of laminated composites to withstand the bending before reaching the breaking point is defined as the flexural strength [38]. It represents the highest stress experienced within the material at its moment of rupture. When a material is bent, only the fibers at the outermost layers are at the largest stress. Therefore, the flexural strength will be determined by the strength of the intact fibers if those fibers are free from defects. Hence, for the same material, it is common to have a higher flexural strength than tensile strength.

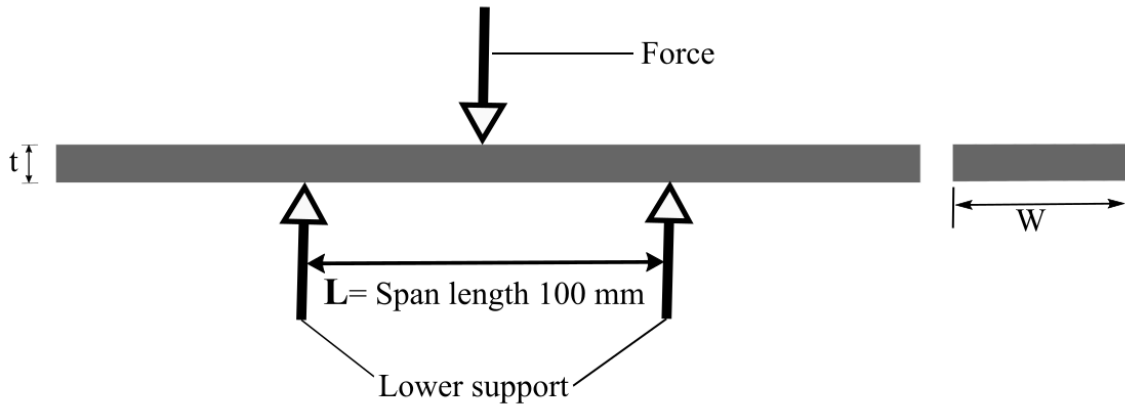


Figure 3.9 Specimen dimension for flexural test

In this experiment, the flexural test has been conducted as per ASTM D 790 [39]. The flexural, or three-point bending test was performed as per the ASTM D 790 standards. The sample had a length of 250mm and a width of 25mm shown in **Figure 3.9**. Universal Testing Machine (UTM), shown in **Figure 3.10**, was used at a cross-head speed of 5mm/min. The UTM that has been used in this research can measure and store the force automatically in different usable format. A three-point bending fixture was used with a span length of 100 mm in all samples. Tests were carried out at a room temperature of 30°C with an average humidity of 60%. The deflection of the specimen was measured upon the application of load. The flexural load and displacement were recorded for five samples of each stacking sequence and an average value was considered for each.



Figure 3.10 Flexural testing equipment with the specimen

Equation (3.2.1) has been used to calculate the maximum flexural stress (MPa)

$$\sigma_f = \frac{3PL}{2bd^2} \dots\dots\dots (3.2.1)$$

In this equation (3.2.1), d (mm) is the depth and b (mm) is the width of the sample. L (mm) denotes the span-length, and P (N) is the recorded total flexural load applied on the composite samples.

Equation (3.2.1) has been used to calculate the maximum flexural strain (%)

$$\varepsilon_f = \frac{6Dd}{L^2} \dots\dots\dots (3.2.2)$$

In this equation (3.2.2), D (mm) is the flexural displacement of the composite specimens.

3.2.2 Finite Element Analysis

Finite element analyses of the experimental data of the composite materials were carried out using ANSYS R20 software to validate the experimental results. To recreate the composite materials, ANSYS Composite Pre/Post (ACP) was used as it provides all the necessary functionalities for the analyses of layered composite structures. The setup was then connected to a Static Structural module to solve its structural problems under static loads for both the flexural and tensile tests.

The Finite Element Analyses was conducted in the following steps:

- Pre-Process: assignment of the properties of the materials, modeling of the parts, creation of mesh
- Process: input of loads and boundary conditions, solution of the assembling equations
- Post-Process: analyses, formation of different formats of the results: animations, graphs and tables.

Initially, the material properties of the plies in the composite were assigned in the engineering data module. Orthotropic material properties were used for both the carbon/epoxy and jute/epoxy plies. Several engineering constants were utilized to completely describe the 3D orthotropic laminates, as presented in *Table 3-4* [40] . The default material of structural steel was assigned to the supports and loads.

Table 3-4 Material properties in Engineering Data, ACP (Pre) [40]

Physical Parameters	Carbon/epoxy laminate	Jute/epoxy laminate
Density (kg/m ³)	1050.7	826.07
E ₁ =E ₂ (MPa)	40000	3400
E ₃ (MPa)	5077	3200
G ₁₂ (MPa)	4000	1574
G ₂₃ =G ₁₃ (MPa)	2277	1536
ν_{12}	0.045	0.08
$\nu_{23} = \nu_{13}$	0.3	0.32

3.2.2.1 Flexural Analysis

A part resembling the experimental flexural test was modeled. A rectangular ply surface of 250x25mm was created in SpaceClaim. The ply was split into four parts using the ‘split’ tool, with two lines defining the position of the supports, and one line defining the one of the loads. Two cylindrical supports and a load-cell were created for better visualization. The support-span length was given as 100mm. The load was given in the centerline of the specimen, along the width.

The model body was meshed with fine mesh using multizone quad/tri method, shown in **Figure 3.11**. The rest of the steps of the construction of the layered composite were done in

ACP Setup. Two fabrics, namely Carbon/Epoxy and Jute/Epoxy, were defined with thicknesses of 0.4mm and 0.6mm, respectively, followed by setting of the rosette. The desired sequence of the layers of plies was created in the modeling group according to the direction set in the oriented selection set.

The shell data from ACP Setup was transferred to the Static Structural stand-alone module. The model was then subjected to appropriate boundary conditions and load, and solved accordingly.

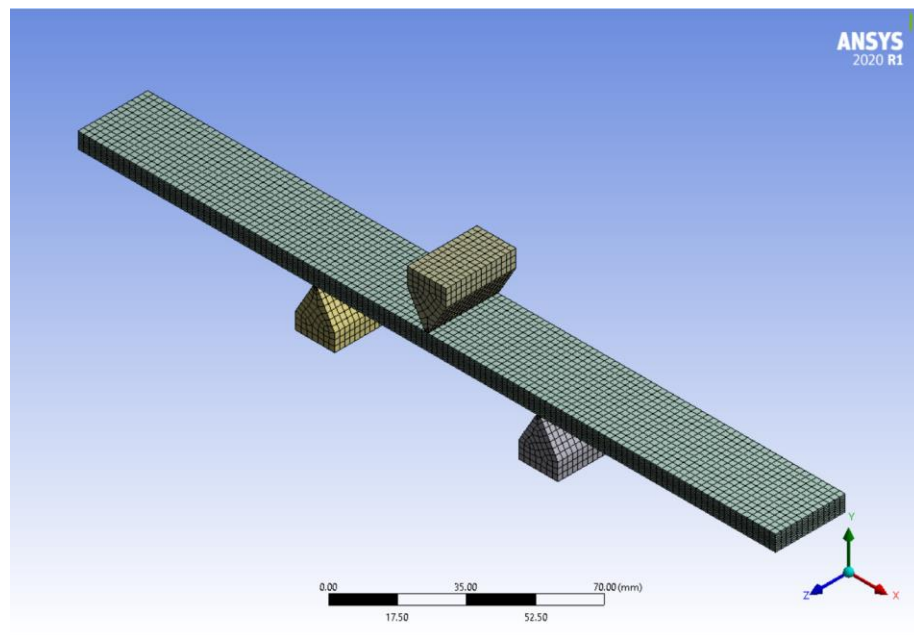


Figure 3.11 Prepared mesh of pusher, base and specimen for flexural test

3.2.2.2 Simulation Steps

ANSYS Workbench was opened and the file was saved as an archive as shown in **Figure 3.12**.

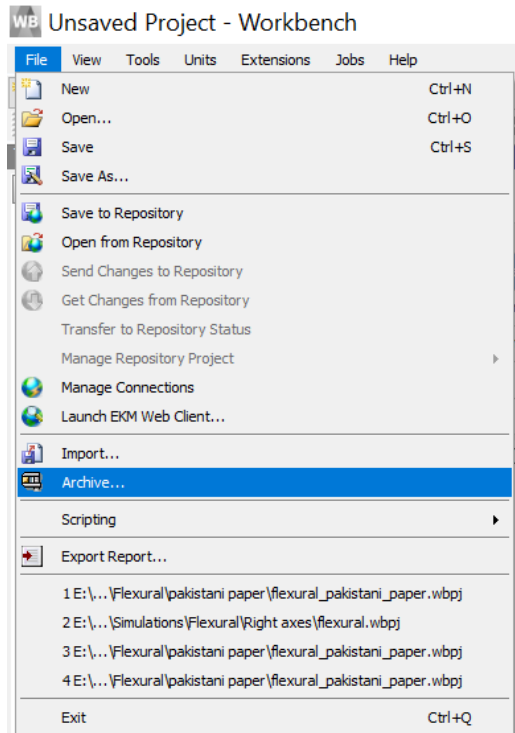


Figure 3.12 Saving file

Under ‘component systems,’ ‘ACP PrePost’ was dragged and made ‘standalone’ as shown in **Figure 3.13**.

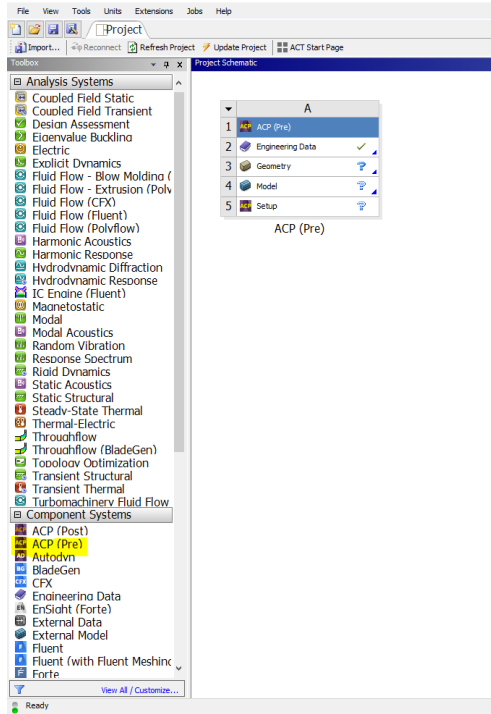


Figure 3.13 Creating ACP PrePost

The section named ‘Engineering data’ was selected.

The orthotropic properties were used in the engineering data section. Orthotropic materials can be 2D and 3D. The 2D ones have been used; meaning one of the planes is the plane of isotropy. Since ANSYS can only input data of 3D orthotropic materials, the properties of the remaining planes and axes were found using the equations 3.2.3 to 3.2.7. It has been explained as follows.

If the plane x_2 - x_3 is a plane of isotropy, there are four relationships between the 9 orthotropic constants, where the symbols have their usual meaning:

$$E_2 = E_3 \quad \dots\dots\dots (3.2.3)$$

$$G_{12} = G_{13} \quad \dots\dots\dots (3.2.4)$$

$$\nu_{12} = \nu_{13} \quad \dots\dots\dots (3.2.5)$$

$$G_{23} = E_2 / (2(1 + \nu_{23})) \dots\dots\dots (3.2.6)$$

$$E = 2G(1 + \nu) \dots\dots\dots (3.2.7)$$

Under the contents of engineering data, two new materials were named: Carbon/Epoxy and Jute/Epoxy.

The property ‘density’ was dragged and dropped from ‘physical properties’, and ‘orthotropic elasticity’ from ‘linear elastic’ to the two materials as shown **Figure 3.14**.

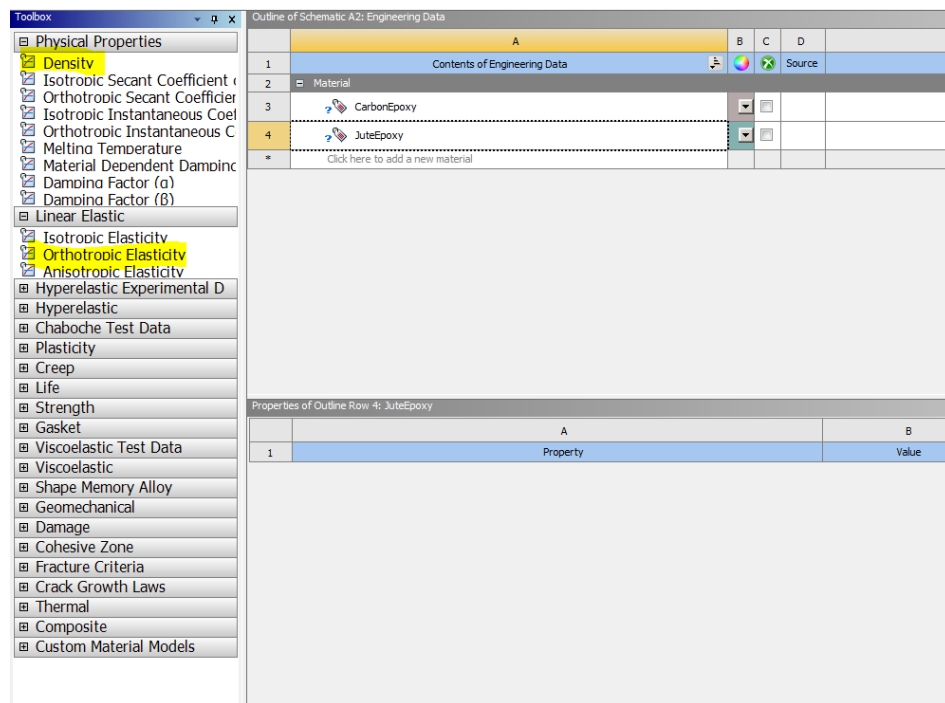


Figure 3.14 Insertion of density and elasticity

The data was entered under ‘property’ using the correct units for both the materials as shown in **Figures 3.15 and 3.16**

Contents of Engineering Data		Source	Description
1	Material		
3	CarbonEpoxy		
4	JuteEpoxy		
*	Click here to add a new material		

Properties of Outline Row 3: CarbonEpoxy			
	A	B	C
1	Property	Value	Unit
2	Material Field Variables	Table	
3	Density	1050.7	kg m ⁻³
4	Orthotropic Elasticity		
5	Young's Modulus X direction	40000	MPa
6	Young's Modulus Y direction	40000	MPa
7	Young's Modulus Z direction	5077	MPa
8	Poisson's Ratio XY	0.3	
9	Poisson's Ratio YZ	0.3	
10	Poisson's Ratio XZ	0.045	
11	Shear Modulus XY	2277	MPa
12	Shear Modulus YZ	2277	MPa
13	Shear Modulus XZ	4000	MPa

Figure 3.15 Properties of carbon/epoxy

Contents of Engineering Data		Source	Description
1	Material		
3	CarbonEpoxy		
4	JuteEpoxy		
*	Click here to add a new material		

Properties of Outline Row 4: JuteEpoxy					
	A	B	C	D	E
1	Property	Value	Unit		
2	Material Field Variables	Table			
3	Density	826.07	kg m ⁻³		
4	Orthotropic Elasticity				
5	Young's Modulus X direction	3400	MPa		
6	Young's Modulus Y direction	3400	MPa		
7	Young's Modulus Z direction	3200	MPa		
8	Poisson's Ratio XY	0.32			
9	Poisson's Ratio YZ	0.32			
10	Poisson's Ratio XZ	0.08			
11	Shear Modulus XY	1536	MPa		
12	Shear Modulus YZ	1536	MPa		
13	Shear Modulus XZ	1574	MPa		

Figure 3.16 Properties of jute/epoxy

The section named 'geometry' was then selected as shown in *Figure 3.17*.

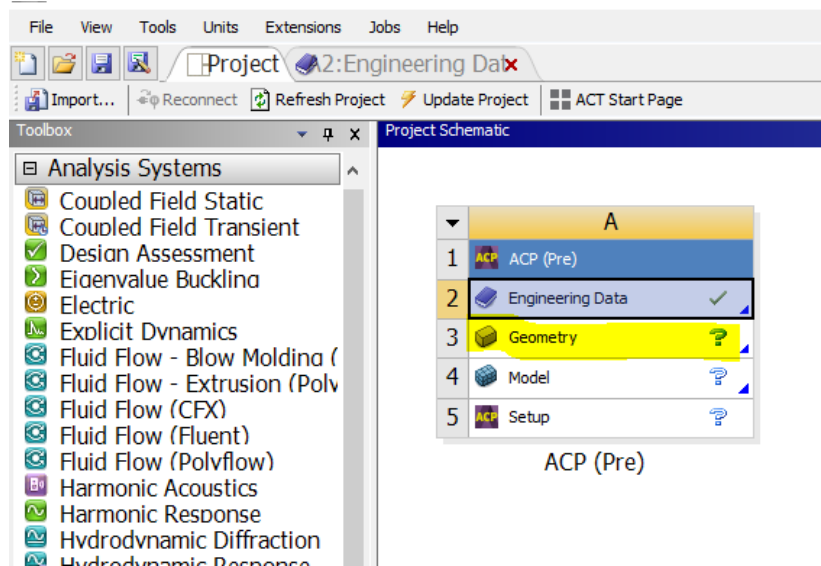


Figure 3.17 Selection of geometry

Spaceclaim was used to draw a rectangular ply surface of 250x25mm in xz plane as shown in *Figure 3.18*.

Span length was given 100mm. It is the distance between two intermediate supports for a structure.

The ply was converted to a 'surface' by using the marked entity.

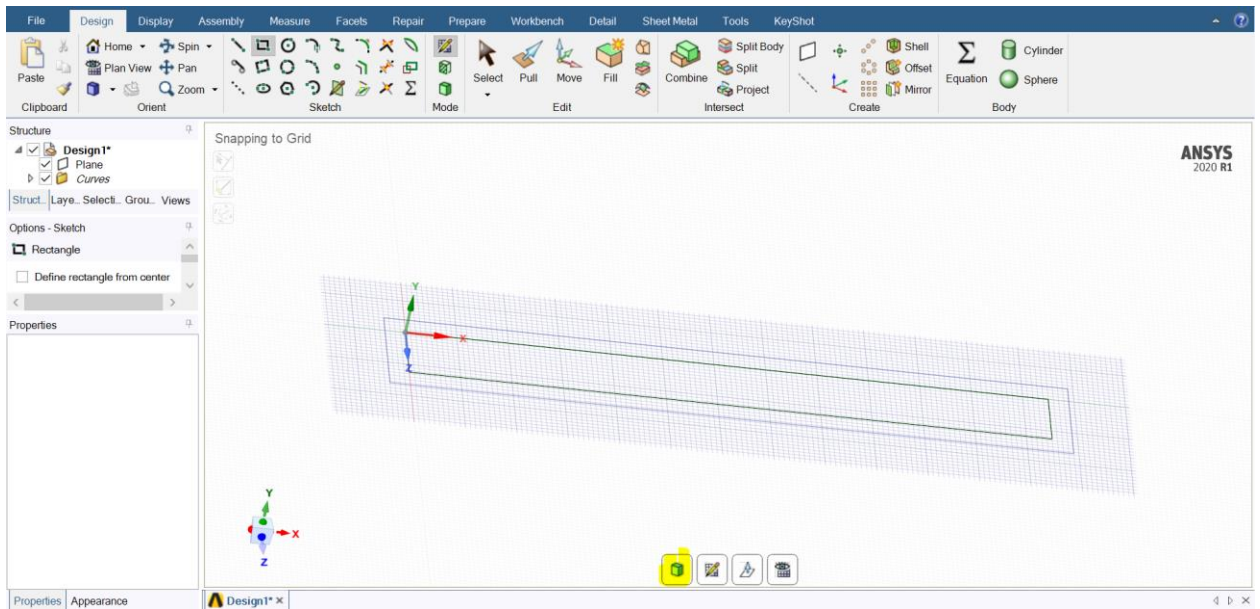


Figure 3.18 Dimension of ply

The ‘split’ option was used to split the surface into four parts. Two lines were used for supports and one line for load as shown in **Figure 3.19**.

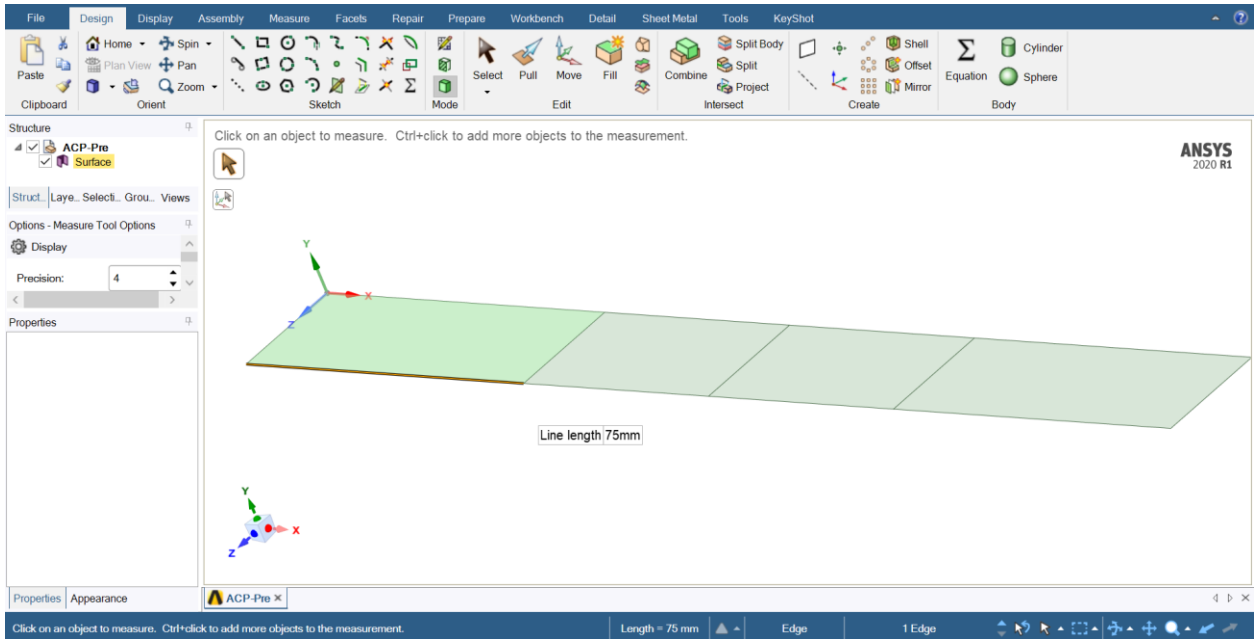


Figure 3.19 The splitting of the ply

The section named ‘mechanical model’ was selected as shown in **Figure 3.20**.

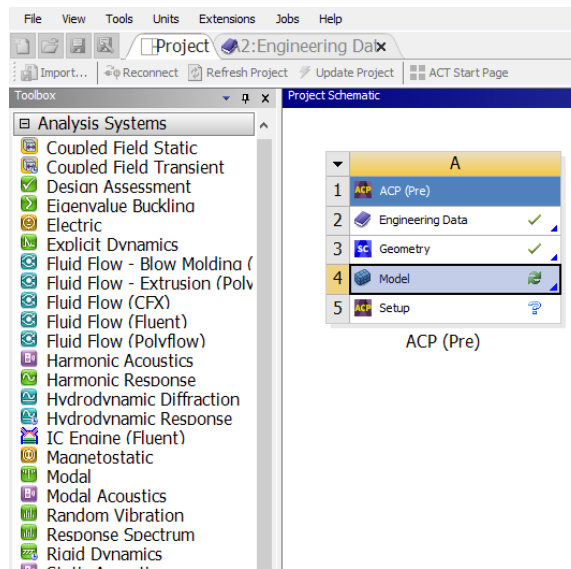


Figure 3.20 Selection of geometry

Arbitrary thickness and material in ‘geometry’ as shown in **Figure 3.21** was given.

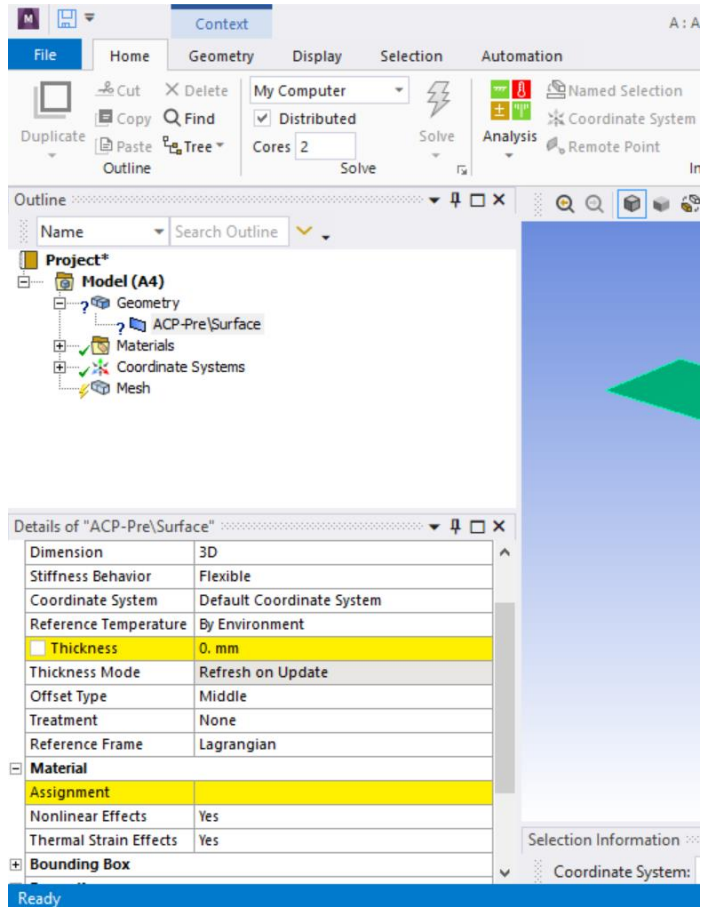


Figure 3.21 The arbitrary assignment of values of properties

In mesh, body sizing was used by selecting the ply. Then ‘hard behavior’ and suitable element size of 0.5mm was selected as shown in **Figure 3.22**.

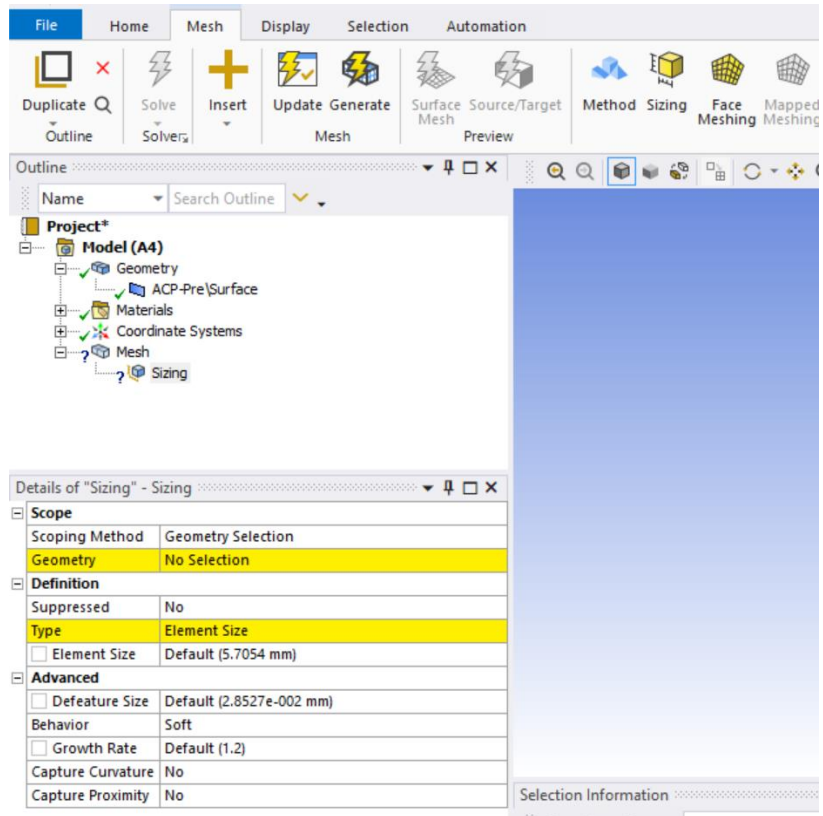


Figure 3.22 The geometry and type of ply

The option 'Method' was used by selecting the ply. The option 'multizone quad/tri' was selected as shown in *Figure 3.23*.

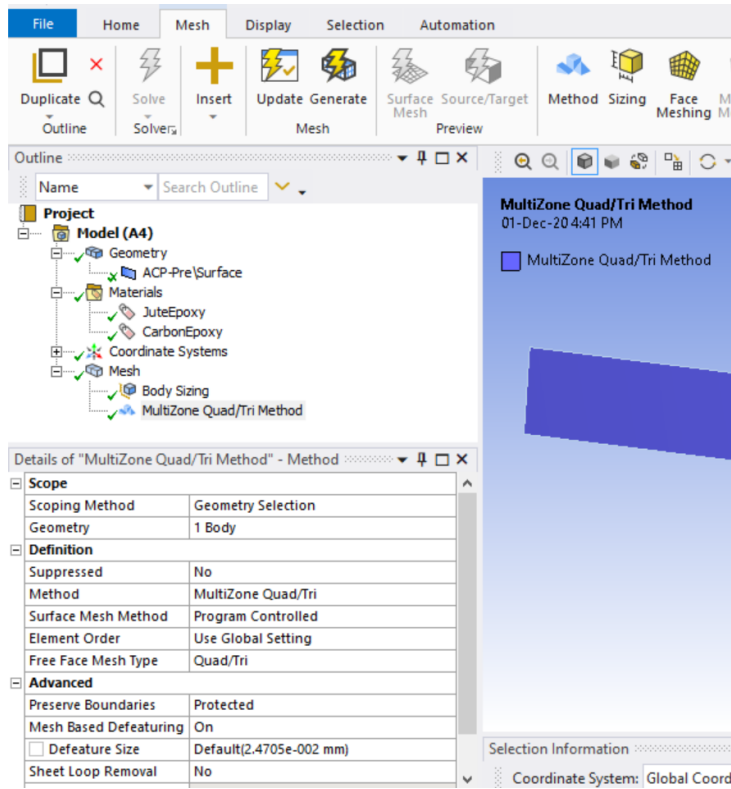


Figure 3.23 Usage of method

The option 'ACP Setup' was then selected as shown in *Figure 3.24*

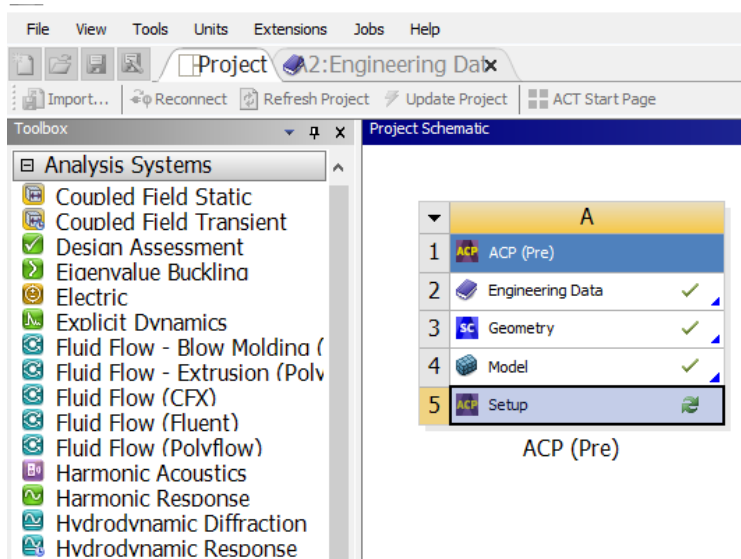


Figure 3.24 Selection of acp setup

In ACP setup, two fabrics were defined: CarbonEpoxy with a thickness of 0.5mm and JuteEpoxy with a thickness of 0.5mm as shown in *Figure 3.25*.

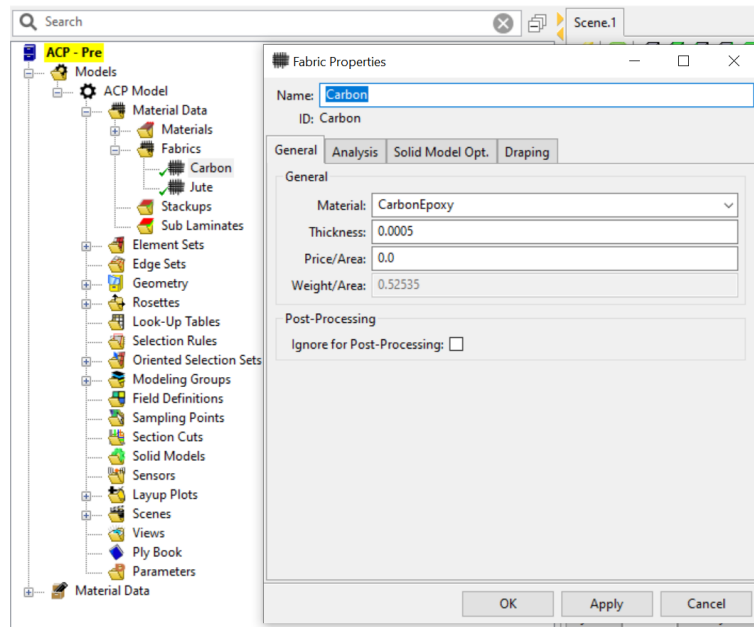


Figure 3.25 Creation of fabrics

In the rosettes, the colors red, green and blue were used for longitudinal fibre direction, transverse fibre thickness, and as the direction normal to the ply, respectively as shown in *Figure 3.26*. This was done by flipping the axes where necessary as shown in *Figure 3.27*.

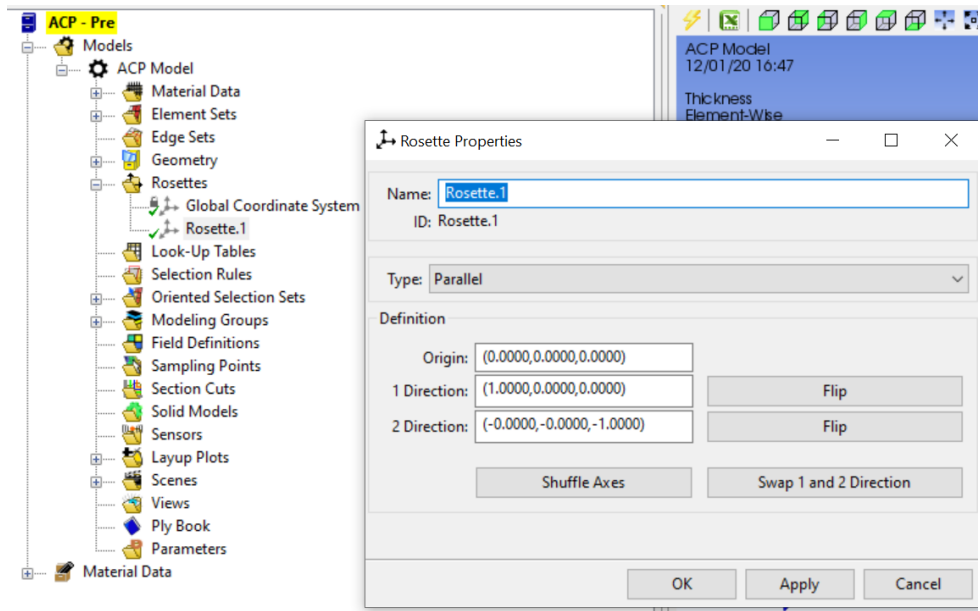


Figure 3.26 Flipping axes

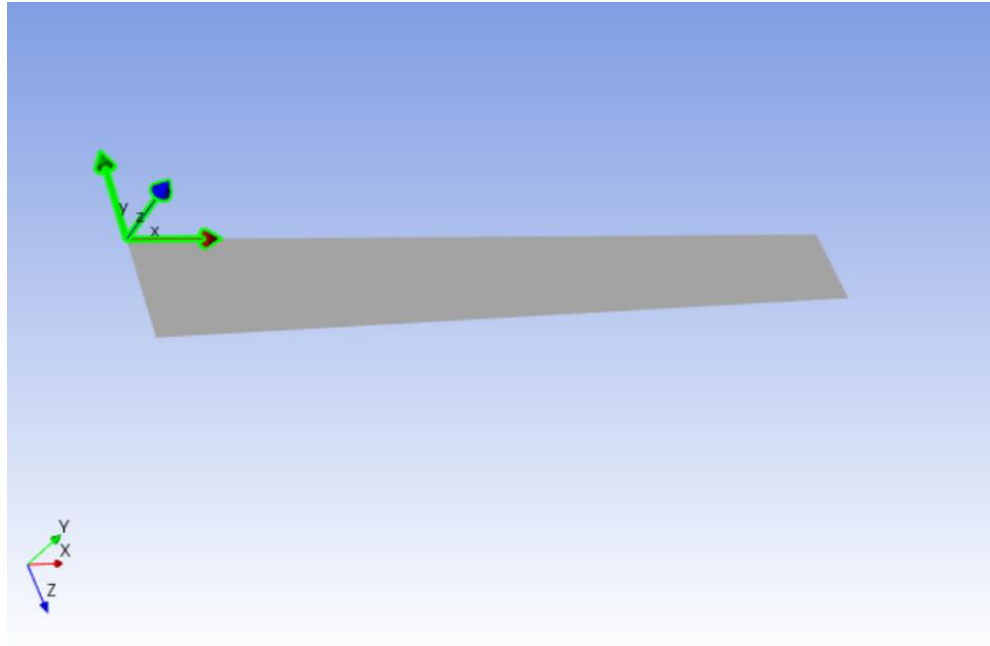


Figure 3.27 Rosette directions

In orientated selection set, the direction was selected upwards which indicates that the stacking would be done from bottom to top as shown in **Figure 3.28** by using **Figure 3.29**

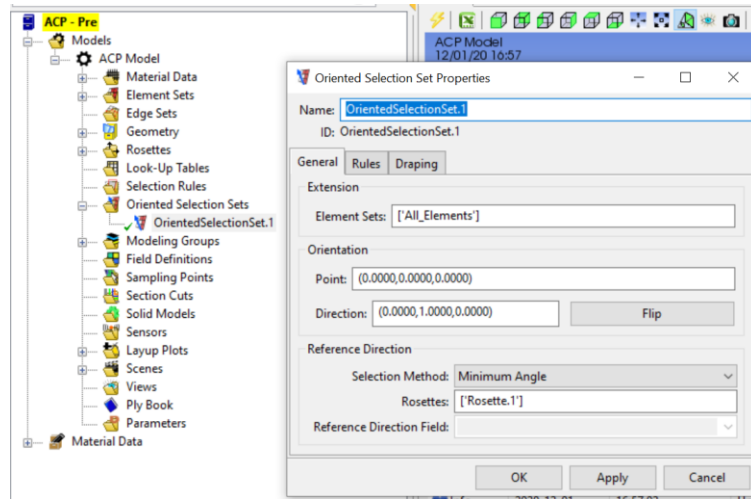


Figure 3.28 Selection of orientated selection set

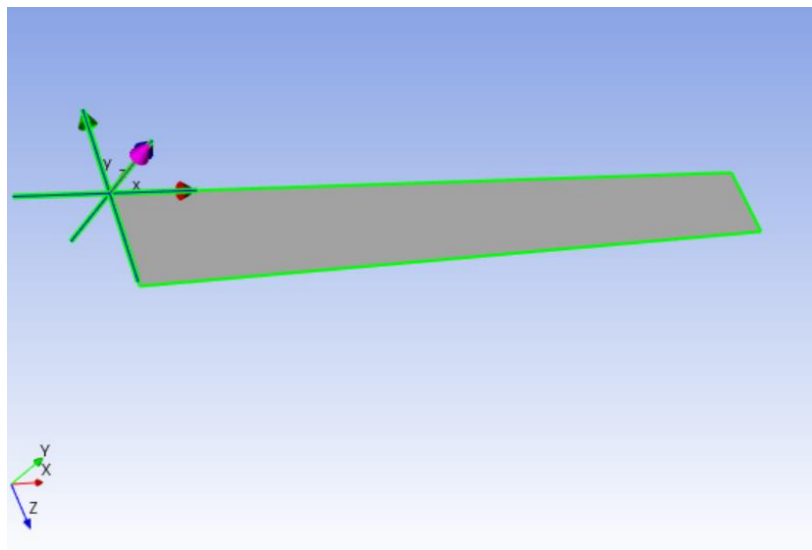


Figure 3.29 Upward direction

In the modelling group, the desired layers of plies were created, as shown in **Figure 3.30**, keeping in mind that stacking would be done from bottom to top.

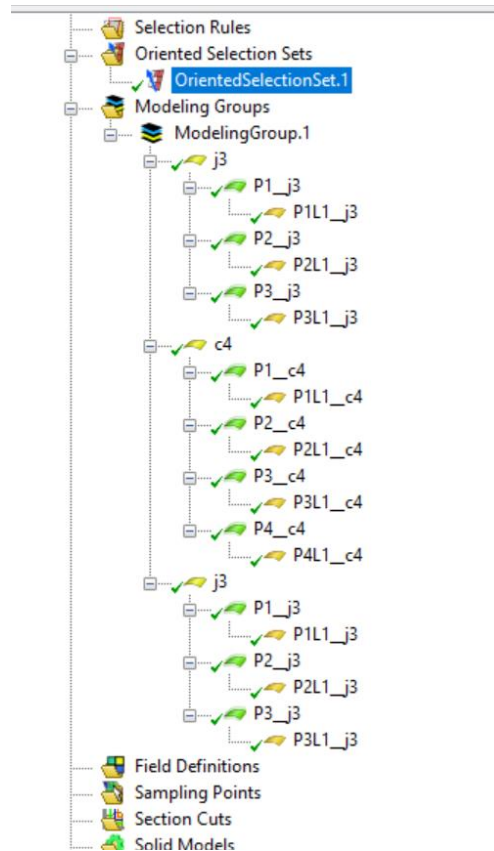


Figure 3.30 Stacking sequence

The model was not converted to a solid as the option ‘simply support’ can only be applied to the edges of a geometry.

‘Stackup’ is to be used in ‘modelling ply’ as shown in **Figure 3.31**.

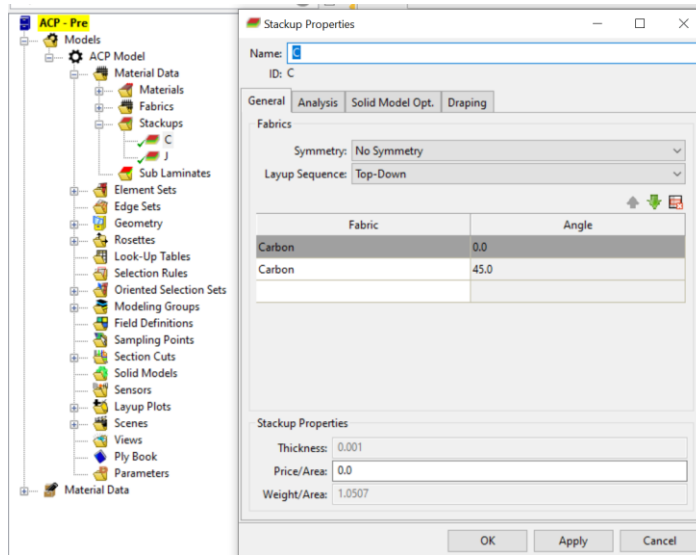


Figure 3.31 Setting of stack up

If the plies are angled, it can be done using the option called ‘stackup’ under ‘material data’.

The section ‘Static Structural’ was made standalone and the section ‘setup’ was dragged to its ‘model’ and ‘shell data’ was transferred as shown in *Figure 3.32*.

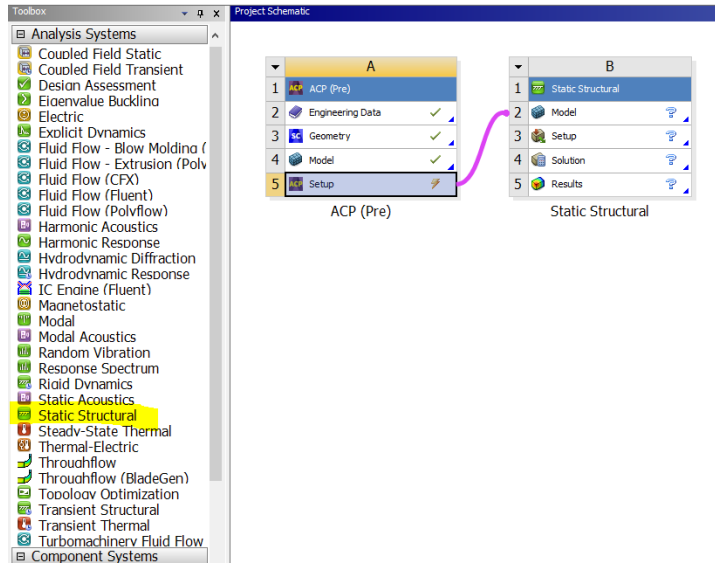


Figure 3.32 Creation of static structural

In 'model', the option 'show mesh' was deselected to work with the 'shell' form as shown in *Figure 3.33*.



Figure 3.33 Deselection of 'show mesh'

Under 'static structural', 'analysis settings' was selected. The following properties were modified as shown in *Figure 3.34*:

- Under step control, Step end time was set to 2
- Under step control, Auto time stepping was set to off

- Under step control, No. of substeps was set to 25
- Under solver controls, Solver pivot checking was set to off
- Under solver controls, Large deflection was set to on
- Under output controls, nodal forces were set to yes
- Under output controls, contact miscellaneous was set to yes

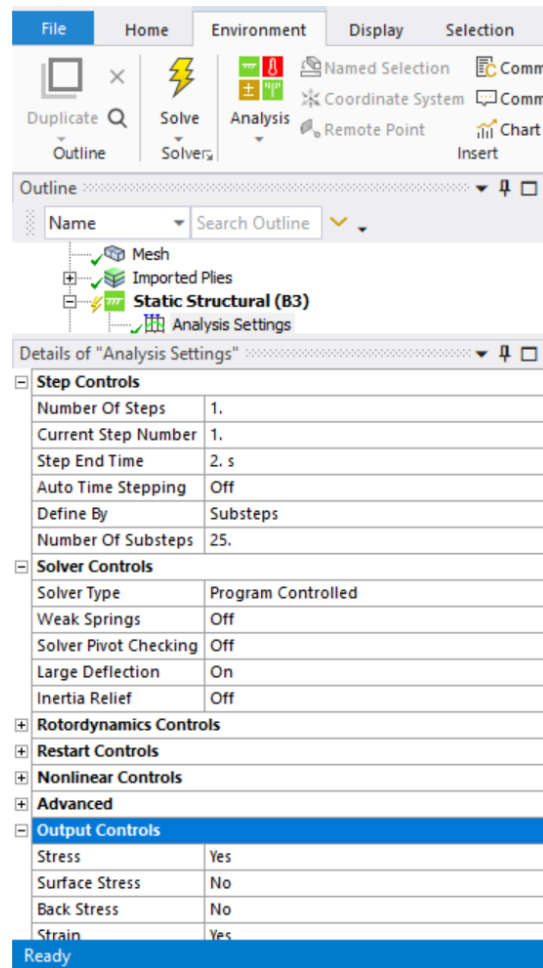


Figure 3.34 Modification of analysis settings

‘Simply support’ was inserted and added to the two span edges as shown in *Figure 3.35*.

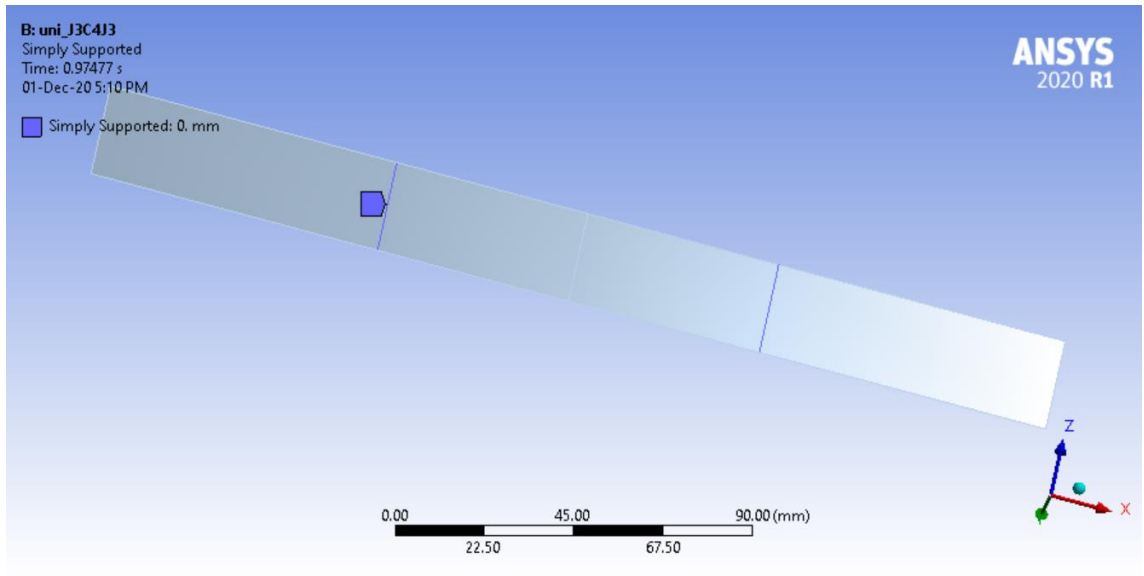


Figure 3.35 Addition of simply support

‘Force’ was inserted and added in the middle of the ply. It was defined by components as shown in *Figure 3.36*.

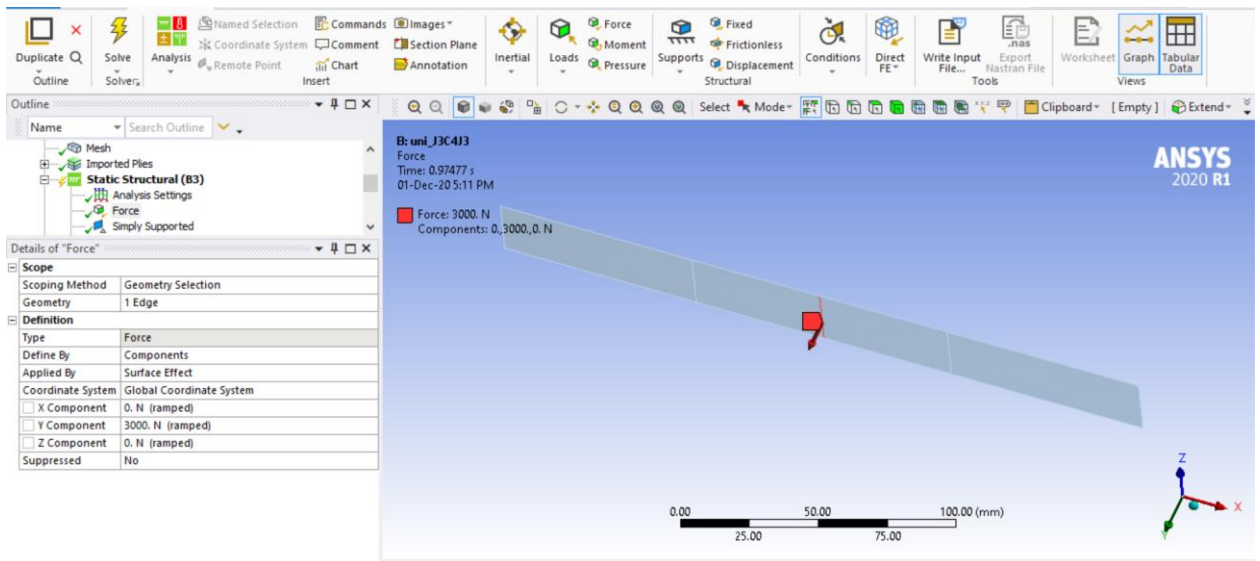


Figure 3.36 Insertion of force

‘Displacement’ was inserted as x and z being 0, and y being -6mm as shown in *Figure 3.37*.

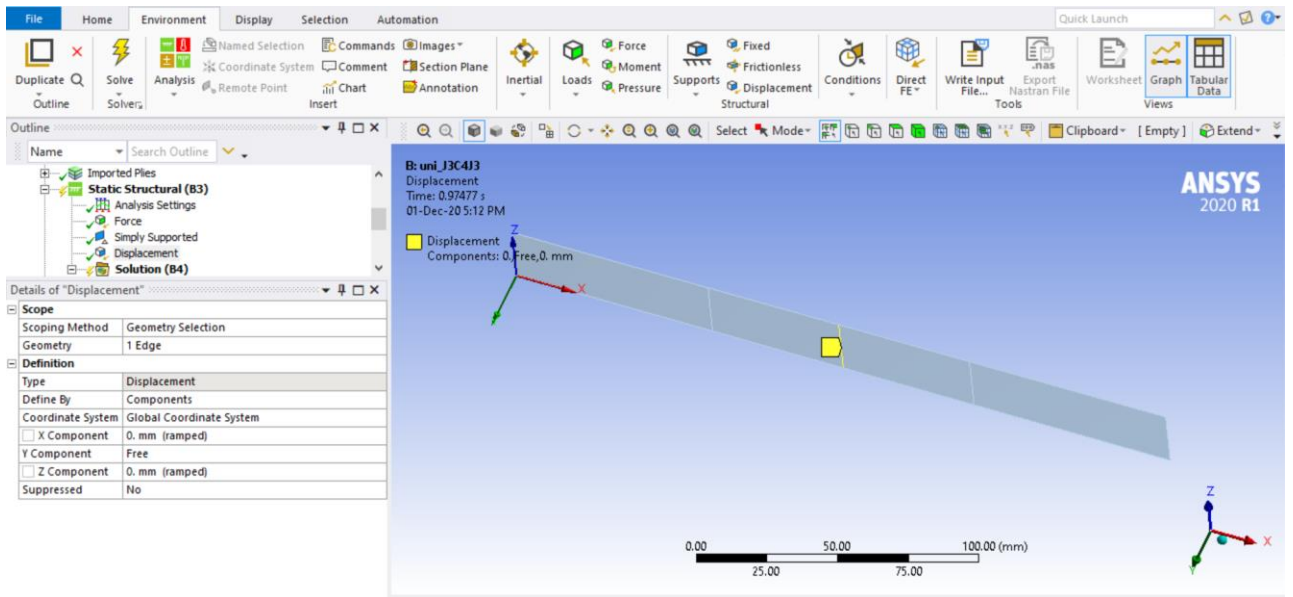


Figure 3.37 Addition of displacement

The option 'solution' was created and the following were inserted as shown in **Figure 3.38**

- Total deformation
- Directional Deformation (for force-displacement graph)
- Equivalent elastic strain: sub scope by-layer
- Equivalent stress: sub scope by-layer

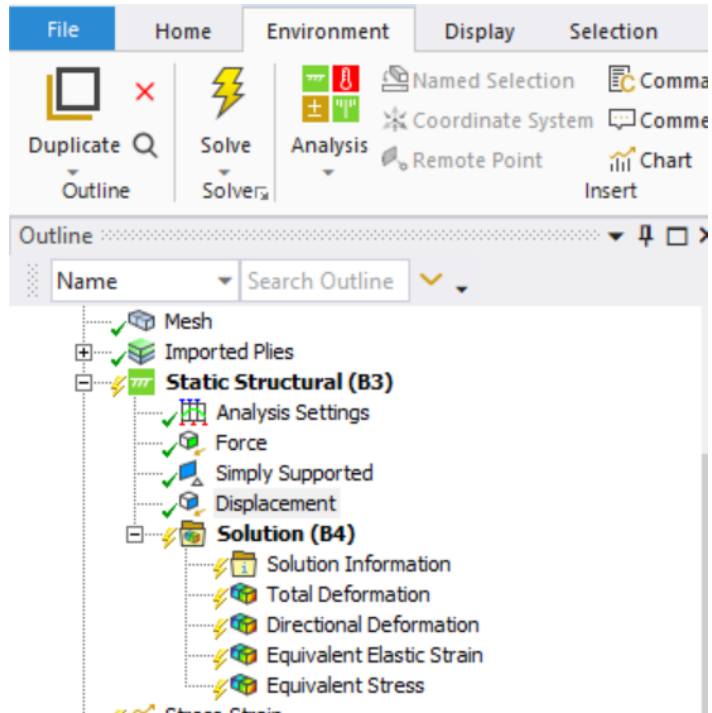


Figure 3.38 Branches of solution tree

The following ‘settings’ were done in ‘chart’ as shown in *Figure 3.39*

- Outline selection: both Equivalent elastic strain and Equivalent stress
- X-axis: equivalent strain (max)
- Time: omit
- equivalent strain (min): omit
- Equivalent stress (min): omit

Details of "Stress-Strain"	
Definition	
Outline Selection	2 Objects
Chart Controls	
X Axis	Equivalent Elastic Strain (Max)
Plot Style	Both
Scale	Linear
Gridlines	Both
Axis Labels	
X-Axis	Strain
Y-Axis	Stress
Report	
Content	Chart And Tabular Data
Caption	
Input Quantities	
Time	Omit
Output Quantities	
[A] Equivalent Elastic Strain (Min)	Omit
Equivalent Elastic Strain (Max)	X Axis
[B] Equivalent Stress (Min)	Omit
[C] Equivalent Stress (Max)	Display

Figure 3.39 Data for graph plotting and animation

The ‘maximum’ and ‘minimum’ tags were selected to determine the highest and lowest properties, respectfully as shown in *Figure 3.40*

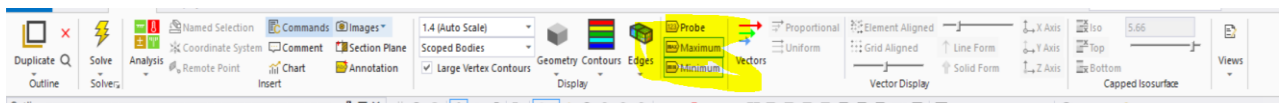


Figure 3.40 Marking of the positions with the greatest and smallest ‘solution’ results

3.3 Tensile Test

3.3.1 Experimental Procedure

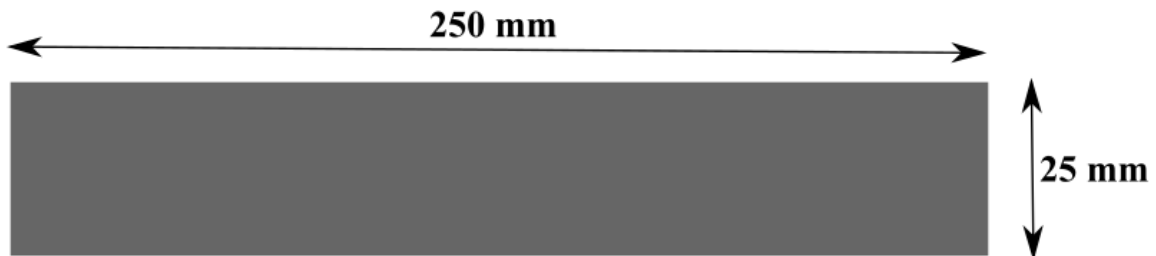


Figure 3.41 Specimen dimension for tensile test

Tensile strength is a measure of the ability of a material to withstand a longitudinal stress, expressed as the greatest stress that the material can stand without breaking. Tensile strength is the amount of load or stress that can be handled by a material before it stretches and breaks. As its name implies, tensile strength is the material's resistance to tension that is caused by mechanical loads applied to the material. The ability to resist breaking under tensile stress is one of the most important and widely measured properties of materials used for structural applications. Tensile specimens were prepared following ASTM D3039 [41] standards. A 250x25mm specimen of 6.8 mm thickness with a variation of 0.2 mm was taken as shown in *Figure 3.41*. The specimen was clamped with two fixtures positioned 100mm apart, 75mm from the edges of the specimen. An increasing load was applied by using a Universal Testing Machine with a cross head speed of 5 mm/min until the specimen failed at room temperature. The load at this point is used to calculate the maximum tensile strength of the composite material. Five different tests were conducted for each stacking sequence and the average value was taken for detailed analysis. The setup is shown in *Figure 3.42*



Figure 3.42 Tensile testing equipment with the specimen

3.3.2 Finite Element Analysis

A solid model having the dimension of 250x25mm was designed in SolidWorks and later on imported in ANSYS. The model was finely meshed using multizone quad/tri method shown in *Figure 3.43*. The Jute/Epoxy and Carbon/Epoxy fabrics were defined with thickness of 0.6mm and 0.4mm, respectively. The Rosette was set with the red arrow defining the longitudinal fiber direction, green being the transverse fiber width, leaving blue representing the direction normal to the ply. Later, modelling groups were created.

Here, the ply is defined with appropriate fabric and number of layers. Finally, a solid model of the specimen is generated.

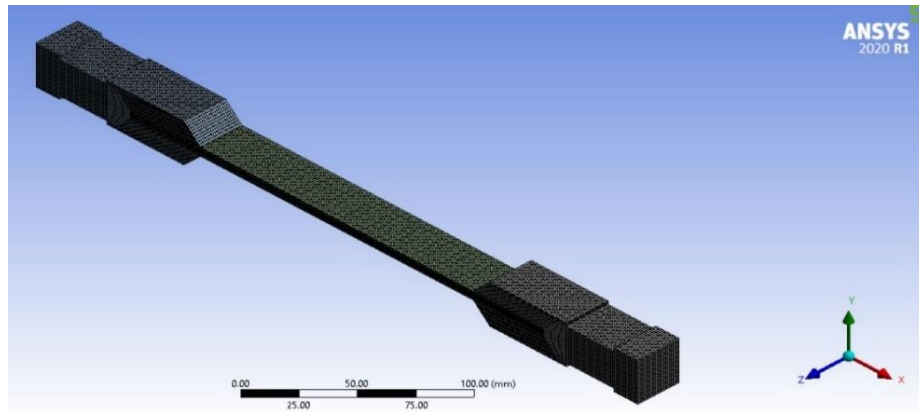


Figure 3.43 Prepared mesh of the fixture and specimen for tensile test

3.3.2.1 Simulation Steps

A specimen was designed in SolidWorks 2017 having dimension of 250x25 mm and a thickness of 1mm, shown in **Figure 3.44**.

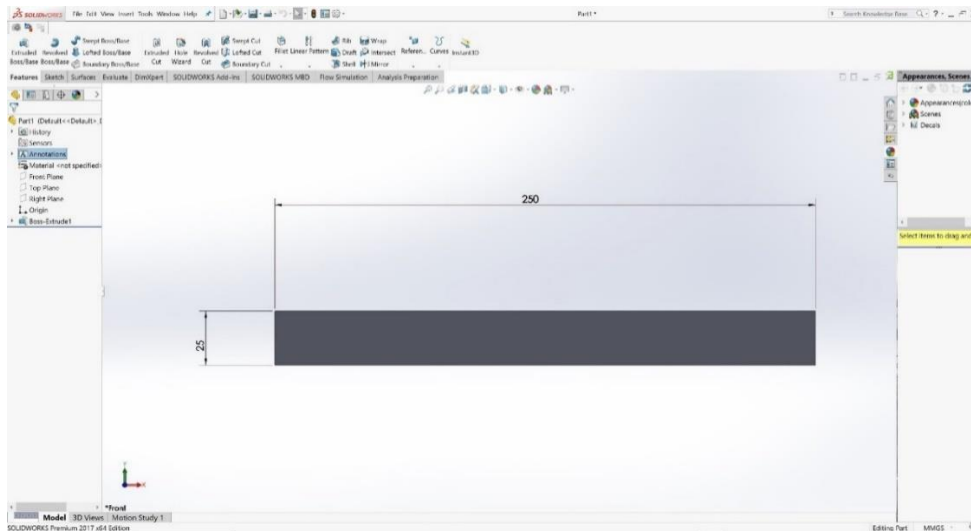


Figure 3.44 Designing the specimen in SolidWorks 2017

Once the specimen is designed, a pair of fixtures was designed in SolidWorks 2017. These fixtures along with the specimen was later imported on ANSYS for simulation.

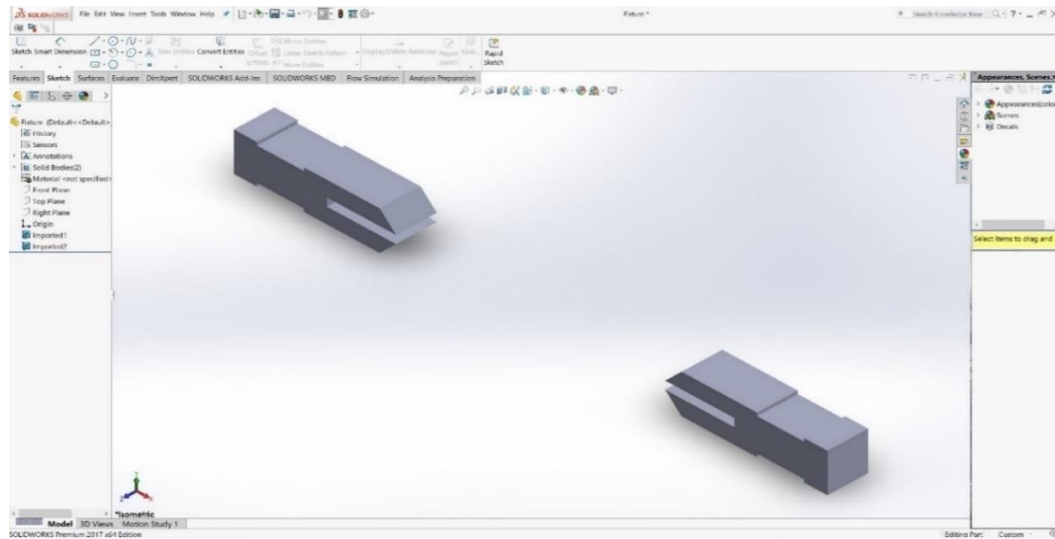


Figure 3.45 Designing fixtures to hold the specimen

The fixture, shown in *Figure 3.45* was designed in such a way to minimize local stress concentration on the specimen. The fixture allows independent application of load on the specimen.

ACP (ANSYS Composite Prepost) was dragged from the left column into the blank space of the workbench as *Figure 3.46*.

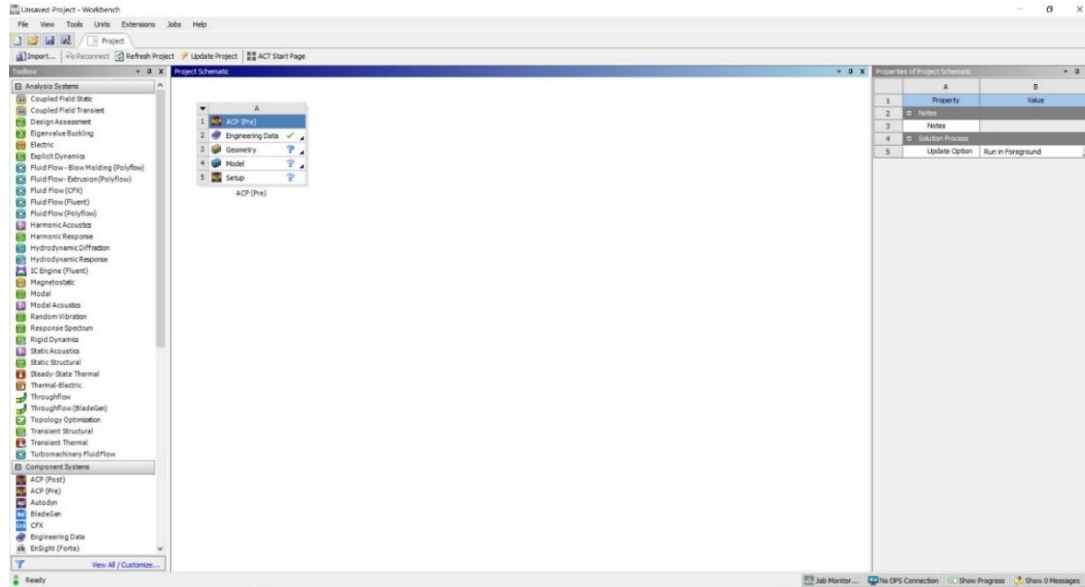


Figure 3.46 Setting up ACP (ANSYS Composite Prepost)

After that **Engineering Data** was clicked to assign materials for the simulation as *Figure 3.47*.

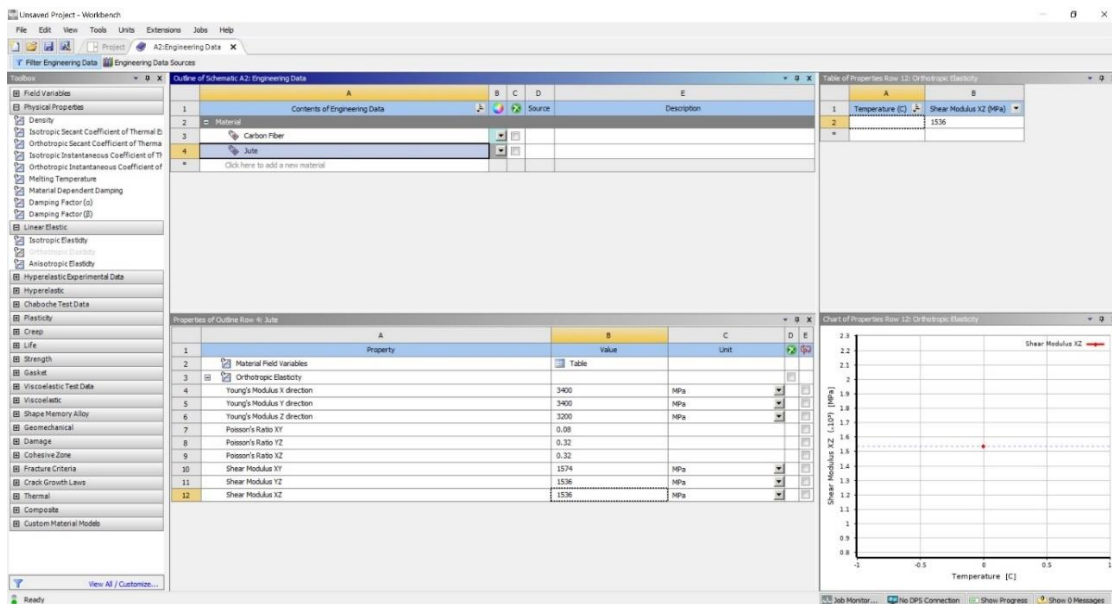


Figure 3.47 Inputting the property values of Carbon Epoxy

Since Carbon Epoxy was not available in ANSYS materials library, so a new material had to be created and its orthotropic elastic values were assigned accordingly.

Just like Carbon Epoxy, a new material naming Jute Epoxy was created and its orthotropic elasticity values were assigned, as shown in *Figure 3.48*.

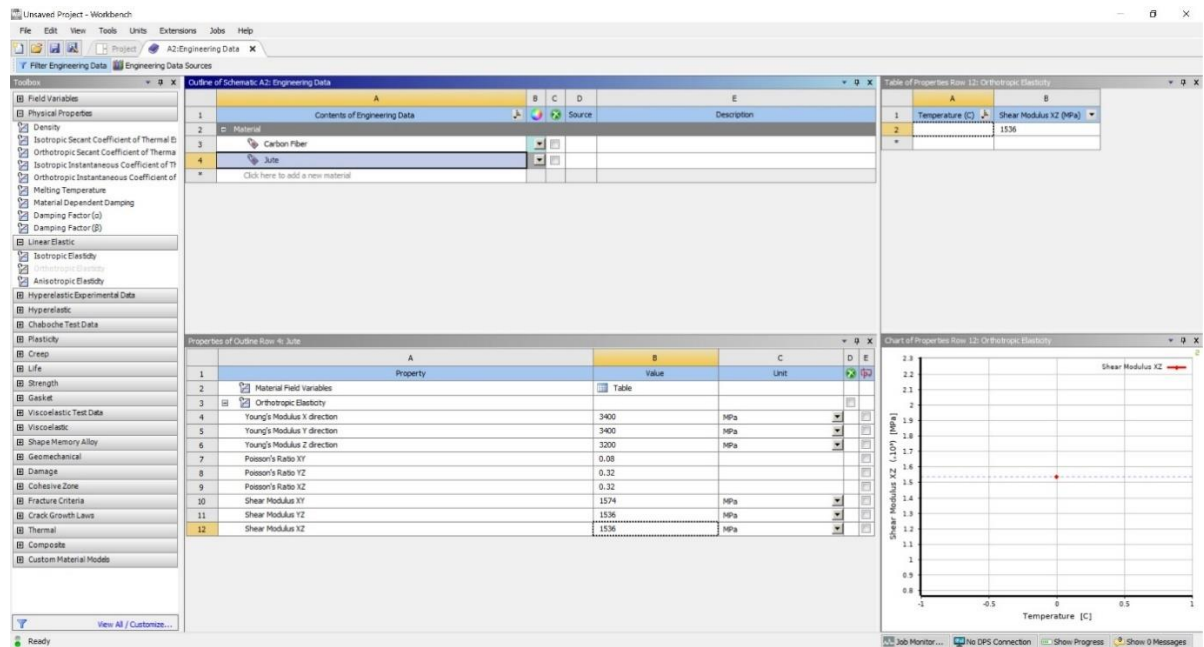


Figure 3.48 Inputting the property values of Jute Epoxy

The specimen drawn and designed on SolidWorks 2017 was imported in the **Geometry** section of the ACP tool, shown in *Figure 3.49* and *3.50*.

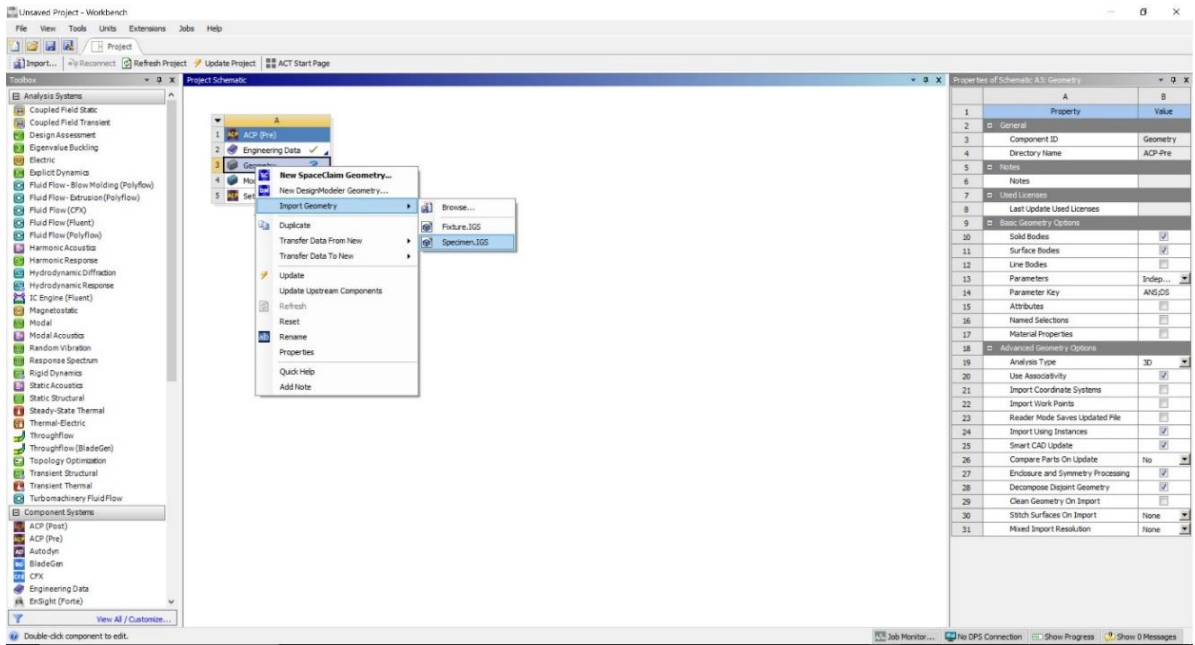


Figure 3.49 Importing the designed specimen into the workbench

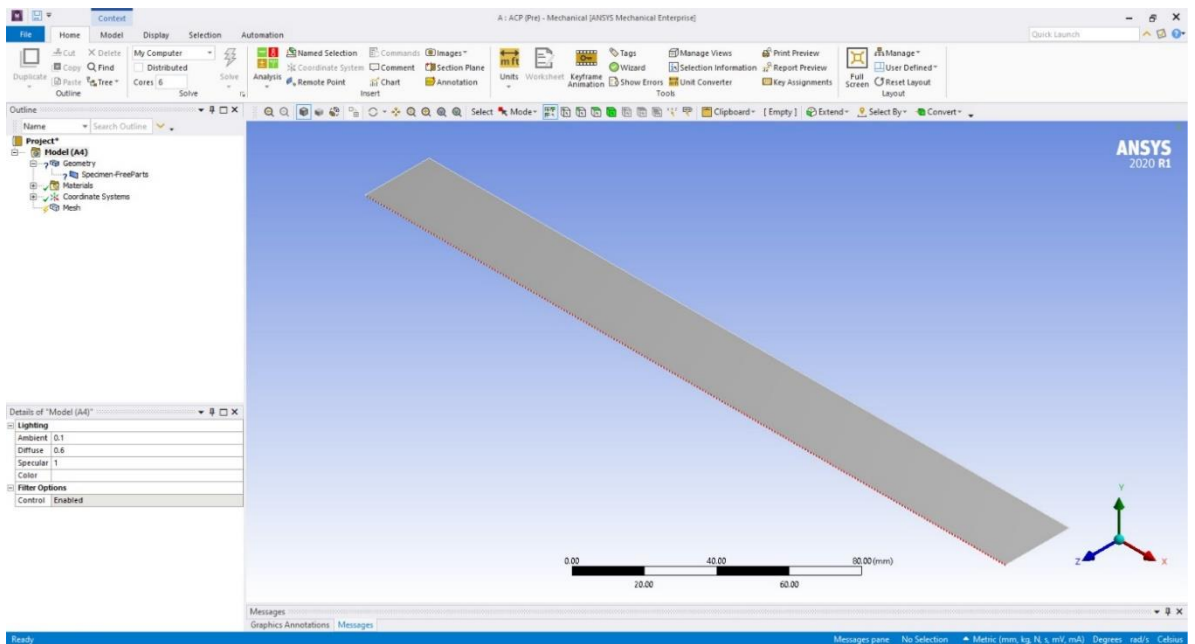


Figure 3.50 Imported specimen on ANSYS ACP

For meshing, the specimen had to be assigned to a fake thickness and in this study, it has been chosen to be 1mm shown in *Figure 3.51*.

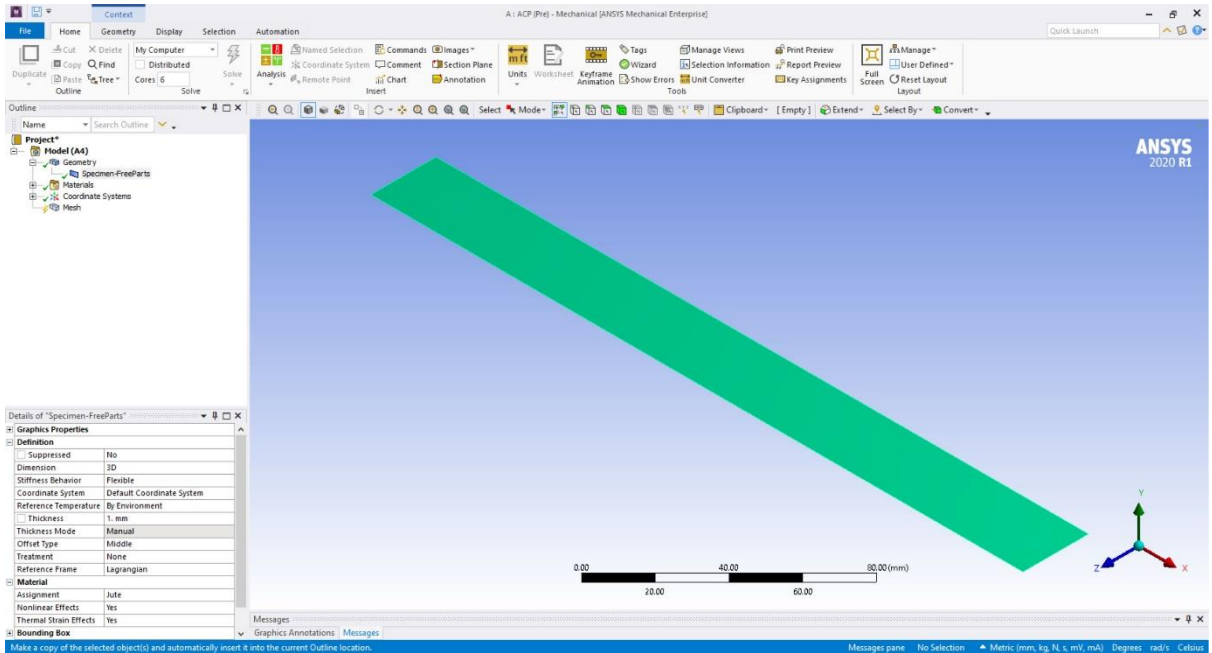


Figure 3.51 Geometry assigned with a fake thickness

Once the fake thickness is defined, the material was assigned to the geometry, like **Figure 3.52**. In this case any one of either Jute or Carbon can be assigned. This was done only for meshing. It is to be noted that once this geometry undergoes preprocessing in ACP, the model will automatically get defined with the corresponding composite material properties and stacking sequence.

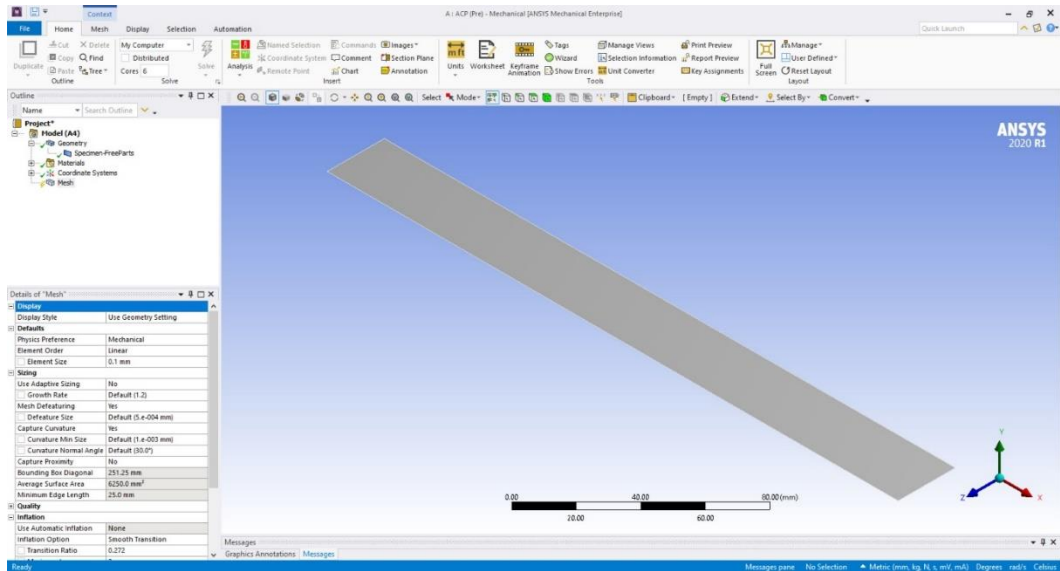


Figure 3.52 Prepared geometry for meshing

The model was finely meshed using multizone quad/tri method shown in **Figure 3.53**. Mesh transition was chosen as smooth and mesh size was assigned as 0.1mm

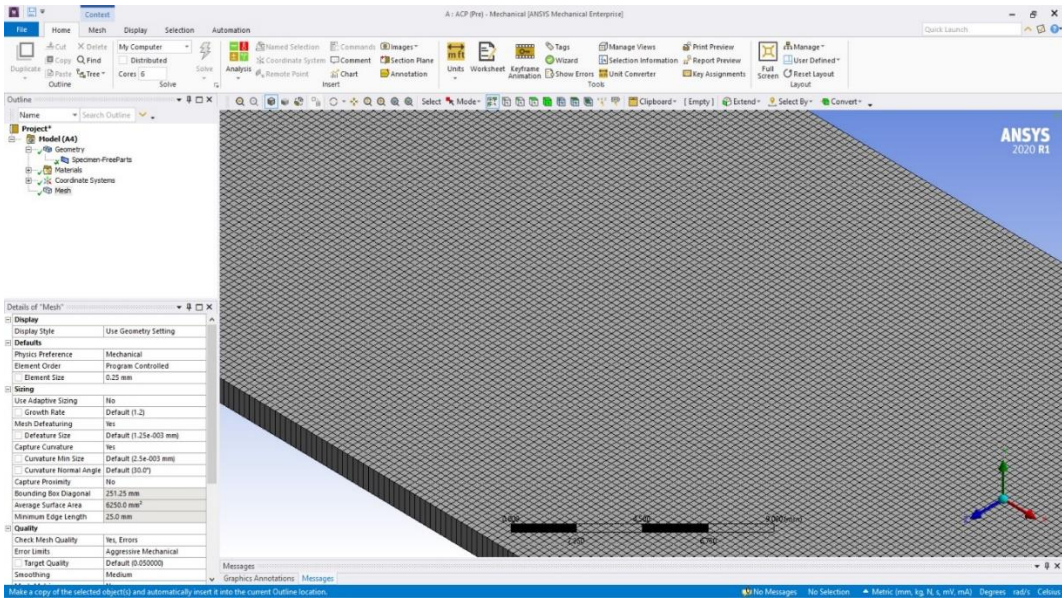


Figure 3.53 Finely meshed model of the specimen

Once the specimen meshing is done, mechanical model was dragged from the left column. This was done to import the fixture geometry. Later a connection was established between the two models. These have been shown in *Figures 3.54* and *3.55*.

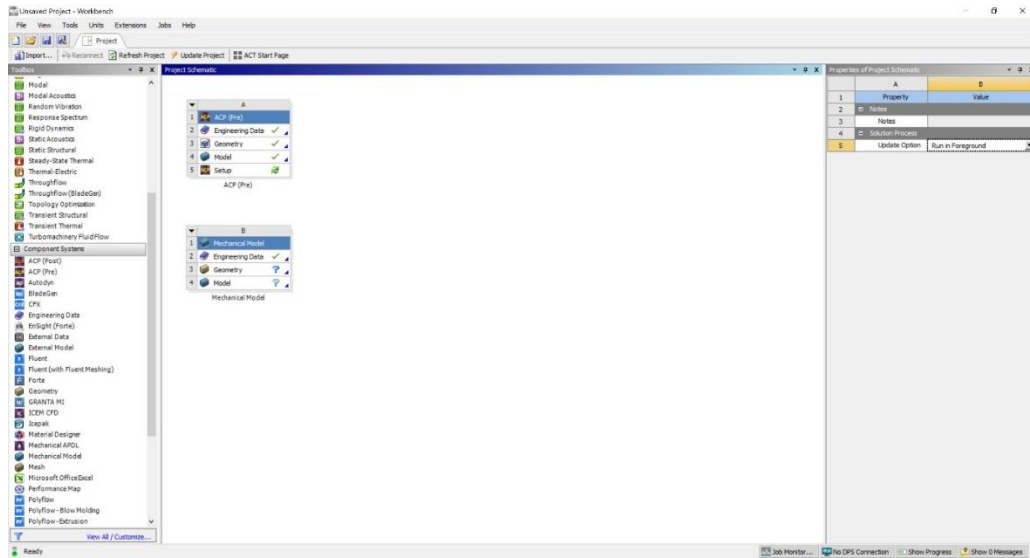


Figure 3.54 Setting up workbench for importing fixture geometry

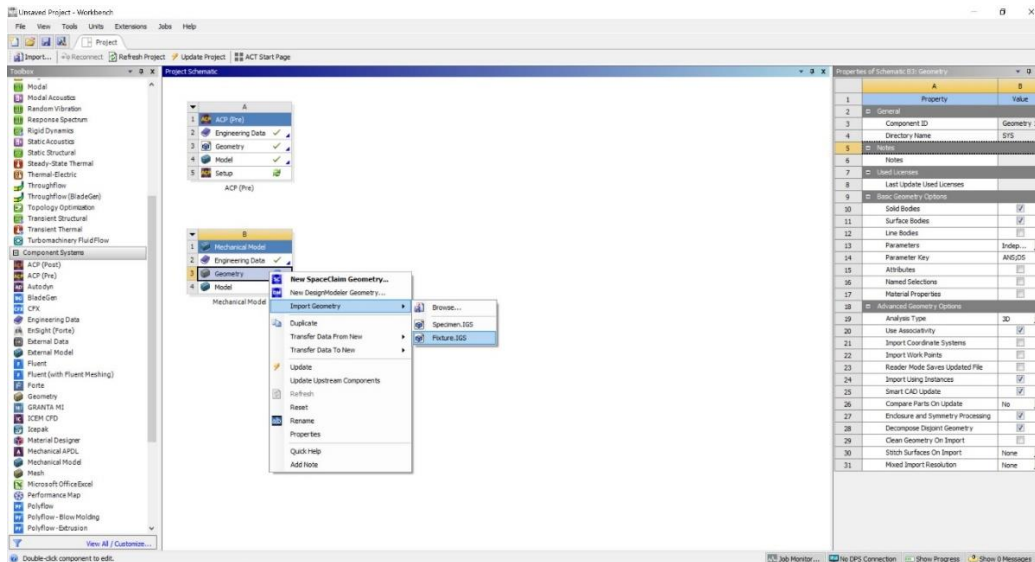


Figure 3.55 Importing the fixture geometry

The fixture that was previously designed on SolidWorks 2017 was converted into IGS format and then imported on the mechanical model.

Once the fixtures are exported, meshing is done on the fixtures, as shown in **Figure 3.56**.

The fixtures are not meshed as finely as the specimen since finding out the stress, strain and deformation of the specimen only was important. The fixture is used in this study so that force can be applied uniformly all over the specimen and to avoid any stress concentration.

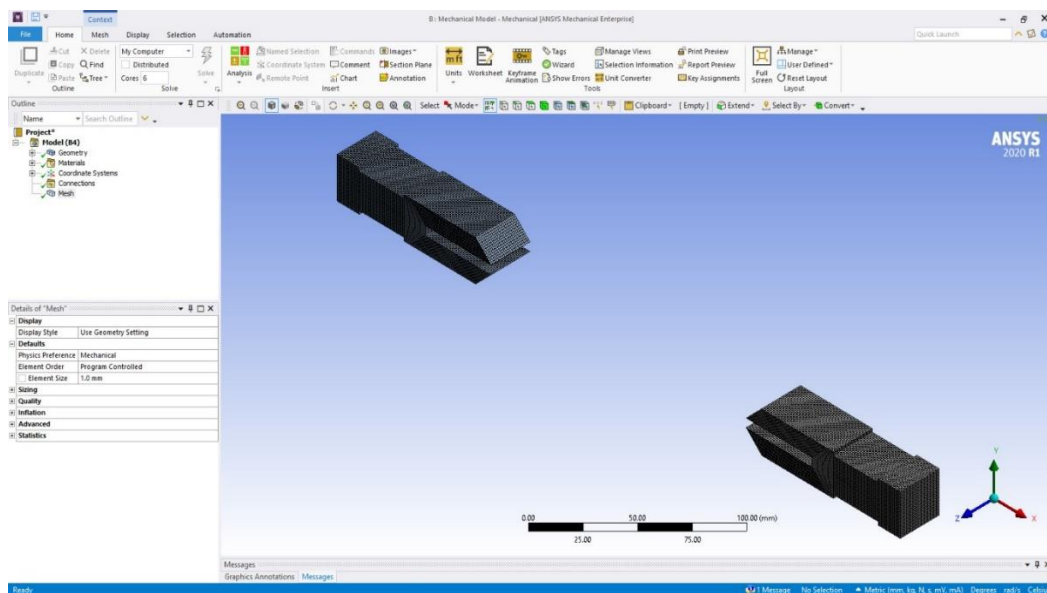


Figure 3.56 Meshed fixtures

Before the specimen is put under simulation, it had to be preprocessed in the dedicated platform for composite material that is on ANSYS ACP. Setup option was clicked on the ACP tool and a new window was opened as shown in **Figure 3.57**.

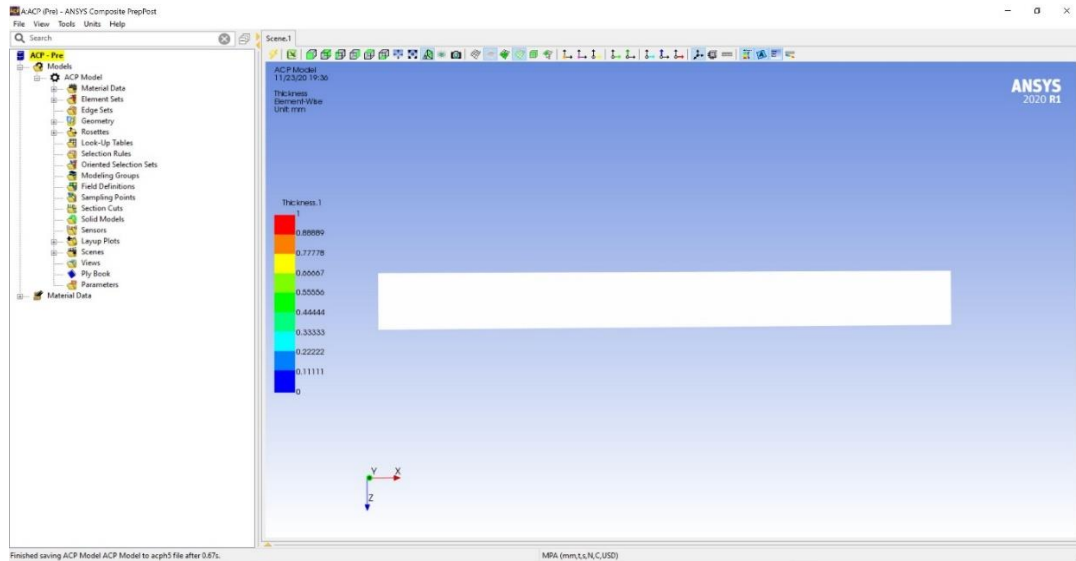


Figure 3.57 Setup window of ACP tool

At first the fabrics were defined. To define and assign the fabrics, the following steps were followed: Material data > Fabric > Create Fabric, shown in **Figure 3.58**.

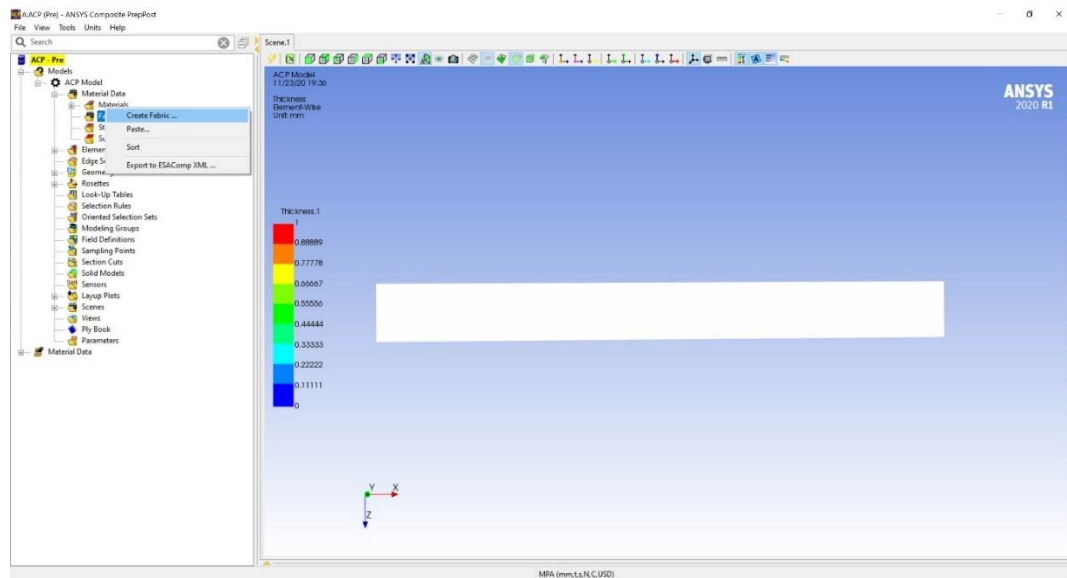


Figure 3.58 Creating fabric on ANSYS ACP

At first Carbon fabric was defined. Thickness section was set to 0.4 according to the thickness of each Carbon fabric. It has been shown in **Figure 3.59**.

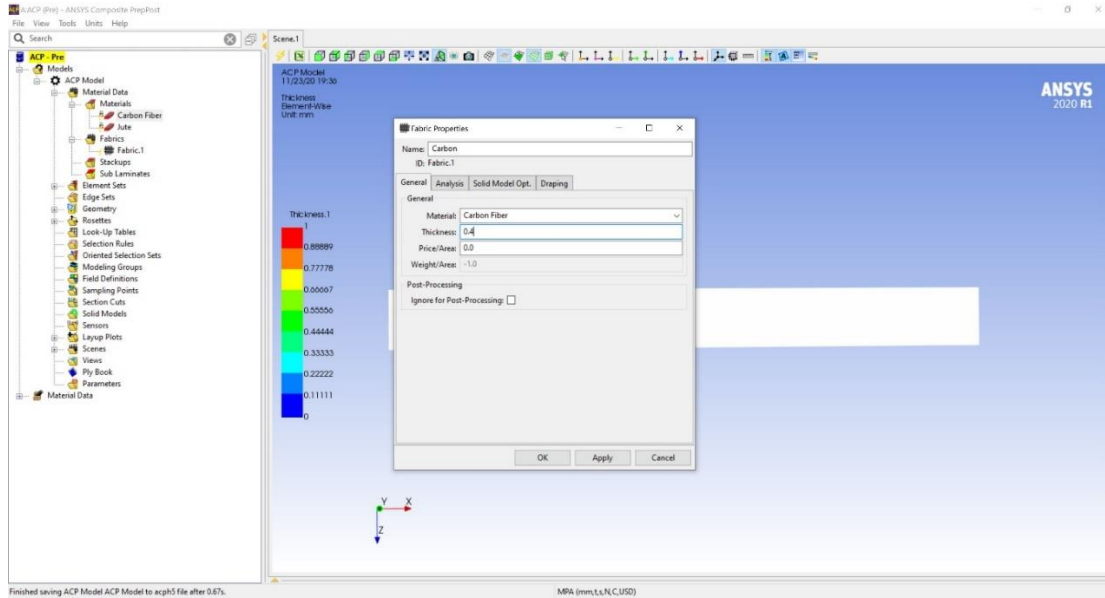


Figure 3.59 Defining Carbon fabric

Once defining Carbon fabric is done, Jute fabric was defined with a thickness of 0.6 mm, shown in *Figure 3.60*.

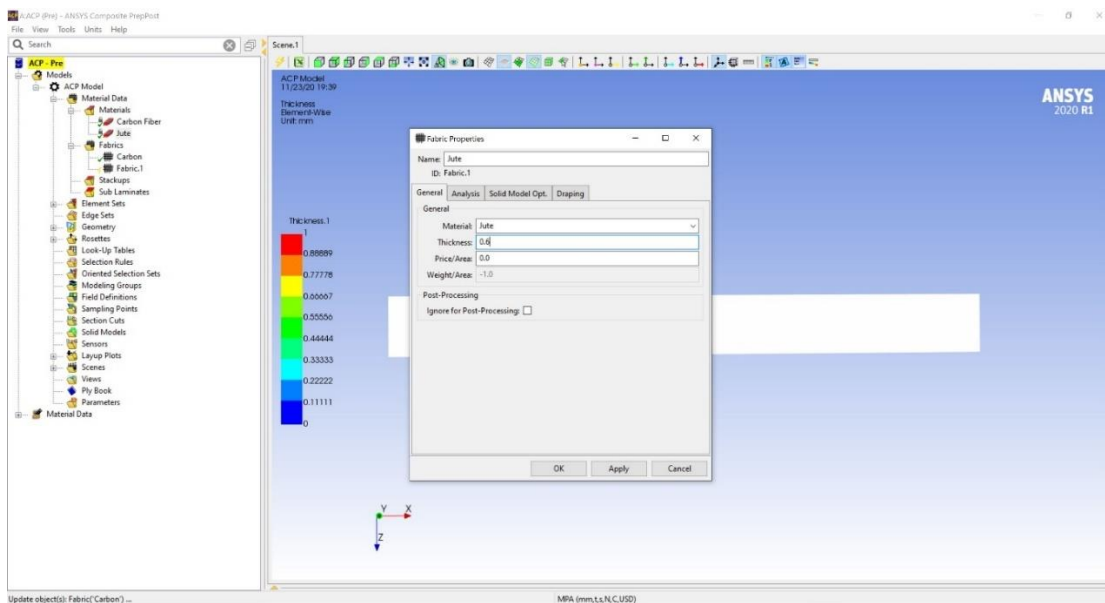


Figure 3.60 Defining Jute fabric

When all the fabric definition was complete, a new rosette was created by the following steps: Rosettes > Create New Rosette, shown in **Figure 3.61**.

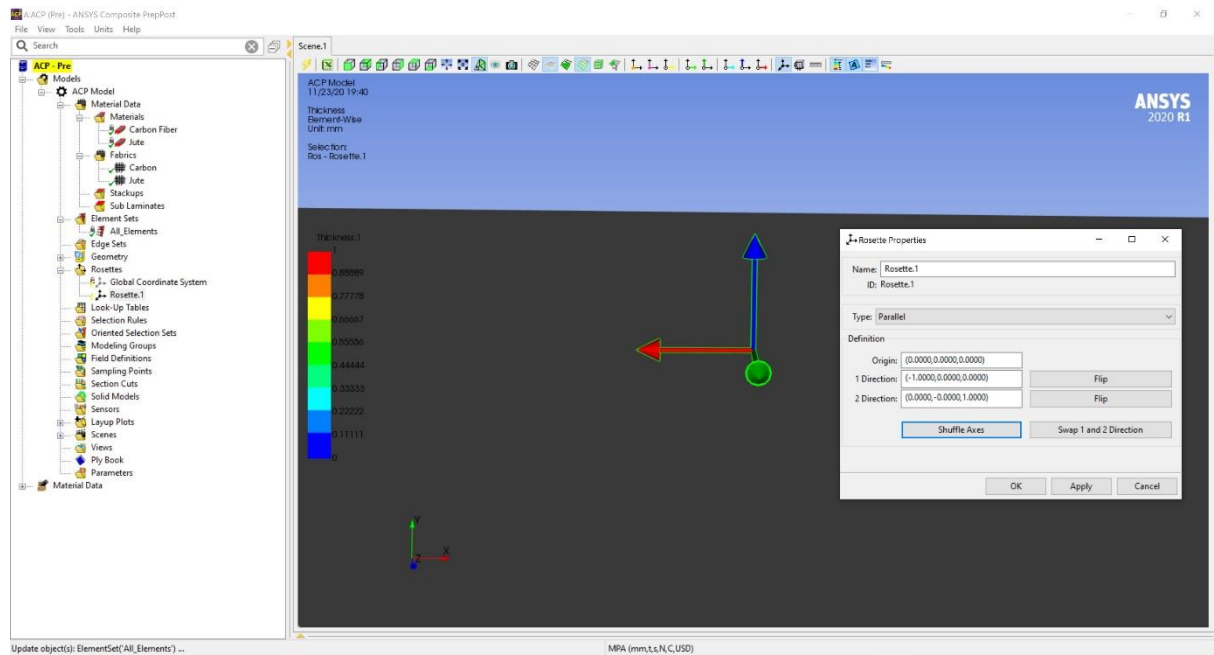


Figure 3.61 Creating new Rosette

While creating the rosette, the convention followed were: Red arrow as the direction of fiber, Blue Arrow as the normal direction and Green Arrow as the direction of width.

After creating rosette, oriented selection sets are defined as shown in **Figures 3.62** and **3.63**.

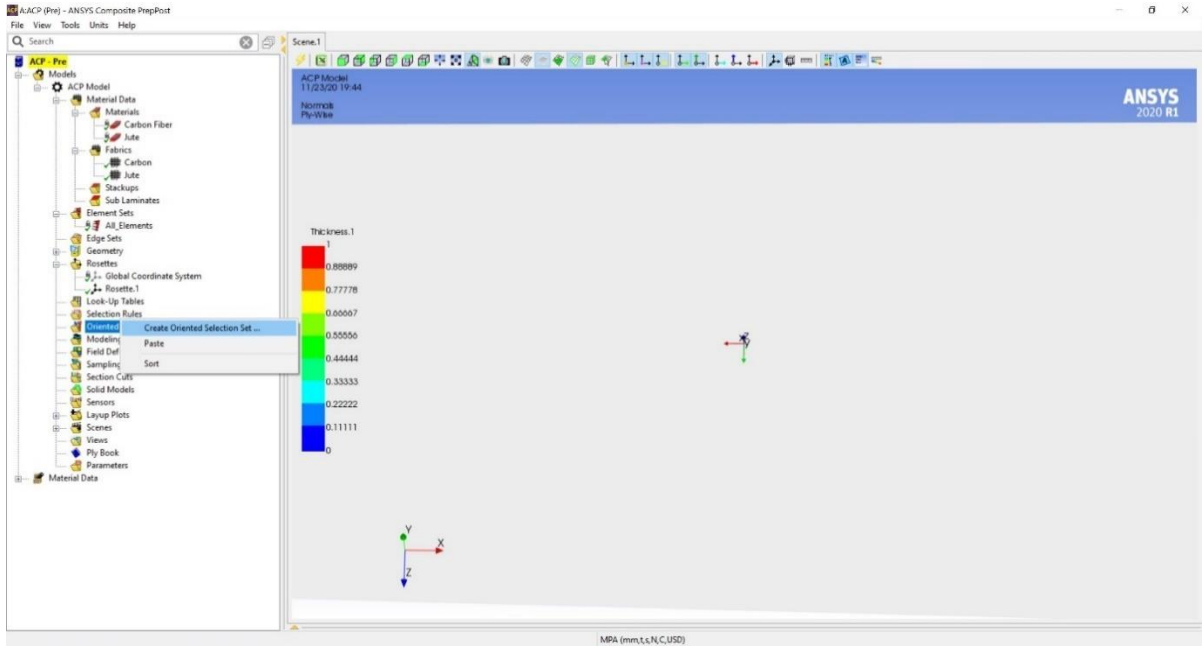


Figure 3.62 Creating Oriented Selection Set

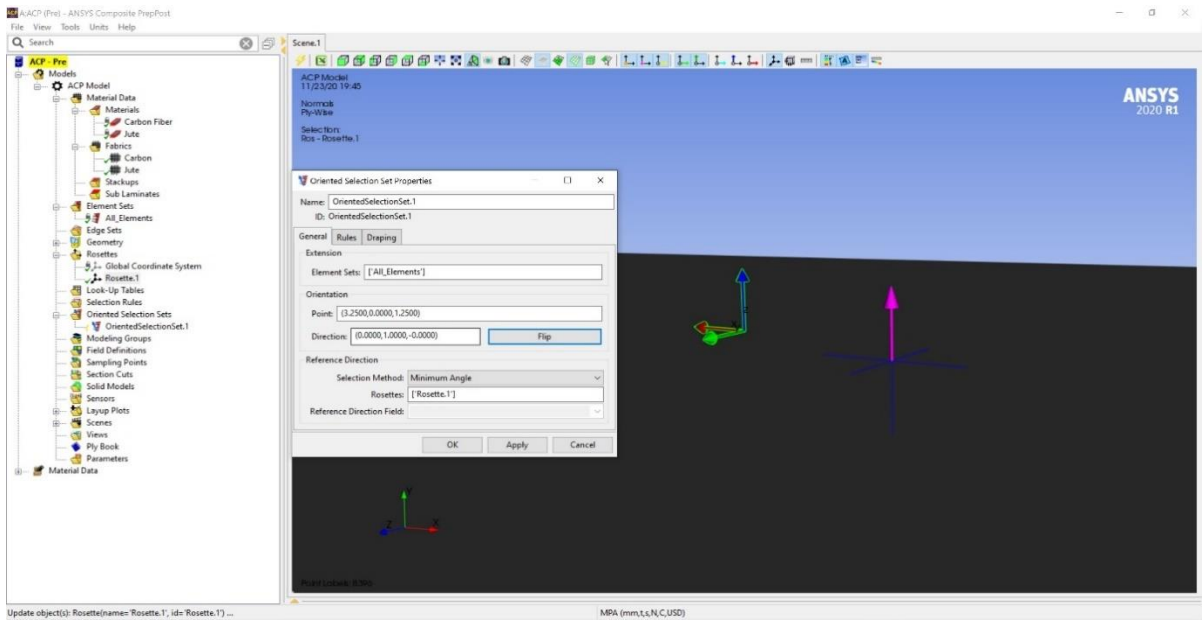


Figure 3.63 Defining coordinates for oriented selection set

Once the setup of rosette and oriented selection set is complete, the fabric will show the direction of fiber and the direction of stacking. Here on the **Figure 3.64** above, the purple and green arrows indicate the stacking direction and fiber direction, respectively.

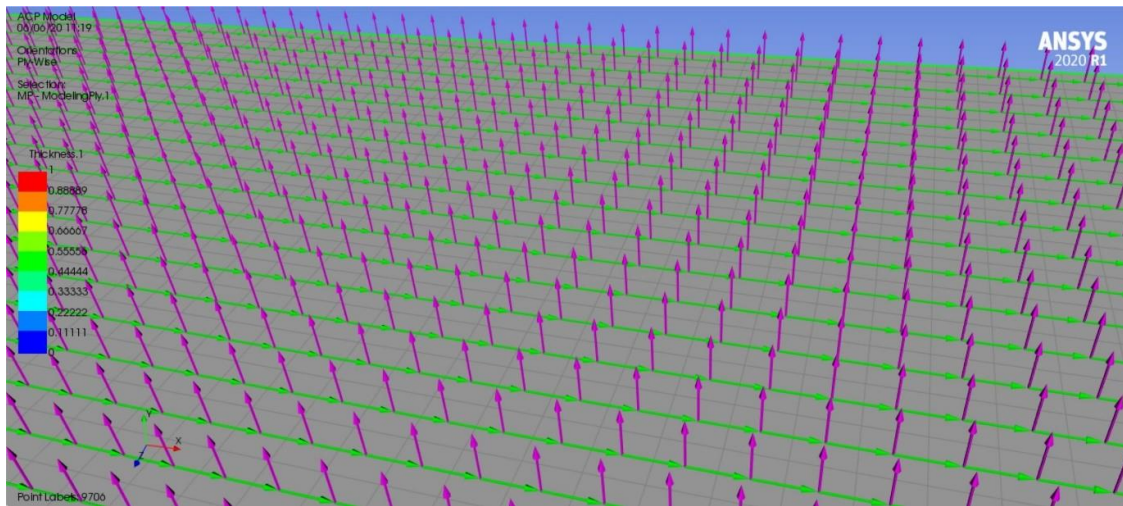


Figure 3.64 Arrows showing the direction of fiber and the normal direction

The final step of the ACP Preprocessing is to create modeling groups. Modeling groups define the number of fabric layers and the stack up sequence. The command is executed by the following process: Modeling groups > Create Modeling Groups as shown in **Figure 3.65**.

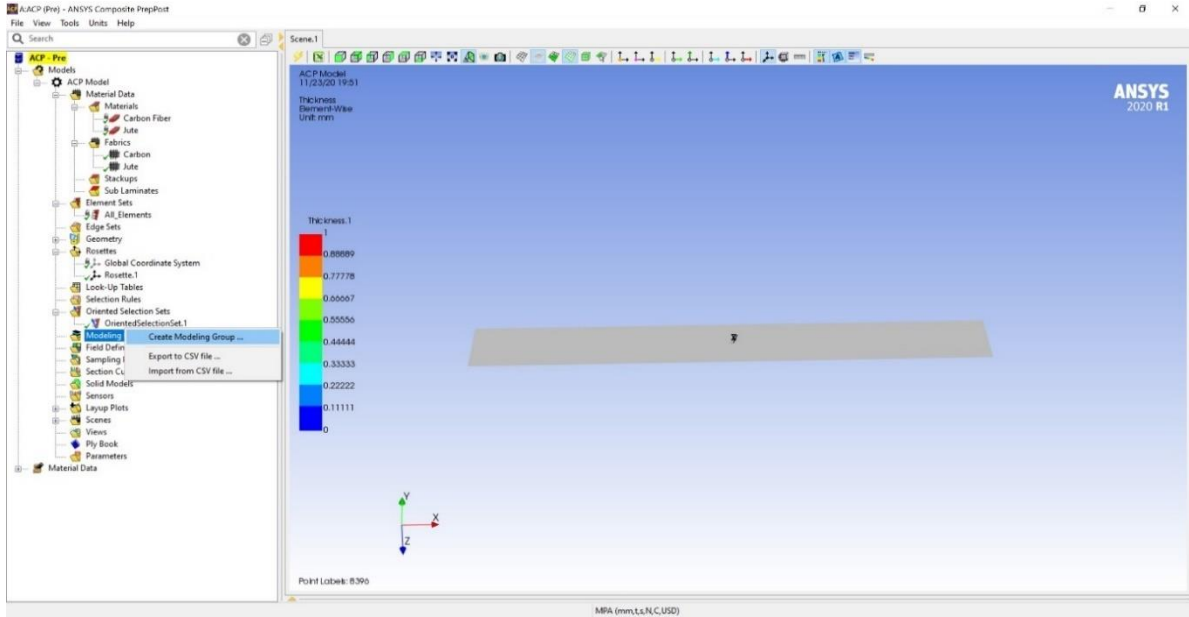


Figure 3.65 Creating Modeling Groups

When a modeling group was created, it facilitated to create necessary number of fabric plies in correct stack up sequence. The result it shown in **Figure 3.66**.

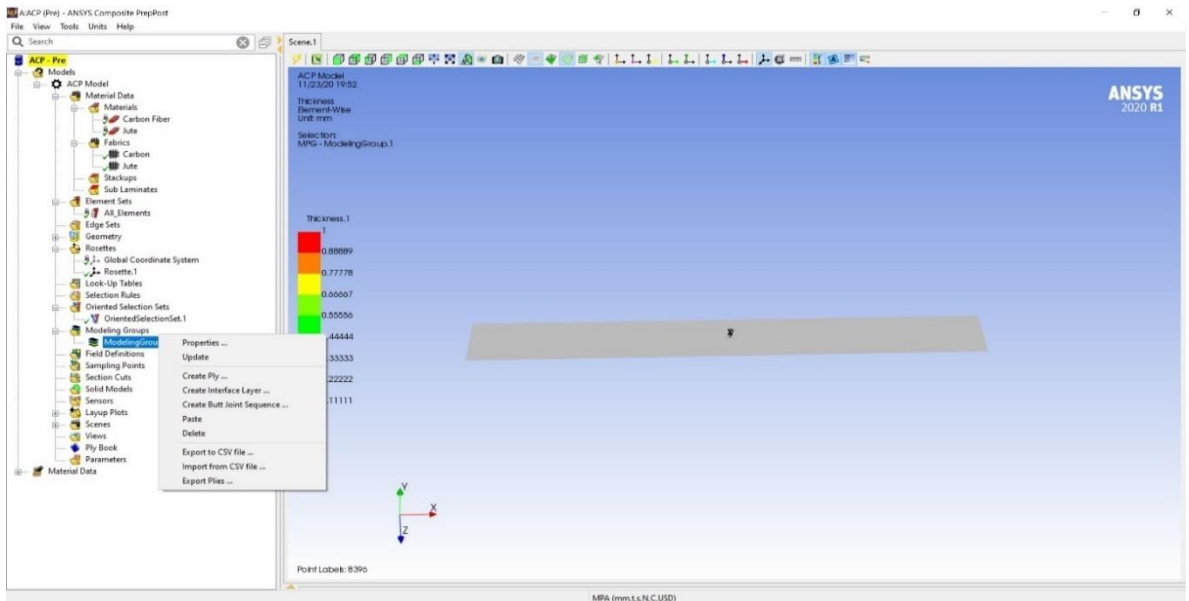


Figure 3.66 Creating composite plies

After the modeling ply properties window toggled up, the necessary data of the plies was inputted. Here on the **Figure 3.67** above, the previously created oriented selection set is selected, ply material is selected as Carbon.

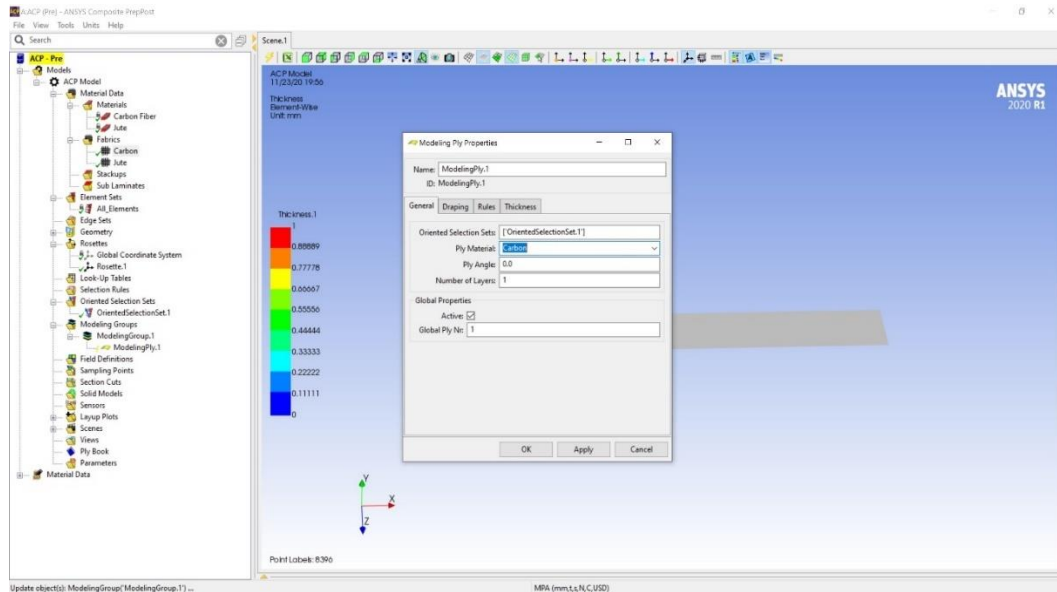


Figure 3.67 Creating Carbon ply

The jute plies are also created following the similar steps as in creating Carbon plies, and is shown in **Figure 3.68**. It is to be noted that the thickness of the fabric was previously assigned while creating fabrics. Therefore, once the solid model is updated, the model will get the exact appropriate thickness as per the number of plies.

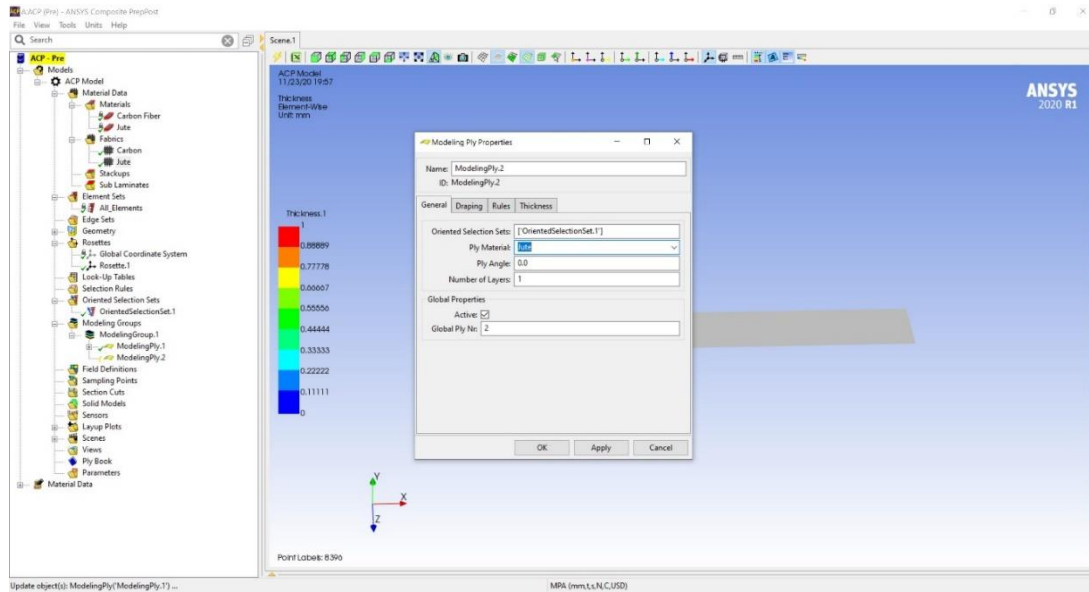


Figure 3.68 Creating ply for Jute

Creating Solid Model is the last step of ACP preprocessing. By creating solid model, the thickness of the specimen was defined. The clearance in the fixture must match with the thickness of the model so that no mesh overlapping takes place. This command is executed by the following step: Solid Model > Create Solid Model, shown in **Figure 3.69**.

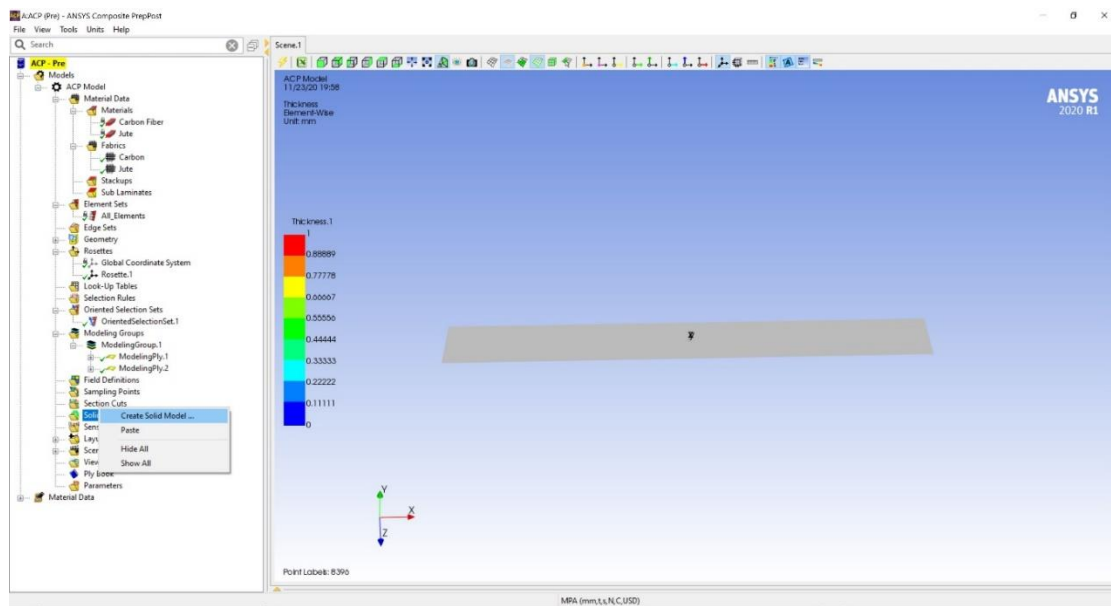


Figure 3.69 Creating Solid Model

Once the Solid Model property window toggles, element set is selected “All elements”, Extrusion method is selected as “Analysis Ply wise”. Shell Normal is selected for offset direction. These have been shown in **Figure 3.70**. It is to be noted that any global drop off material was not selected. It is because the properties that are inputted in the very beginning in Engineering data section is for Epoxy Jute and Carbon Epoxy. If the value of Jute and Carbon fibers are inputted only, then Epoxy resin as global drop off material is to be input.

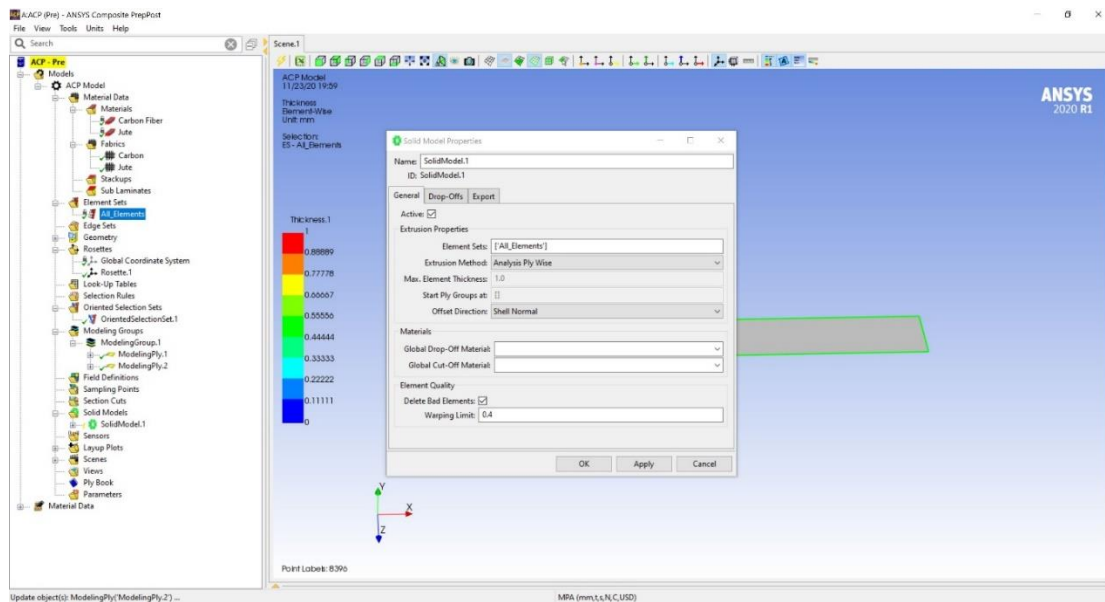


Figure 3.70 Inputting necessary data for creating solid model

Section cut is created to illustrate various section throughout the specimen. This is created by executing the following command: Section Cut > Create Section Cut, shown in **Figure 3.71**.

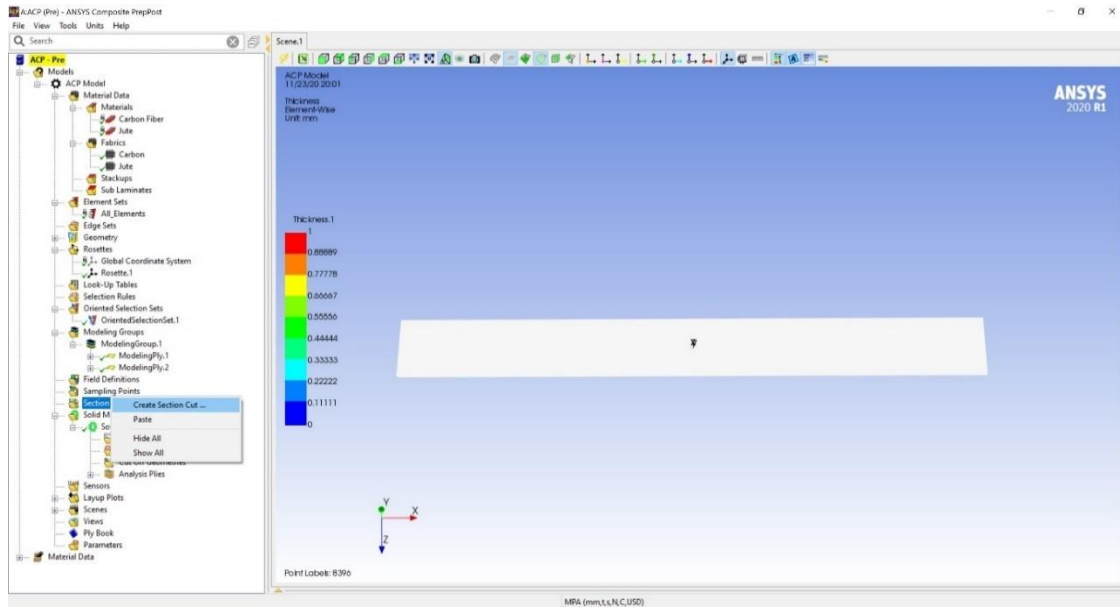


Figure 3.71 Creating Section Cut

All parameters were set as default. Section cut was applied and apply and updated, as shown in *Figure 3.72*.

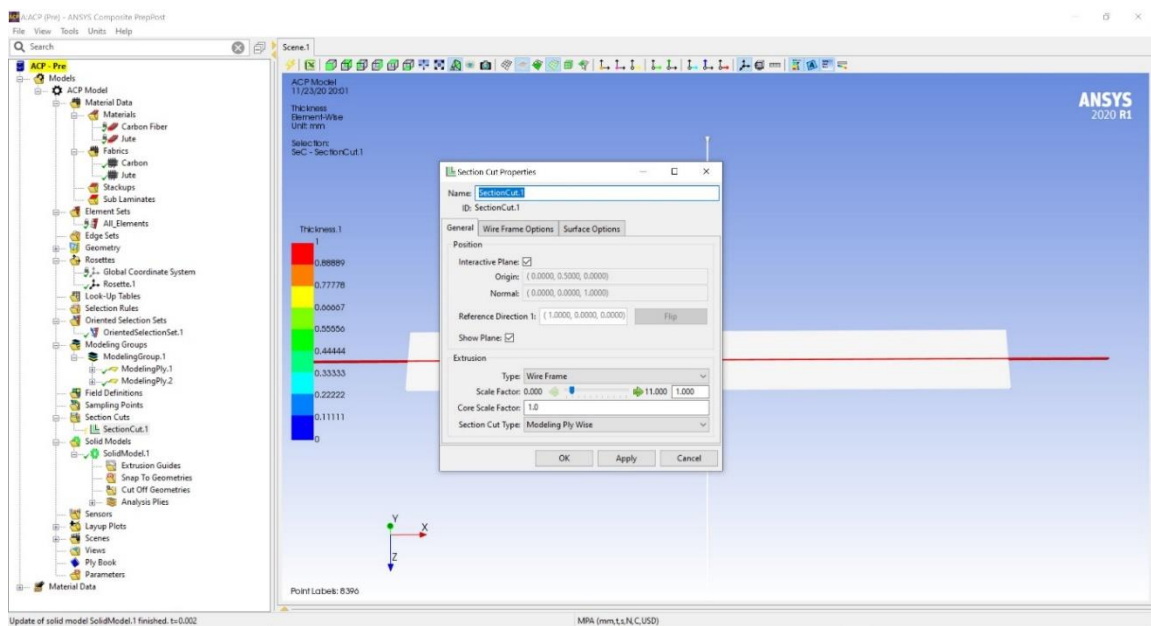


Figure 3.72 Section Cut Window

The green lines indicate the boundary of the fabric layers. This is done to check whether the created composite model is appropriate in thickness and number of plies. The result is shown in *Figure 3.73*.

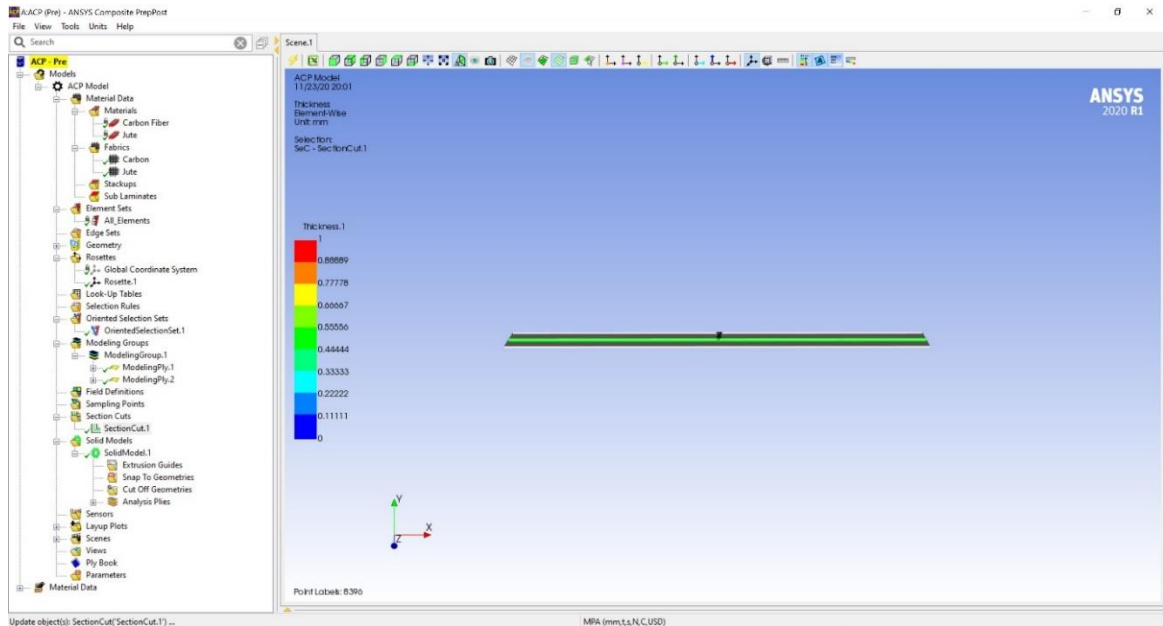


Figure 3.73 Specimen after executing section cut

Creating solid model and section cut was the final step in ACP pre processing. Once the model is pre processed and all other parameters are well defined, static structural tool was dragged from the left column and then it was connected with the previously set **ACP** tool and **Mechanical model** where the fixture was imported and meshed, as shown in *Figure 3.74*.

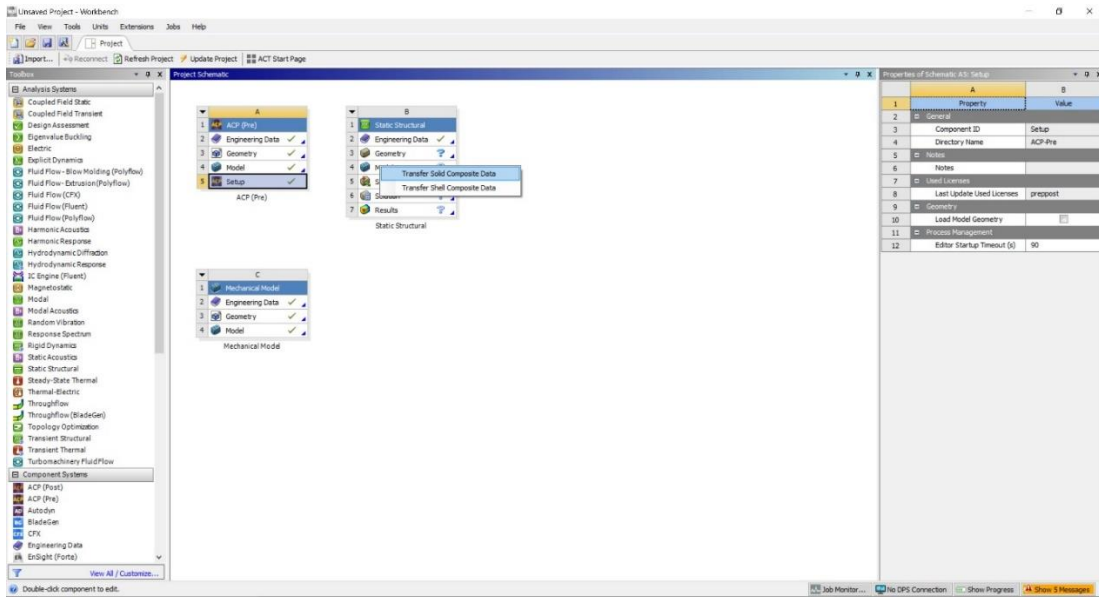


Figure 3.74 Setting up static structural tool and connecting with ACP tool

The tools are connected by dragging the “Setup” section of ACP into the model section of **Static Structural**. While doing this, ANSYS will ask for confirmation of transferring parameters of solid composite data or shell composite data. Since the specimen is a solid model, “Transfer solid composite data” was selected.

The mechanical model is connected by dragging the “Model” section and dropping it into the “Model” section of Static Structural tool as shown in **Figure 3.75**.

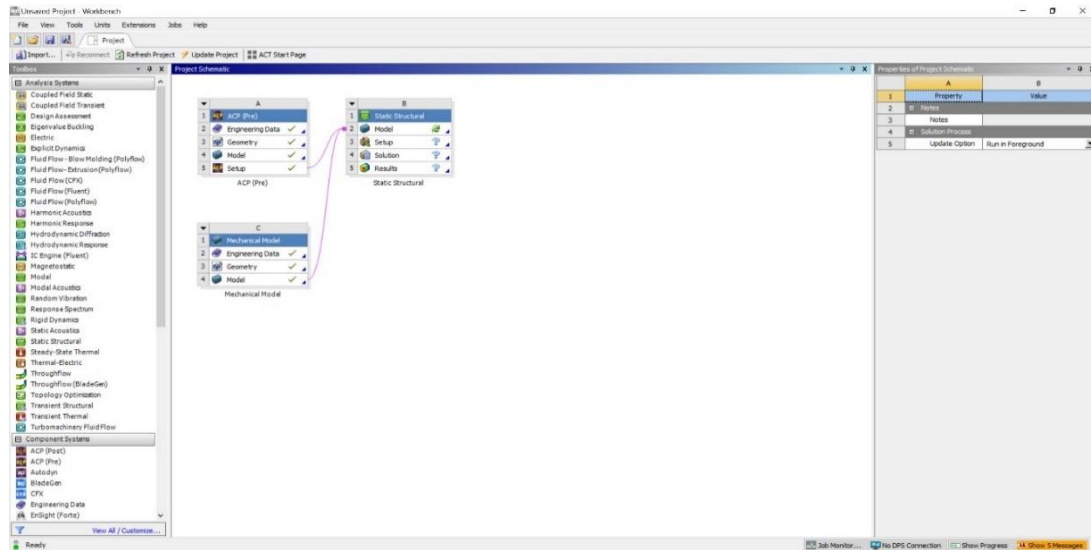


Figure 3.75 Connecting ACP and Mechanical model with Static Structural

The combined model of specimen was opened and fixture by double clicking on “Model” section of Static Structural, shown in **Figure 3.76**. It is to be noted that both fixture and specimen were meshed previously in Mechanical Model and ACP tools respectively.

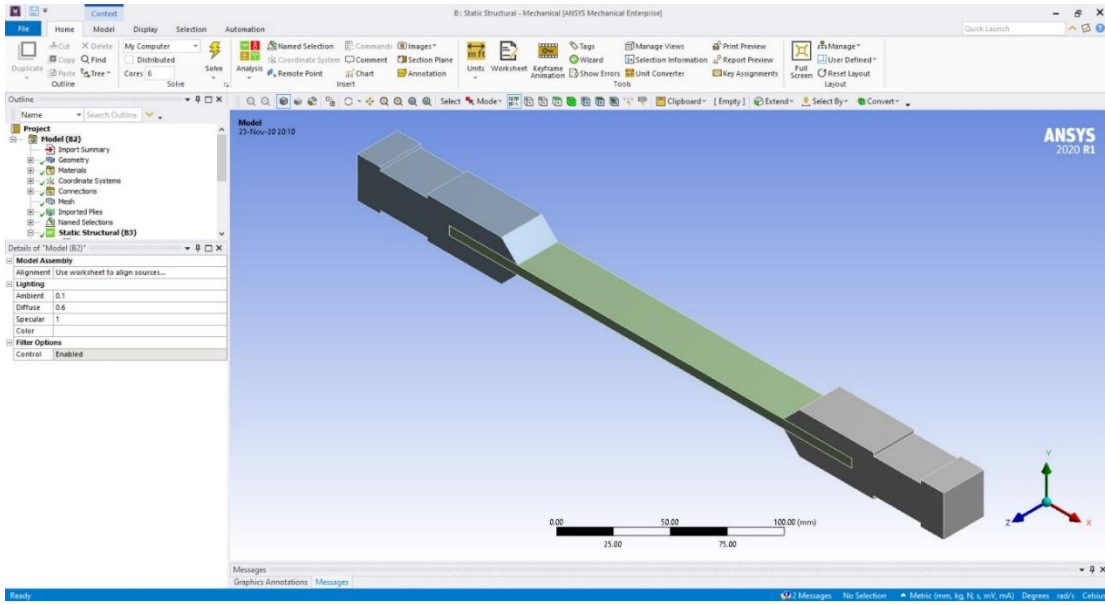


Figure 3.76 Combined model of specimen and fixture in ANSYS Mechanical

While meshing, the nature and quality of mesh for both specimen and fixture was similarly maintained, however, the number of elements and nodes were kept different for specimen and fixture. The mesh is shown in **Figure 3.77**.

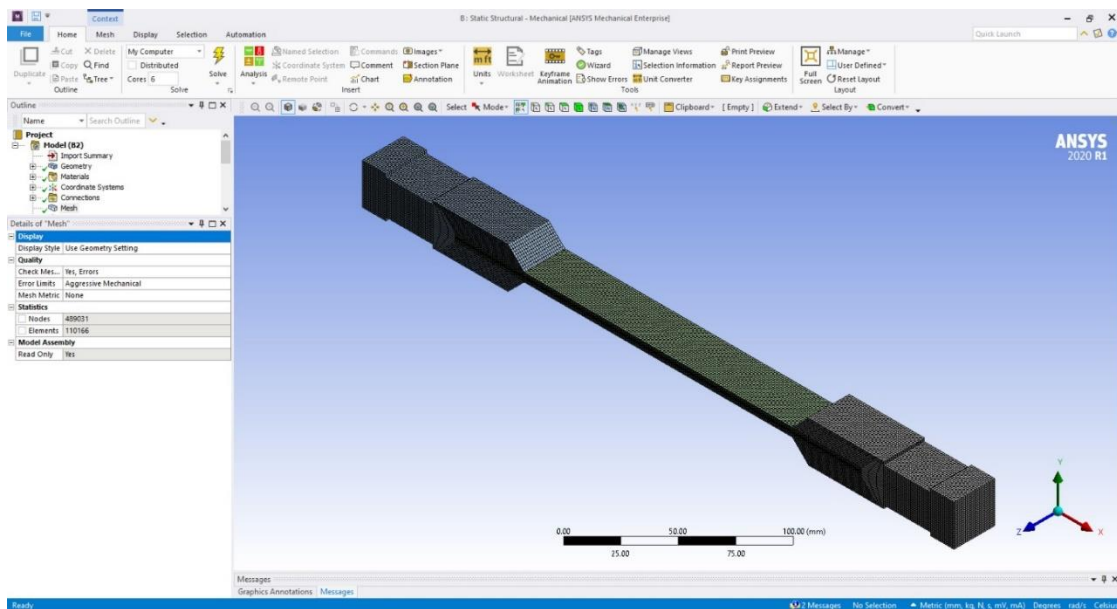


Figure 3.77 Illustration of prepared mesh in both specimen and fixture

In order to perform a tensile test, one fixture has to be kept fixed and load is to be applied on the other fixture. The fixed support is defined by the following commands: Static Structural > Fixed Support. The blue square area on the figure above shows that section is fixed and is constrained to all kinds of motion, shown in **Figure 3.78**.

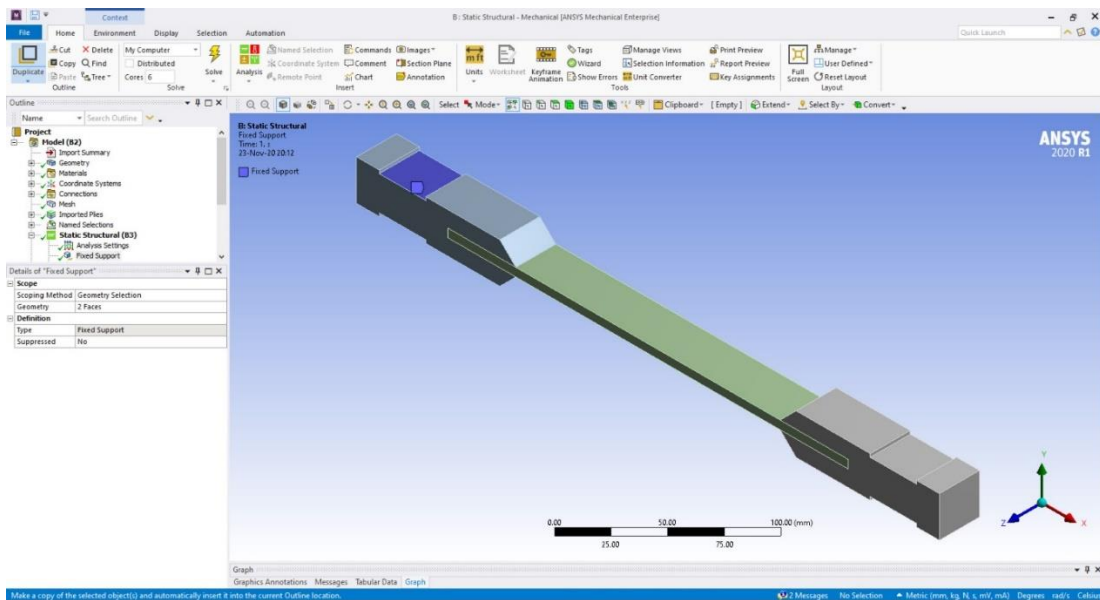


Figure 3.78 Defining fixed support

A load of 25 kN was applied on the red square area on the other fixture, which is not assigned as fixed support, shown in *Figure 3.79*.

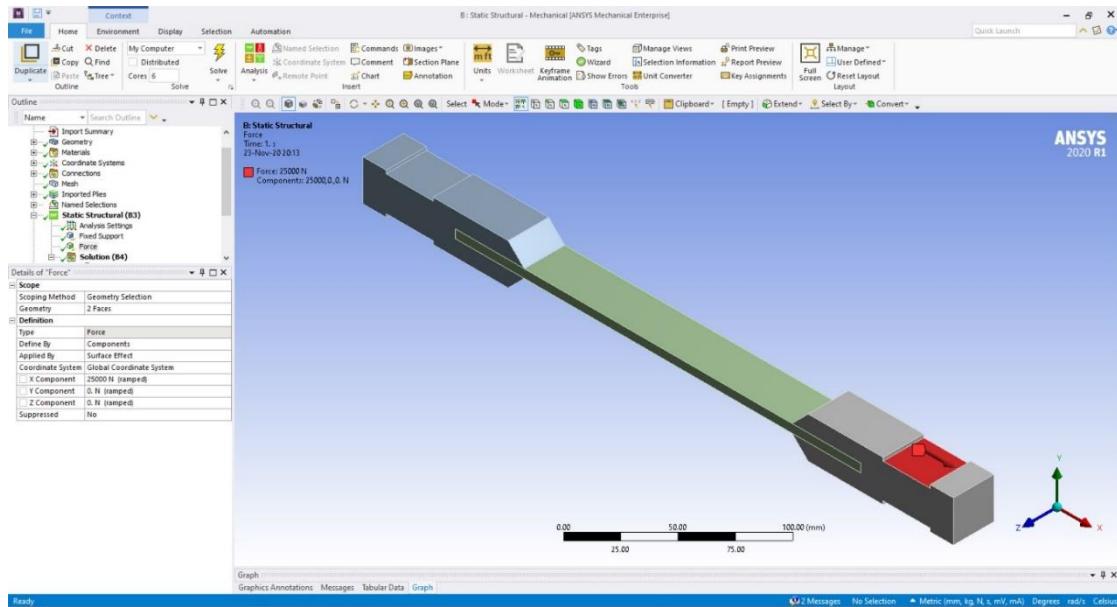


Figure 3.79 Assigning load on the fixture

It is to be noted that as per the figure above, the load is applied towards the X direction only and no force acts on other two directions.

Once all boundary condition is assigned, the simulation option is manipulated as per requirement. For calculating Equivalent stress, the simulation is sub scoped by layer and not by plies. With all parameters set, the simulation is run by clicking solve button on the top. The parameters are shown in *Figure 3.80*.

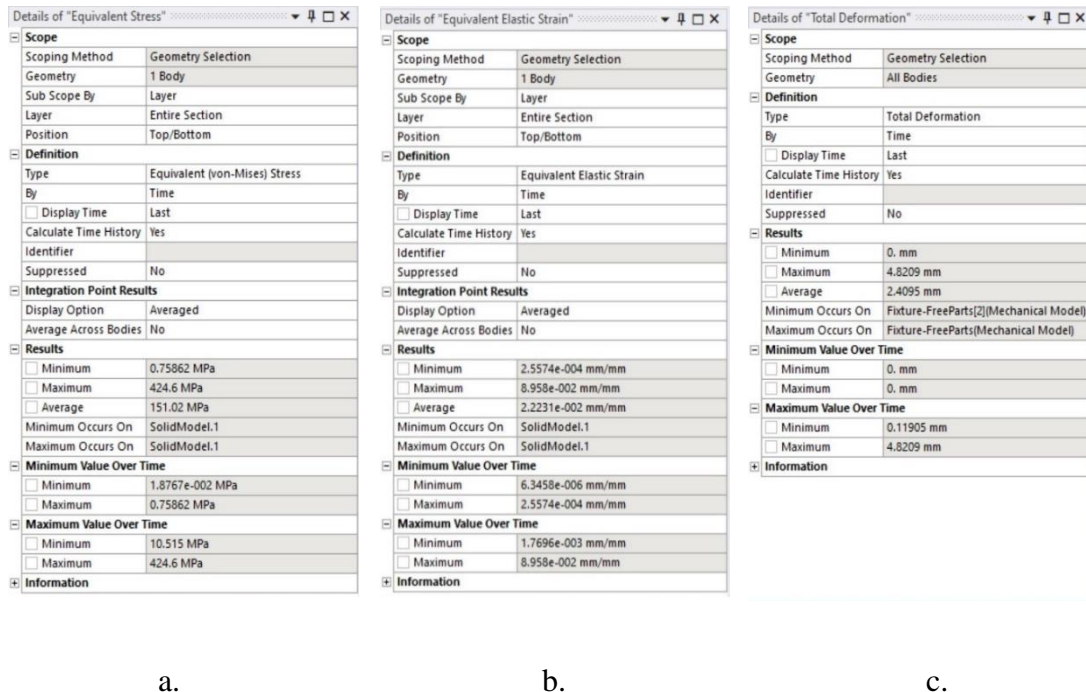


Figure 3.80 Simulation option parameters for (a) Equivalent Stress (b) Equivalent Elastic Strain (c) Total Deformation

Chapter 4. Results and Discussion

In this study, the tensile and the flexural properties of jute-carbon reinforced epoxy composite material was analyzed. First, the composites in four different stacking sequence was fabricated, all of which were in the same unidirectional orientation. Later the composites in standard dimensions was cut and analyzed in the lab to attain their tensile and flexural properties following the procedure that has been already mentioned in the previous chapter. After that the exact specimen dimensions was taken and FEA model of the specimen was generated and then tensile test and flexural test was simulated in ANSYS APDL. Later both the experimental data and the data acquired from the numerical analysis were compared and validated in order to achieve a more reliable conclusion.

In this chapter, the experimental and numerical result has been discussed in two major sections divided according to the type of the analysis, and within which there are total 4 sub-sections. The first sub-section evaluates results achieved from the experimental analysis of tensile properties and then in the second sub-section, the attained results from the FEA simulation was first stated and then a comparative discussion on findings was made and the results were validated. In the third and fourth sub-section the same format for the flexural test was repeated and results are discussed.

4.1 Tensile Test Result Analysis

4.1.1 Experimental Result Analysis

A complete picture of the result that is obtained from the experimental analysis has been presented in **Figure 4.1** it is observed that various stacking sequence has quite significant effect on the tensile behavior. At the point when the fibers were arranged unidirectionally, the force was parallel to the adjusted long and continuous fibers. Thus, unidirectional composites laminates had the option to show most extreme resistance from the deformation to the applied force. An eminent measure of variety was seen in the Ultimate Tensile Strength (UTS) among the four diverse stacking successions. The highest UTS has been recorded for $J_3C_4J_3$, which is 571 MPa and $J_2C_2J_2C_2J_2$ has the second highest UTS which is 548 MPa. $C_2J_6C_2$ gives the lowest UTS of 496 MPa and $C_2J_3C_2J_3$ has the second lowest UTS of 510 MPa.

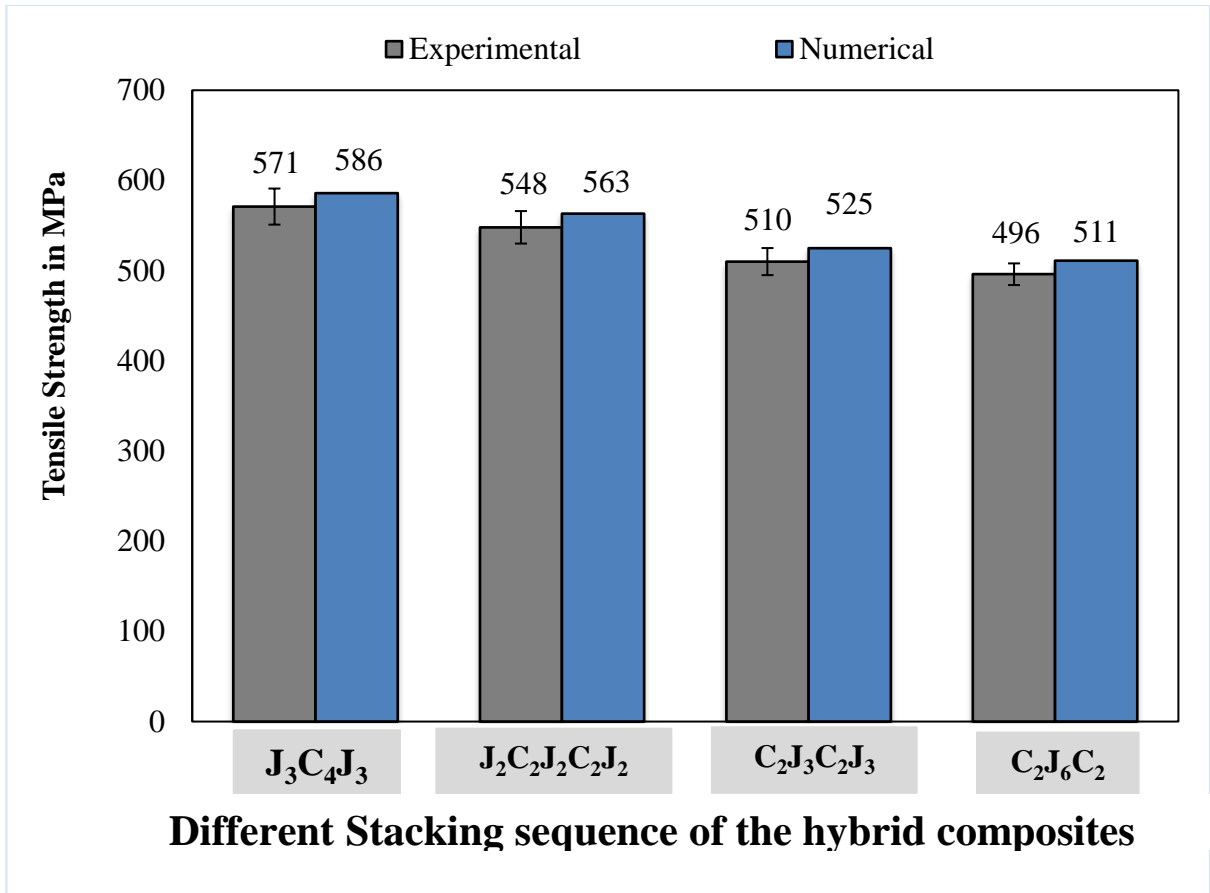


Figure 4.1 Experimental and numerical tensile test result for all the composite laminates

Since the fibers were oriented in a single direction, the load was parallel to the fibers. Because of the delamination and debonding occurring in the sample composite, the tensile strength is shifted in spite of not altering the volume of the fiber in each of the hybrid composites. Putting the jute plies halfway hinders the carbon interaction and furthermore expands the debonding and delamination, causing a decline in the ultimate tensile strength. Because of these, the ultimate tensile strength was discovered greatest while jute laminate was set to the exterior surface and the carbon laminate was set in the center of the sample. Carbon fibers are sturdier and firmer than the jute strands, explaining the sudden increment

in the ultimate tensile strength. In this way, utilizing carbon fiber has resulted in better properties in the hybrid composites in contrary to its natural fiber partners. Jute fibers are naturally fragile. Because of this, jute fibers broke down in a brief timeframe, while the carbon fibers kept on withstanding the load until the all layers failed.

Rosen's failure model is shown in **Figure 4.2**, where Rosen analyzed strength distribution of fiber enforced composite materials. There in the figure one fiber is broken when the rest of the fibers are yet intact. Therefore, when either on load, the volume element of the fibers changes its size or the fractured fiber increases. As a result, a redistribution of the stress takes place around the fracture. This stress takes place in between the two broken fiber ends. For this reason a high amount of stress takes place in a short distance as shown in **Figure 4.2**. The stress increases from zero to σ_f , which is the break to stress level, but the composite material stress level is far from the break. As a result, a fiber-pull-out problem is occurred after a fiber fracture.

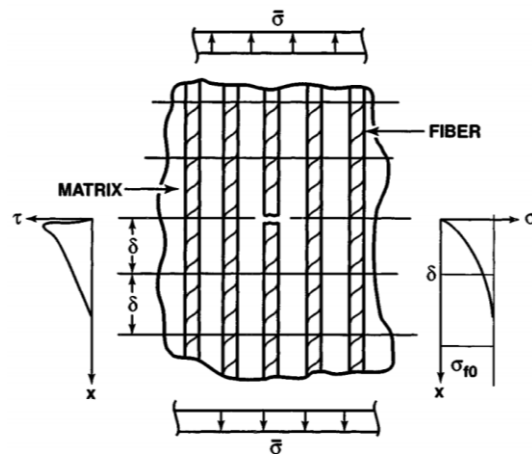


Figure 4.2 Rosen's Tensile Failure Model

In this condition, a fiber reinforced composite material failure may happen in two ways. One way can be the failure of the matrix surrounding the area due to the shear stress. Which means the bond between the fiber and the matrix is broken. On the other hand, there might be an over all failure of the composite if the fracture is propagated through out the fibers along with the matrix.

The tensile properties of a composite material depend on the position of the delamination and deboning that occurs during an tensile test. It is also observed if the jute fibers are positioned in the middle, the delamination & deboning significantly increase. Therefore, to increase the tesile strength of jute-carbon compsite, the jute fibers should be as close to the surface as possible.

It is also observed that the tensile strength of the composite increases significantly if the carbon fibers are positioned as the cores (*Figure 4.1*). This happens due to the carbon fibers being stronger and stiffer in nature then the jute fiber. Due to the improved tensile property of carbon fiber when hybridized with jute fiber, the composite showed significant amount of boost in mechanical properties over the jute fiber.

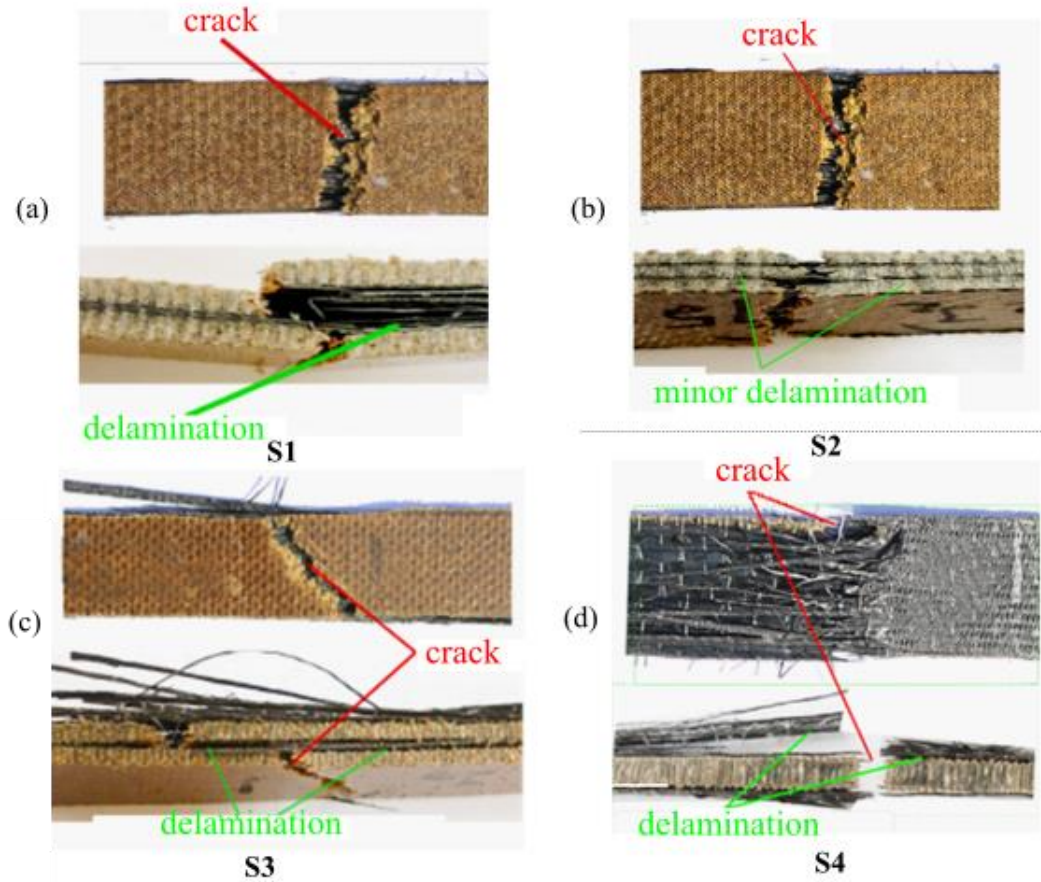


Figure 4.3 Fracture condition of Unidirectional composite (S1-S4) material after tensile test(a-d)

Due to the brittle nature of jute fibers, it breaks earlier than the carbon fibers used in the composite. Gradually all the fibers in the composite fracture and result in failure of all the layers.

The jute carbon fiber reinforced composite material tensile failure is observed in **Figure 4.3 (a-d)**. It is seen that for all the cases there is delamination occurring at the surface of the composite samples. For the sample S4, the delamination at the surface showed the most **Figure 4.3 (d)** and also, it showed the least UTS among all the four stacking sequences.

4.1.2 FEA Simulation Results of Tensile Properties

The generated FEA model was approved by contrasting the stress strain attributes of the composite laminates acquired by means of experimental and simulated tensile test. The result that is obtained from numerical analysis is also presented on the **Figure 4.4**. It is observed that numerical results are quite close to the experimental ones. J₃C₄J₃ gives the maximum UTS of a magnitude of 586 MPa and C₂J₆C₂ gives the minimum UTS of 511 MPa. In case of the experimental result, the same tensile behavior is observed. The numerical results are close to the experimental ones because of preparing and modeling the composite specimens in ACP before simulating in ANSYS APDL. Total deformation of the model under the application of tensile load is pictured in **Figure 4.4**

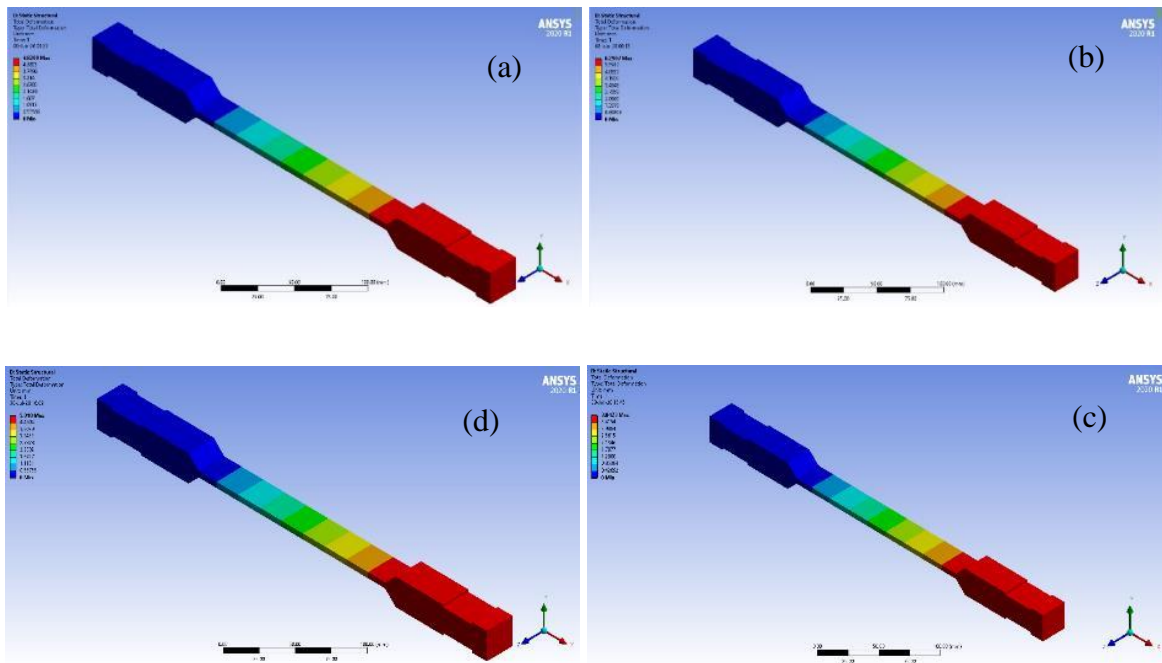


Figure 4.4 Total deformation after tensile load. (a) S1 = J₃C₄J₃, (b) S2= J₂C₂J₂C₂J₂C, (c) S3 = C₂J₃C₂J₃, (d) S4= C₂J₆C₂

It is observed that the stress strain characteristics of numerical outcomes displayed almost close pattern of experimental findings. It is found that the result of numerical analysis is higher than that of the experimental findings. It might be because of the explanation, that during simulation, the laminates were considered as homogeneous and neither any void nor any crack formation was present in the composites. Progressively, the plies are not homogeneous which brought about voids and event of fiber-matrix breaking and cracking during the tensile test experiments.

4.2 Flexural Test Result Analysis

4.2.1 Experimental result analysis

The flexural properties of jute-carbon composite laminates vary significantly from the flexural property of pure jute fiber laminates or pure carbon fiber laminates as shown in *Figure 4.5*. The flexural properties have also observed to be depended on the number of plies used for a laminate and also on the sequence of stacking. The flexural performances of composites had proven to be increased if the carbon fiber is used on the outer/skin layers as top ply or bottom ply of a laminate. This happens as the flexural test eventually causes compression on the top ply, tension on the bottom ply and shear stress for the middle plies. The impact on flexural properties due to stacking sequence can be observed from Figure 1, it is observed that the flexural strength of S1 and S2 is 142 MPa and 280 MPa is significantly lower than the flexural strength of S3 and S4, which are 320 MPa and 445 MPa. The higher flexural properties of S3 and S4 are results of their stacking sequence. In addition, from further observation, comparing the results of S2 with S3 and S3 with S4 it is found that using Carbon ply as skin layer showed a significant improvement of the flexural properties.

The claim can be strengthened further by observing the stacking sequence of S3 (C₂J₃C₂J₃) and S4 (C₂J₆C₂), where the S3 sequence had 2 Carbon fabrics as the top plies and the S4 had 2 carbon fabrics as top plies another 2 Carbon fabrics as bottom plies. As a result, the S4 laminate showed the maximum flexural performance. The S3 laminate showing significantly higher flexural strength than S1 and S2, but strengthening less than S4 can also be explained from the stacking pattern. Therefore, finally it can be stated that the hybridization of the Carbon-Jute composites significantly improves its flexural performance; the flexural properties are highly depended on the number of plies used for lamination and the stacking pattern of the laminate. In addition, it is evident that flexural properties are highly depended on the skin layers; reinforced layers such as carbon fabric used as skin layers resulted in significant improvement of flexural properties.

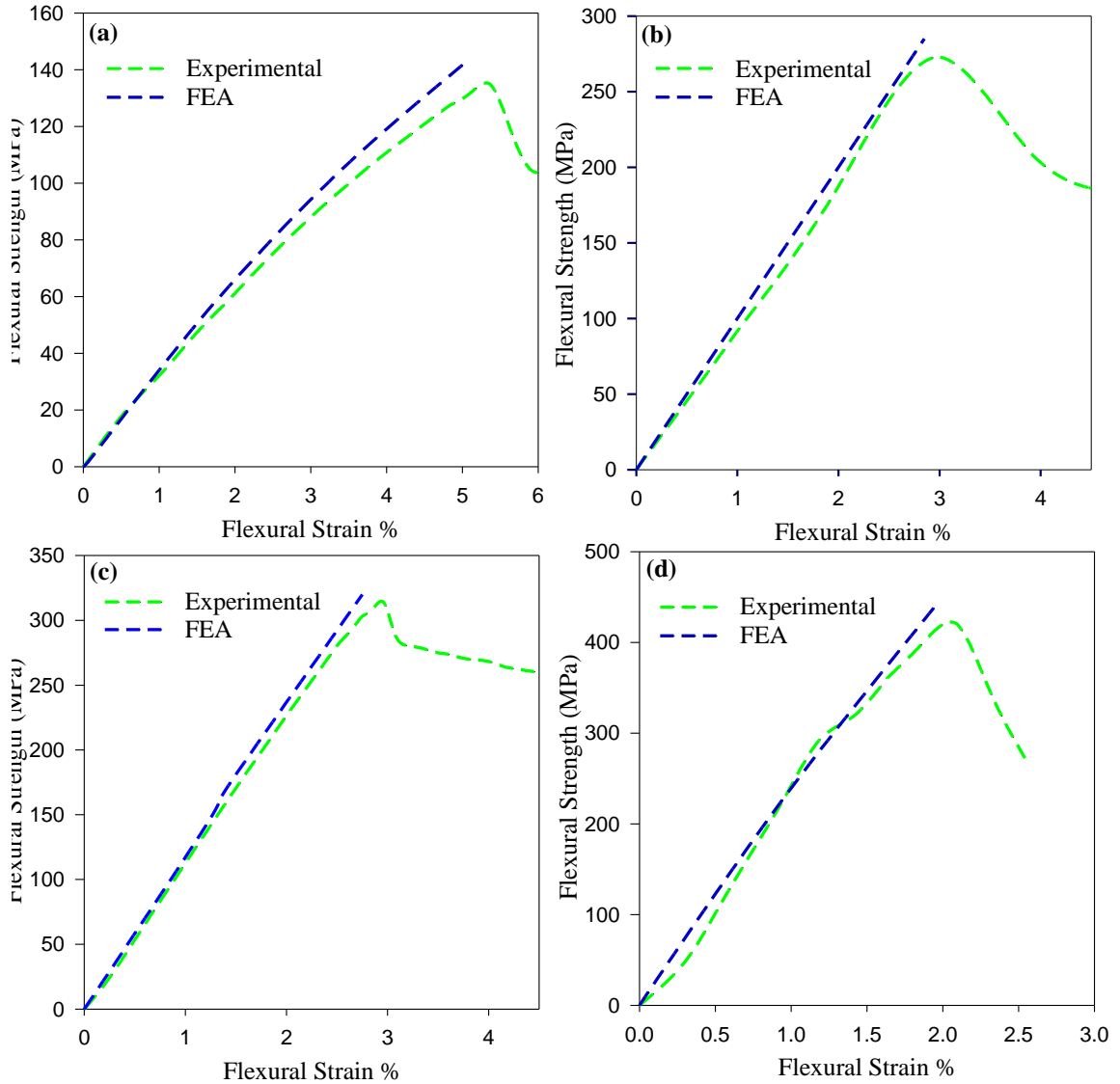


Figure 4.5 Flexural stress vs Strain curve experimental and FEA (a) $J_3C_4J_3$ (b) $J_2C_2J_2C_2J_2$
(c) $C_2J_3C_2J_3$ (d) $C_2J_6C_2$

The **Figure 4.5** correlates the flexural strain of unidirectional composite with response to the flexural strength observed under the applied flexural force. From the **Figure 4.5** it can be observed very clearly how the flexural stress varies among the four different stacking sequences. The patterns of fracture in which the four different stacking sequence took place was showed in **Figure 4.6**. They clearly show signs of delamination, matrix cracking, fiber

buckling in *Figure 4.6*. The sample S4 from *Figure 4.6 (d)* showed the maximum amount of delamination, one important factor here is that for S4 the carbon fiber was used on both the compression side and tensile side. It is due to the weak bonding between the carbon fiber and jute fiber. The highest flexural strength of 460 MPa was found for S4 (*Figure 4.5 and Figure 4.6*) and for S1 *Fig 4.6 (a)* sample was 135 MPa (*Fig 4.5 and Fig. 4.6*) which was the lowest flexural strength among all the samples. For S3 sample (315 MPa) which was the 2nd highest flexural strength observed, it is 31% less than the flexural strength of S4.

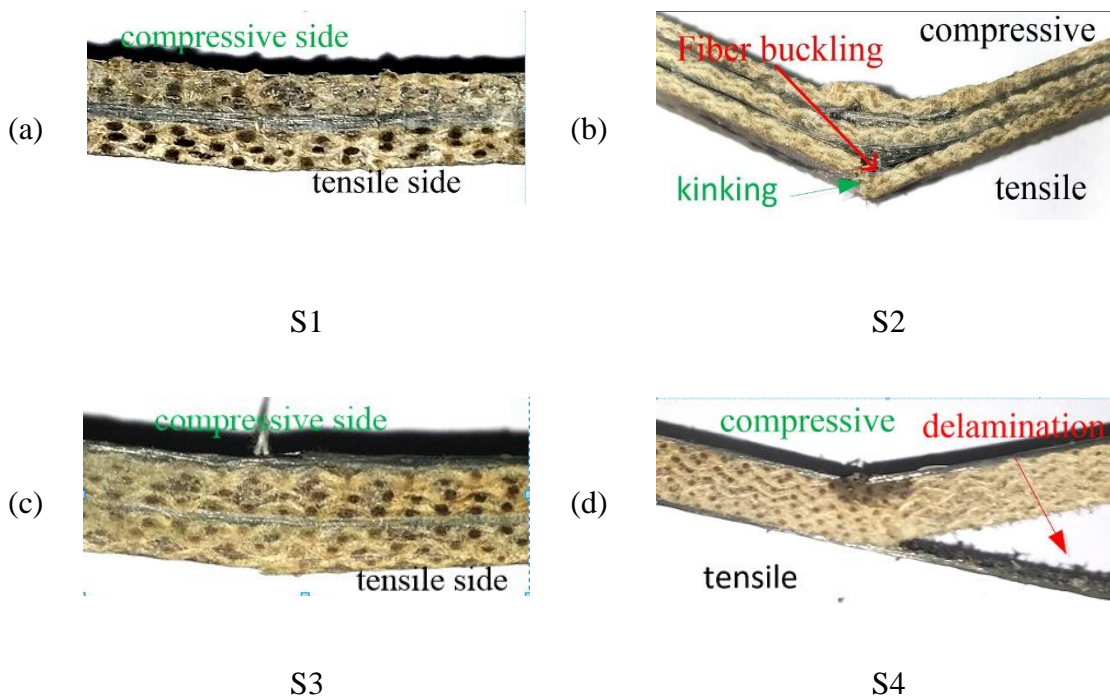


Figure 4.6 Fracture configuration of the sample after the flexural test (a-d) for sample S1-S4 (unidirectional)

4.2.2 FEA Simulation Results of Flexural Properties

The FEA model was generated and simulated in ANSYS, ACP module was used to generate the specimen and then flexural test was simulated in ANSYS APDL. The results that are achieved from the simulation was validated by the experimental flexural test results of stress-strain diagram. Here in Figure 1 the results found from both the experimental analysis and FEA analysis of flexural properties were plotted. Flexural strain-flexural strength graph for S1 ($J_3C_4J_3$), S2 ($J_2C_2J_2C_2J_2$), S3 ($C_2J_3C_2J_3$) and S4 ($C_2J_6C_2$) of both experimental and FEA analysis were plotted. From the graphs of Figure 1, it can be observed that the simulation results show a similar trend as the experimental results for all laminates of different stacking sequences. However, the data gathered from FEA analysis gives ideal curve and the flexural strengths achieved at similar flexural strains is slightly higher than the experimental analysis. It is due to the lack of homogenous structure of the experimental specimen, on the other hand in case of FEA analysis a completely homogeneous specimen was considered. Total deformation of 3D modeled specimen during flexural numerical analysis is illustrated in *Figure 4.7*. In practical experiments, while producing the composite specimen avoiding any fiber matrix crack or avoiding formation of small voids between resin-enforced plies is impossible. Due to these, an overall enhancement of flexural performance in FEA analysis can be seen. Therefore, considering these unavoidable technical difficulties, observing the flexural strength-flexural strain graphs of both experimental and FEA analysis it is noticed that the results are converging and thus the numerically acquired data from this simulation can be considered reliable and satisfactory.

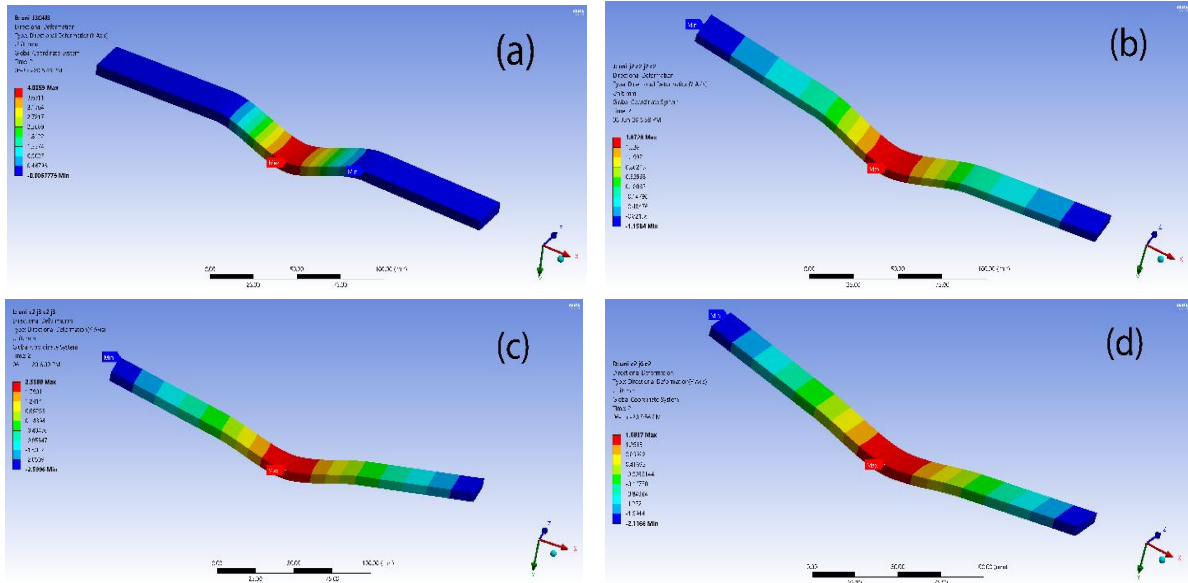


Figure 4.7 Total deformation of FEA 3D specimen under flexural load of (a) $J_3C_4J_3$

(b) $J_2C_2J_2C_2J_2$ (c) $C_2J_3C_2J_3$ (d) $C_2J_6C_2$

Chapter 5. Conclusion

The purpose of the work was to find out and describe the properties of jute-Carbon fiber composites, also to investigate the possibilities of using the composite for wide range of applications by testing and discussing its tensile and flexural properties. Due to achieving higher mechanical properties at a lower material density and less material cost the modern production companies are getting more involved in natural fiber composites and laminates. As the Jute-Carbon composite materials exhibits higher mechanical properties and it is proven to be more cost efficient therefore, it has a significant importance for modern industries. However, considering the possibilities despite many research and development of testing the anisotropy properties of composite in past few years, accurately predicting the tensile & flexural properties and failure mechanism of Jute-Carbon composite materials are still a challenge, which is due to the non-homogenous structure and properties of jute fiber. So, from the above discussion of our study, these following conclusions can be drawn :

- Hybridization of natural fibers such as jute fiber with carbon fiber can be a more economical alternative of synthetic composites without significantly compromising the mechanical properties such as tensile strength and flexural strength.
- The mechanical behaviors of Jute-Carbon composite were highly dependent on the number of plies used in a laminate, also on the position of carbon plies and jute plies in a sequence. Using carbon ply as skin layer of a laminate resulted in significant improvement of flexural behavior, however it didn't seem to affect the tensile properties of the specimen.

- The overall comparison among S1(J₃C₄J₃), S2(J₂C₂J₂C₂J₂), S3(C₂J₃C₂J₃) and S4(C₂J₆C₂) sequences revealed that tensile behaviors doesn't differ significantly for different stacking sequences of Jute-Carbon hybrid composites. Tensile strength was found maximum of 571 MPa for S1(J₃C₄J₃) and minimum of 511 MPa for S4(C₂J₆C₂) during the experimental analysis. However, the numerical analysis resulted in slightly higher tensile strength for each of the sequence due to the pre-assumptions of isometric conditions, no void formation, proper bonding of fiber/matrix and homogeneity of specimen during FEA simulation.
- On the contrary, similar comparison among the sequences revealed that the flexural behavior differs significantly for different stacking sequences of Jute-Carbon hybrid composites. Flexural strength was found maximum of 420 MPa for S4(C₂J₆C₂) and minimum of 130 MPa for S1(J₃C₄J₃) during the experimental analysis. And the results clearly indicate the superiority of flexural properties for S4 and S3 due to the existence of carbon fiber as skin layers. Here again the numerical analysis resulted in slightly higher flexural strength for all the specimen for the same reasons explained in the previous point.
- Comparing with experimental results the tensile and flexural simulation results to be reliable was found. The data achieved through ANSYS ACP simulation showed to be converging with the data found by experimental analysis for both the tensile and flexural properties.

- These simulations were also very accurate in determining realistic failure zone for the specimen during these analyses.

From these above-mentioned points, it can be confidently claimed that the hybridization with natural composites holds a significant potential for future manufacturing industries and the cost of the future research and development can be drastically reduced using FEA simulations with even more accuracy using less mesh dimensions and anisometric properties. Moreover, increasing natural composite applications can produce a huge impact on climate change by lowering the synthetic wastes and carbon foot prints. The above study of Jute-Carbon composite can be improved further by analyzing specimen with complex shapes at anisometric conditions, further calibration of parameters for simulations, and investigation of mesh sensitivity can reduce computational time and increase accuracy of validation for numerical analysis.

Chapter 6. References

- [1] M. Boopalan, M. Niranjanaa, and M. J. Umapathy, “Study on the mechanical properties and thermal properties of jute and banana fiber reinforced epoxy hybrid composites,” *Compos. Part B Eng.*, vol. 51, pp. 54–57, 2013.
- [2] S. H. Han, H. J. Oh, H. C. Lee, and S. S. Kim, “The effect of post-processing of carbon fibers on the mechanical properties of epoxy-based composites,” *Compos. Part B Eng.*, vol. 45, no. 1, pp. 172–177, 2013.
- [3] X. S. Yi, *Development of multifunctional composites for aerospace application*. Elsevier Inc., 2015.
- [4] R. Park and J. Jang, “Performance improvement of carbon fiber/polyethylene fiber hybrid composites,” *J. Mater. Sci.*, vol. 34, no. 12, pp. 2903–2910, 1999.
- [5] S. Ashworth, J. Rongong, P. Wilson, and J. Meredith, “Mechanical and damping properties of resin transfer moulded jute-carbon hybrid composites,” *Compos. Part B Eng.*, vol. 105, pp. 60–66, 2016.
- [6] D. K. Rajak, D. D. Pagar, P. L. Menezes, and E. Linul, “Fiber-Reinforced Polymer Composites : Manufacturing, Properties and Application,” *Polymers (Basel)*, vol. 11, no. 1667, pp. 1–37, 2019.
- [7] K. K. Chawla, *Composite Materials*. Springer New York, 1998.
- [8] M. Ramesh, K. Palanikumar, and K. H. Reddy, “Mechanical property evaluation of sisal-jute-glass fiber reinforced polyester composites,” *Compos. Part B Eng.*, vol. 48, pp. 1–9, 2013.

- [9] B. Koskova, *Mechanical properties of textile fibres*. 1981.
- [10] H. N. Dhakal, Z. Y. Zhang, R. Guthrie, J. MacMullen, and N. Bennett, "Development of flax/carbon fibre hybrid composites for enhanced properties," *Carbohydr. Polym.*, vol. 96, no. 1, pp. 1–8, 2013.
- [11] T. M. Aranno *et al.*, "Fabrication, experimental investigation of jute fiber reinforced epoxy composites and hybrid composites," *IOP Conf. Ser. Mater. Sci. Eng.*, vol. 628, no. 1, 2019.
- [12] A. S. Sujon and N. Mehfuz, "Experimental and numerical investigation on the tensile and water absorption behavior of jute / carbon reinforced epoxy," *Int. J. Mech. Eng. Technol.*, vol. 11, no. 2, pp. 130–140, 2020.
- [13] and Y. H. Lei Shao, Qing Gao, Xie, Jianzhong Fu, Meixiang Xiang, "Ce Pte Us Pt," *Mater. Res. Express*, pp. 0–12, 2019.
- [14] A. K. Bledzki and J. Gassan, "Composites reinforced with cellulose based fibres," *Prog. Polym. Sci.*, vol. 24, no. 2, pp. 221–274, 1999.
- [15] A. C. Karmaker and J. A. Youngquist, *Injection molding of polypropylene reinforced with short jute fibers*, vol. 62, no. 8. 1996.
- [16] J. Gassan and A. K. Bledzki, *The influence of fiber-surface treatment on the mechanical properties of jute-polypropylene composites*, vol. 28, no. 12. 1997.
- [17] Z. S. Ng, L. C. Simon, and A. Elkamel, *Renewable agricultural fibers as reinforcing fillers in plastics: Prediction of thermal properties*, vol. 96, no. 1. 2009.
- [18] C. Pavithran, P. S. Mukherjee, and M. Brahmakumar, *Coir-Glass Intermingled Fibre*

Hybrid Composites, vol. 10, no. 1. 1991.

- [19] I. A. Hakim, S. L. Donaldson, N. G. Meyendorf, and C. E. Browning, “Porosity Effects on Interlaminar Fracture Behavior in Carbon Fiber-Reinforced Polymer Composites,” *Mater. Sci. Appl.*, vol. 08, no. 02, pp. 170–187, 2017.
- [20] S. Biswas and M. Engineering, “Characterization and Performance Analysis of Natural Fibres as Reinforcement in Polymer Composite,” 2010.
- [21] H. Ismail, J. M. Nizam, and H. P. S. Abdul Khalil, *Effect of a compatibilizer on the mechanical properties and mass swell of white rice husk ash filled natural rubber/linear low density polyethylene blends*, vol. 20, no. 2. 2001.
- [22] H. Ismail and R. M. Jaffri, *Physico-mechanical properties of oil palm wood flour filled natural rubber composites*, vol. 18, no. 5. 1999.
- [23] H. Ismail, M. R. Edyham, and B. Wirjosentono, *Bamboo fibre filled natural rubber composites: The effects of filler loading and bonding agent*, vol. 21, no. 2. 2002.
- [24] E. Selver, N. Ucar, and T. Gulmez, “Effect of stacking sequence on tensile, flexural and thermomechanical properties of hybrid flax/glass and jute/glass thermoset composites,” *J. Ind. Text.*, vol. 48, no. 2, pp. 494–520, 2018.
- [25] D. K. Jesthi and R. K. Nayak, “Influence of glass/carbon fiber stacking sequence on mechanical and three-body abrasive wear resistance of hybrid composites,” *Mater. Res. Express*, vol. 7, no. 1, 2020.
- [26] M. Ramesh and P. Sudharsan, “Experimental Investigation of Mechanical and Morphological Properties of Flax-Glass Fiber Reinforced Hybrid Composite using

- Finite Element Analysis,” *Silicon*, vol. 10, no. 3, pp. 747–757, 2018.
- [27] M. Jawaid and H. P. S. Abdul Khalil, “Cellulosic/synthetic fibre reinforced polymer hybrid composites: A review,” *Carbohydr. Polym.*, vol. 86, no. 1, pp. 1–18, 2011.
- [28] M. Asim, M. Jawaid, N. Saba, Ramengmawii, M. Nasir, and M. T. H. Sultan, *Processing of hybrid polymer composites-a review*. Elsevier Ltd, 2017.
- [29] M. A. Abd El-Baky and M. Kamel, “Abrasive Wear Performance of Jute–Glass–Carbon-Reinforced Composites: Effect of Stacking Sequence and Fibers Relative Amounts,” *J. Nat. Fibers*, vol. 00, no. 00, pp. 1–16, 2019.
- [30] R. Rahman and S. Z. F. S. Putra, *Tensile properties of natural and synthetic fiber-reinforced polymer composites*. Elsevier Ltd, 2018.
- [31] L. Vinšová and T. Urban, *Testing of mechanical properties of thick-walled carbon fiber composite for FEM simulations*, vol. 4, no. 5. Elsevier Ltd, 2017.
- [32] M. Nirbhay, A. Dixit, R. K. Misra, and H. S. Mali, “Tensile Test Simulation of CFRP Test Specimen Using Finite Elements,” *Procedia Mater. Sci.*, vol. 5, pp. 267–273, 2014.
- [33] H. W. Wang, H. W. Zhou, L. L. Gui, H. W. Ji, and X. C. Zhang, “Analysis of effect of fiber orientation on Young’s modulus for unidirectional fiber reinforced composites,” *Compos. Part B Eng.*, vol. 56, pp. 733–739, 2014.
- [34] “FAdetails @ indiantextilejournal.com.” .
- [35] F. Corrales, F. Vilaseca, M. Llop, J. Gironès, J. A. Méndez, and P. Mutjè, “Chemical modification of jute fibers for the production of green-composites,” *J. Hazard.*

Mater., vol. 144, no. 3, pp. 730–735, 2007.

- [36] E. Nisini, C. Santulli, and A. Liverani, “Mechanical and impact characterization of hybrid composite laminates with carbon, basalt and flax fibres,” *Compos. Part B Eng.*, vol. 127, pp. 92–99, 2017.
- [37] J. Flynn, A. Amiri, and C. Ulven, “Hybridized carbon and flax fiber composites for tailored performance,” *Mater. Des.*, vol. 102, pp. 21–29, 2016.
- [38] D. B. Dittenber and H. V. S. Gangarao, “Critical review of recent publications on use of natural composites in infrastructure,” *Compos. Part A Appl. Sci. Manuf.*, vol. 43, no. 8, pp. 1419–1429, 2012.
- [39] D790, “{ASTM} Standard test method for flexural properties of unreinforced and reinforced plastics and electrical insulating materials,” *Annu. B. ASTM Stand.*, vol. 10, pp. 1–11, 2010.
- [40] A. Ali *et al.*, “Experimental and numerical characterization of mechanical properties of carbon/jute fabric reinforced epoxy hybrid composites,” *J. Mech. Sci. Technol.*, vol. 33, no. 9, pp. 4217–4226, 2019.
- [41] A. International and indexed, “Designation: D 3039/D 3039M – 00 Standard Test Method for Tensile Properties of Polymer Matrix Composite Materials 1,” vol. 15, 2002.